BLOOD VESSEL DEVELOPMENT

APPROVED BY SUPERVISORY COMMITTEE

Ondine Cleaver, Associate Professor

Thomas Carroll, Associate Professor

Eric Olson, Associate Professor

Melanie Cobb, Associate Professor

Dedication

To my parents:

Kyung Ah Cho and Bon Sik Koo

For their eternal love and support.

BLOOD VESSEL DEVELOPMENT

By

YEON SEUNG KOO

DISSERTATION

Presented to the Faculty of the Graduate School of Biomedical Sciences

The University of Texas Southwestern Medical Center at Dallas

In Partial Fulfillment of the Requirements

For the Degree of

DOCTOR OF PHILOSOPHY

The University of Texas Southwestern Medical Center at Dallas

Dallas, Texas

December, 2014

ACKNOWLEGDEMENTS

First, I would like to thank my mentor, Dr. Ondine Cleaver for her support, guidance, and patient advice. Since I joined Cleaver Lab, I have seen her motivating and encouraging people with describing of excitement of science all the time. She enjoys challenges and seeks for new ideas. It was a great inspiration. I am also in dept to her help and caring through my graduate life.

Secondly, I am very grateful to committee members, Dr. Thomas Carroll(Chair), Dr. Melanie Cobb, and Dr. Eric Olson for their invaluable suggestions and advice. Their critical questions during committee meetings and their wise insights helped me to focus on the right direction for my project.

In addition, I would like to thank my previous and current lab members, Ke Xu, Diana Chong, Allethia Villasenor, Stryder Meadows, Peter Fletcher, Stephen Fu, Lyndsay Ratliff, Leilani Marty Santos, David Barry, Caitlin Braitsch, and Berfin Azizoglu. Because of them, I could enjoy working in family-like environment. I also appreciate their help and assist for carrying out experiments and developing ideas.

Last but not least, I would like to thank my boyfriend, Josh Chang, my parents, Bonsik Koo and Kyung Ah Cho, my sister, Eunice Koo, and my brother Woongmo Koo for their support, understanding, and unconditional love.

BLOOD VESSEL DEVELOPMENT

YEON SEUNG KOO, Ph.D.

The University of Texas Southwestern Medical Center at Dallas, 2014

Supervisor: ONDINE CLEAVER, Ph.D.

Cardiovascular system is the first developing functional organ in vertebrates, and one of the fundamental organ systems through adulthoods. Cardiovascular function depends on patent blood vessel formation by endothelial cells. In this dissertation, a careful analysis of different aspects of blood vessel development was conducted in order to expand our understandings of the biology of blood vessel. In brief, Chapter 2 provides an in depth description of vessel anatomy during formation of the first arteries and veins in developing murine embryos, and a stepwise acquisition of arteriovenous fate in these vessels. The dorsal aortae, the first intraembryonic vessels initiate arterial specification before complete circulation occurs, and gradually express a subset of arterial genes. The first veins then establish their fate later than the first arteries. It was also shown that the arteriovenous specification does not require hemodynamic flow, but the flow affects maintenance of select arterial genes. Chapter 3 focuses on the function of Rasip1 in vasculogenesis, angiogenesis and vessel maintenance in developing embryo and in adults. An observation of transient Rasip1 localization at apical membranes in endothelial cells during in vitro tube formation provided an insight where Rasip1 possibly functions. Mice lacking Rasip1 showed

that Rasip1 is critical for lumen formation likely via recruiting Myosin to endothelial apical membranes to alter cell cytoskeleton during vasculogenesis. Rasip1 was also shown to be required for proper vessel remodeling and lumen formation during angiogenesis. I found, however, it is dispensable for adult established blood vessel lumen maintenance, making it a promising therapeutic target for anti-angiogenesis. Finally, in Chapter 4, I show my preliminary findings regarding the role of Arhgap29, a Rasip1 binding partner, during embryonic development. Genetic ablation of Arhgap29 in mice led to allantois-chorion fusion and cardiovascular defects during embryonic development. Arhgap29 expression patterns were correlated with the sites of defects, as Arhgap29 transcripts were seen in allantois and cardiovascular tissues. From these results, its potential role in regulation of cell adhesion, likely via RhoA, was suggested. Overall, this thesis describes basic aspects of vascular development and uncharacterized molecules in different aspects of cardiovascular function.

TABLE OF CONTENTS

PRIOR PUBLICATIONS

Chong D., Koo Y, Xu K, Fu S, Cleaver O. Stepwise arteriovenouse fate acquisition during mammalian vasculogeneiss. *Dev Dyn.* 2011 Sep;240(9):2153-65.

Lee, E., Koo Y, Ng A, Wei Y, Luby-Phelps K, Juraszek A, Xavier RJ, Cleaver O, Levine B, Amatruda JF. Autophagy is essential for cardiac morphogenesis during vertebrate development. *Autophagy.* 2014 Apr;10(4):572-87.

PRESENT WORK

Koo Y., Xu K, Tanikaki K, Mineo C, Fu S, Davis GE, Cleaver O. Rasip1 is essential to angiogenic blood vessel growth. (in preparation)

LIST OF FIGURES

CHAPTER 1

CHAPTER 2

CHAPTER 3

CHAPTER 4

CHAPTER 5

LIST OF TABLES

LIST OF APPENDICES

LIST OF ABBREVIATIONS

aPKC – Atypical Protein Kinase C

Arhgap29 – Rho GTPase activating protein 29

AV – Atriovenous

E – Embryonic day

EC – Endothelial cell

ECM – Extra cellular matrix

GFP – Green Fluorescent Protein

GAP – GTPase Activating Protein

GTP – Guanosine Triphosphate

ISV – Intersomitic/Intersegmental Vessel

Rasip1– Ras interacting protein 1

PECAM – Platelet Endothelial Cell Adhesion Molecule

PODXL – Podocalyxin

S – Somite

SMA – Smooth Muscle Actin

SMC – Smooth Muscle Cell

Tie2 – Tyrosine kinase with Immunoglobin-like and EGF-like domain 2

VCAM-1 – Vascular Cell Adhesion Molecule 1

VE-cadherin – Vascular Endothelial cadherin

Chapter 1. INTRODUCTION

1.1 BLOOD VESSEL DEVELOPMENT

1.1.1 Introduction to blood vessel

Blood vessels and their function

The formation of cardiovascular system is one of the earliest events during embryonic development, and a critical process that occurs during tissue growth, regeneration and pathologies in adults. The vascular system is a highly branched and organized hierarchical network of tubes, which penetrates every organ. The blood vessel provides a tunnel-structure, or 'tube', allowing blood circulation to supply nutrients and respiratory gasses, as well as remove wastes, and dissemination of immune cells throughout the body. The endothelial cell (EC), which is a fundamental building block of blood vessel, lines the inner surface of the vascular tubes. The monolayer of ECs provides regulates blood flow, control thrombosis by platelet adherence and modulates inflammatory responses by controlling immune cell permeability. In addition, ECs regulate vessel growth and provide vessel wall and extracellular matrix (ECM) components. The endothelium, which lines the entire vascular system, plays a critical role as a multifunctional organ.

The significance of blood vessel studies

As the cardiovascular system is one of the fundamental organs, abnormal vasculature formation causes critical pathological problems. Aberrant development of blood vessel can causes critical defects during embryonic development, leading to embryonic lethality. Inadequate vessel maintenance causes ischemia in diseases such as atherosclerosis, stroke,

neurodegeneration, and obesity-associated disorders. Excessive vascular growth contributes cancer, retinopathy, and inflammatory diseases. Driven by clinical demand, vascular studies for pro- or anti- angiogenic therapies have been developed, but the issue still presents challenges. The basic understanding of blood vessel development and its regulators will provide us insights to comprehend EC behavior and facilitate vascular research.

1.1.2 Blood vessel development – Vasculogenesis

Vascular development is highly conservative among vertebrates. Embryonic blood vessel starts with de novo blood vessel formation, termed 'vasculogenesis', which happens via precursor EC assembly **(Fig. 1.1 A)**. During vasculogenesis, EC precursors, called 'angioblasts', emerge and assemble to form vascular plexus. Then, angioblasts undergo morphogenesis to form functional vascular tubes. After initial blood vessel formation, the vascular network is expanded by a process called 'angiogenesis' **(Fig. 1.1 B)**. During angiogenesis, new vascular networks are formed: by extension of new vessels and by remodeling of existing vessels. Once ECs assemble into newly formed vascular tubes, they undergo maturation. Vascular tubes become covered by pericytes (on smaller capillaries), smooth muscle cells (SMCs, on larger vessels), and ECM, and become established functional blood vessels.

The origin of endothelial precursor cells

The origin of angioblasts has long been controversial. It has been established that angioblasts are mesodermally derived and differentiate into ECs in close contact with endoderm (Wilt, 1965). Using chick embryo culture, it was shown that blood island formation from mesoderm was positively regulated by endoderm. In the absence of endoderm, pre-angioblast mesodermal cells failed to differentiate to ECs.

Mesodermal cells give rise to two different angioblast populations, intra- and extra-embryonic angioblasts. Early mesodermal cells migrate into the yolk sac and form extraembryonic yolk sac mesoderm, which become ‘blood island’(Flamme, 1987). During embryonic development, blood islands are the first observable vascular structures, which present as aggregates of cells. They consist of peripheral angioblasts and inner hematopoietic stem cells, forming bag-like structure that contain blood precursors surrounded by EC precursors (Risau and Flamme, 1995). Individual bags extend toward each other and fuse to form vascular plexus, as their lumens become continuous.

Intraembryonic vasculogenesis

Shortly after yolk sac vasculature takes shape, the first intraembryonic angioblasts appear as scattered cells at the lateral edges of the anterior intestinal portal (AIP) within embryonic tissues (Coffin and Poole, 1988). The angioblasts arise from fetal liver kinase (Flk1), or vascular endothelial growth factor receptor (VEGFR2), expressing mesoderm during mouse embryo development between E6.5 to E8.5 (Drake and Fleming, 2000). These $VEGFR2^{+}$ dispersed cells start to gather and establish cell-cell contacts. These linear aggregates of vascular progenitors represent primordial blood vessels. These linear and aggregated angioblasts do not yet form lumens at this stage, and are called ‘cords’. The cords initiate lumen formation and connect nascent endothelial tubes of the yolk sac to construct a complete vascular network that allows blood circulation. During this de novo vessel formation, ECs undergo a complex series of processes, including EC migration, specification, and maturation, which result in the reorganization from individual angioblasts into a continuous tubular endothelium.

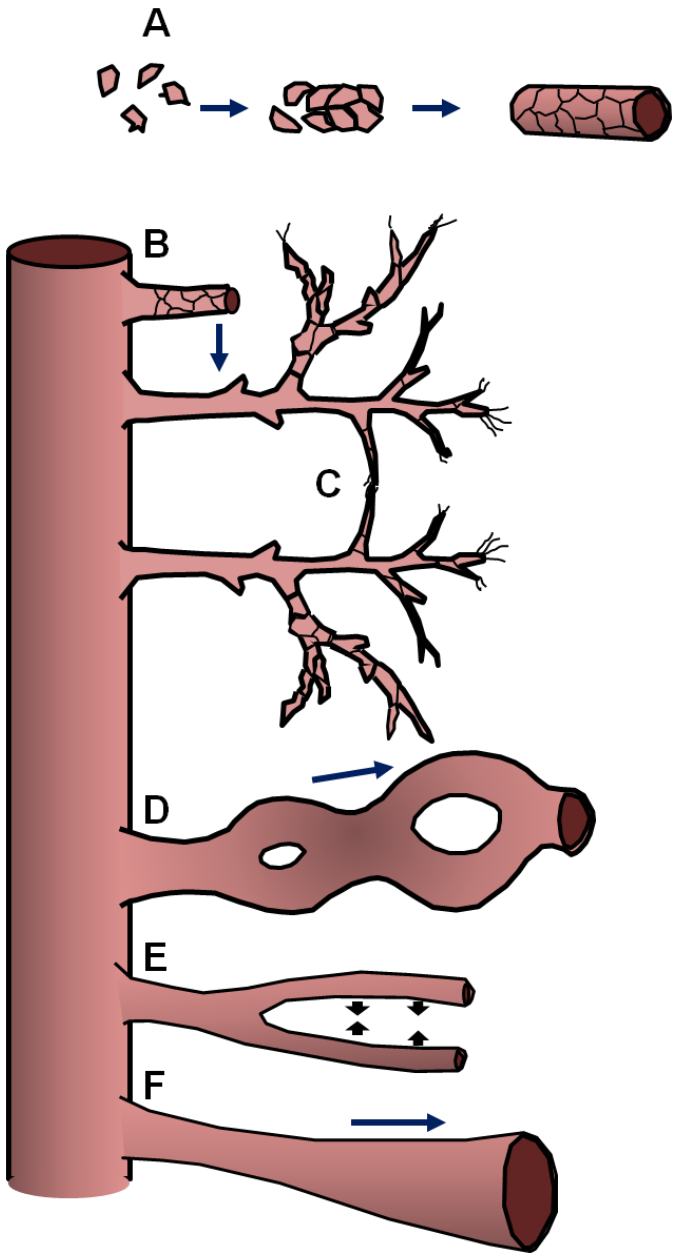

Figure 1.1 Vasculogenesis and angiogenesis models. (A) Vasculogenesis: angioblasts aggregate to form cord, and then form lumenized vessels. **(B)** Angiogenesis: endothelial cells form sprouts and branches. **(C)** Anastomosis: sprouts form vascular plexus. **(D)** Intussusception: a vessel splits into two pillars. **(E)** Reversed intussusception: fusion of blood vessels. **(F)** Intercalated growth of blood vessels': vessel expansion via increase in diameter and length.

1.1.3 Blood vessel development – Angiogenesis

After formation of primitive vasculature, the vascular system extends by process called 'angiogenesis' **(Fig. 1.1 B)**. Angiogenesis is classified into two broad categories. One is 'sprouting angiogenesis', in which ECs extend filopodia and new vessels sprouts as growing extensions from pre-existing blood vessels, usually toward avascular zones, thereby branching out to form a plexus. The other is called 'angiogenic remodeling', a process of vessel reorganization characterized by vessel splitting, fusion, or enlargement.

sprouting angiogenesis

Sprouting angiogenesis is the most easily observed mechanism and therefore, has been well described and the most studied to date (Folkman and Shing, 1992). During development, sprouting vessel formation occurs in intersomitic spaces, CNS, limb bud, embryonic kidney, lung, and retina. In the adult, sprouting angiogenesis can be observed during tissue regeneration and pathological processes, such as wound repair, inflammation, and tumorigenesis, and it has been referred to as 'neovascularization'.

Sprouting of new vessels is induced by induction of angiogenesis signaling. Pro-angiogenic factors include vascular endothelial growth factor family (VEGF), and fibroblast growth factors (FGF). It is thought that angiogenic factors are broadly expressed in the embryo, and are recognized by ligand specific receptors on ECs. For instance, VEGF is expressed in almost all embryonic tissues, while VEGFR2 is exclusively endothelial. On the other hand, there are anti-angiogenic factors secreted by notochord, lens and cornea, which creates avascular space within the embryo and allows for highly regulated patterning of the early blood vessels. Blood vessel growth is highly regulated by this balance between pro- and anti- angiogenic factors.

Once vessels are stimulated by angiogenic stimuli, ECs of the vessel wall produce proteases. Although the basement membrane of embryonic ECs is poorly developed, the proteolytic activity is critical for ECs to break down surrounding obstacles, such as ECM, to migrate towards the stimuli. ECM degradation is mediated by matrix metalloproteases (MMPs) which continue to be secreted from migrating ECs as they extend and the vessel grows.

Within the sprouting vessels, the leading endothelial is defined as the 'tip cell', and the following cells are called stalk cells. Tip and stalk cells are known to be controlled by the Notch signaling pathway (Phng and Gerhardt, 2009). The tip cell expresses high levels of notch ligand, Dll4, and this ligand is received by neighboring stalk cells via Notch1, the most critical Notch receptor during angiogenesis. Stalk cell Notch1 is activated and has been shown to inhibit tip cell phenotype. Disruption of Notch signaling in angiogenic sprouts results in excessive tip cell formation (Hellstrom et al., 2007; Suchting et al., 2007). In contrast to Dll4, another Notch ligand, JAGGED1 (Jag1) is preferentially expressed in the stalk cells, and poorly interacts with glycosylated Notch in the tip cells (Benedito et al., 2009). Dll4 and Jag1 coordinate to regulate tip and stalk cell formation via spatial control of Notch signaling.

Once the tip and stalk cell identities have been selected by ECs within a vessel, new sprouts extend and form a functional vascular plexus via step-wise tubulogenesis, anastomosis (fusion of tubes) **(Fig. 1.1 C)**. and remodeling. The tip cell leads the sprout toward attractants, and the stalk cells follow behind. While tip cells rarely proliferate, stalk cells drive sprout elongation by proliferation (Gerhardt et al., 2003). Meanwhile, lumen formation is occurred in the extending stalk cells. Lumen formation starts proximally as the vessel maintain continuous lumen from the pre-existing lumen. It has been proposed that lumen formation happens via two distinct mechanisms: intercellularly or intracellularly, resulting in continuous tubule formation. These two processes will be described in the following section.

In addition to sprouting and lumen formation, neighboring sprouts also undergo a process called ‘anastomosis’ to form the growing vascular network **(Fig. 1.1 C)**. Anastomosis is defined as the connection of two tubular structures. Studies have shown that neighboring sprouts express vascular endothelial (VE)-cadherin (VE-cad) at the tip cell filopodia. Two sprouts recognize each other via VE-cadherin interaction and extend junctions between them (Almagro et al., 2010). Recent data has demonstrated that the interaction between two sprouts is facilitated by macrophages (Checchin et al., 2006). When the new connections become stable, the separate lumens in each sprout are connected to be perfused.

Non-sprouting angiogenesis – Angiogenic remodeling

Once the primary vessels are initially formed, they undergo remodeling. This is called ‘angiogenic remodeling’, which is non-sprouting angiogenesis. Compared to sprouting angiogenesis, angiogenic remodeling is poorly understood. One form of angiogenic remodeling is called ‘intussusception’ **(Fig. 1.1 D)**. Intussusception is initiated by proliferation of ECs within a vessel, resulting in enlarged vessel, and then the vessel splits by the formation of intervening ‘pillars’(Burri and Tarek, 1990). Enlargement of these pillars essentially splits a single vessel into two separate vessels. This type of vessel growth has been found predominant in developing lung, kidney, and in tumors. Another form of non-sprouting angiogenesis consists of a ‘reversed’ intussusception, or vessel coalescence (or anastomosis) **(Fig. 1.1 E)**. In this type of remodeling, two capillary loops are merged as they fuse, filling in the space between two pillars, resulting in one enlarged vessel. One example of this process takes place during embryo development when two dorsal aortae fuse to form a single midline mature aorta. The last known mechanism is the ‘intercalated growth of blood vessels’ to increase diameter and length (Folkman and Klagsbrun, 1987) **(Fig. 1.1 F)**. In this process, EC proliferation drives vessel increase in diameter and length. This phenomenon is found in wound healing, and growth of coronary arteries (Bogers et al., 1989).

Vessel regression

After formation of blood vessels, ECs undergo vascular remodeling, patterning, differentiation and maturation to form a well organized, hierarchical vascular network. Vascular remodeling occurs via angiogenesis, including sprouting angiogenesis and angiogenic remodeling as described above, as well as vessel regression. During vessel regression, certain vessel branches are removed by cell death or pruning. Vessel regression by cell death is associated with nuclear condensation, increased intracellular vacuole, lumen narrowing, and cessation of blood flow. During the pruning process, ECs in regressing vessels retract and integrate into adjacent vessels without associated cell death, essentially rearranging their positioning relative to other ECs.

Vessel regression has been reported in a number of tissues of developing vessels, including limb vasculature, ocular capillaries, and neonatal hyaloids and retinal vessels. However, how the vessel is selected for regression remains to be understood. It has been demonstrated that vessel regression is possibly due to intrinsic features, associated with different mechanisms. One example is the regressing hyaloids vasculature which is essential for proper vision. Wnt7b ligand secreting macrophages induces apoptosis of hyaloids ECs during neonatal retinal development (Lobov et al., 2005). Anti-angiogenic factors have been proposed as a regression cues in the developing limb bud. Production of anti-angiogenic molecules in interdigital tissues and prechondrogenic zone of limb have been shown to lead to vessel regression required for shaping of limbs (Feinberg et al., 1986; Latker et al., 1986).

It has also been reported that hemodynamic forces are the major forces for vascular remodeling. Studies of yolk sacs in chick and mouse have demonstrated that blood flow induces vessel enlargement, while vessels with little flow regressed. Chick embryos, in which lack of blood circulation was caused by experimental heart removal, displayed failure in vessel

remodeling (Manner et al., 1995). The exposure of ECs in cell culture to fluid shear stress is known to induce EC behavior changes, and this can influence remodeling, including EC migration and proliferation. Although *In vitro* and *in vivo* studies show that mechanotransduction induces vascular remodeling, the mechanism of action is still unclear and further studies are needed to clarify these events.

1.1.4 Blood vessel development – Vessel maturation

During embryonic development, early vessels that have just formed are immature and incomplete. Without proper maturation, immature vessels undergo rapid change and remodeling. Once these vessels are established, EC starts maturation process. Maturation involves formation of a basement membrane as a result of deposition of ECM, as well as recruitment of mural cells, which are composed of pericytes and SMCs.

ECs synthesize a wide variety of ECM components that together form basement membrane. Basement membranes consist of fibronectin, laminin, collagen, and heparin sulfate proteoglycan. The basement membrane not only provides basal support for blood vessels, but also regulates EC behavior. During embryo development, ECM deposition contributes to establish cell polarity. In the adult, ECM supports ECs by providing stability.

Larger arteries and veins are surrounded by a thick vascular wall, which is composed of pericyte and SMCs. Recruited mural cells promote vessel wall association by angiopoietin1 signaling, and undergo differentiation by Transforming growth factor β-1 (TGFβ1) signaling. TGF-β stimulates mural cell recruitment, proliferation and differentiation. Mice lack of TGF-β signaling lead impaired mural cell development (Pardali et al., 2010). Pericyte recruitment is controlled via platelet-derived growth factor receptor β (PDGFR-β) signaling (Gaengel et al., 2009). PDGFB expressing ECs stimulate PDGFR-β expressing pericyte to migrate and

proliferate. Loss of PDGF-β induction causes pericyte deficiency, resulting in vascular dysfunction. The association between mural cells and ECs lead to vessel wall stabilization. This stabilization is reversible when the vessels need to undergo remodeling or angiogenesis.

1.1.5 Blood vessel Maintenance

Once blood vessel become established and mature, the vessels generally stay quiescent until they are activated. The quiescent vessels need to be actively maintained to sustain their integrity and tissue homeostasis. While new vessel formation has been extensively studied, the maintenance of mature blood vessels has not been studied as extensively. Vessel maintenance, however, recently has attracted more attention, because vascular therapies demonstrated that it is important to prevent vessel regression as well as regulate neovascularization. In addition, cancer therapies to normalize tumor vasculature are emerging as a new approach. The conversion of leaky tumor vessels, which have inefficient perfusion to well-sealed vessels resulted in improved tumor control.

Maintenance of blood vessels is also proposed to be an active process required to control tissue homeostasis. Quiescent ECs play an essential barrier function between blood and surrounding tissues to control exchange of fluids and immune cells. Endothelial barrier function is regulated by endothelial intercellular junctions, which are composed of adherens, tight and gap junctions. One of the well-characterized adhesion protein in ECs is VE-cadherin, an endothelial specific adherens junction component, which regulates EC-EC junctions and connects to the actin cytoskeleton. In resting ECs, VE-cadherin associated junctions are continuously reorganized, hence allowing ECs to be sensitive to extracellular stimuli. EC barrier is also dependent on other adhesion proteins, such as occludins and junctional adhesion molecule (JAM) family. Vessel barrier function in resting ECs is highly regulated by orchestrated

growth factors, junctional molecules and signaling components. Vessel maintenance is one of many fundamental and necessary processes required for stability of mammalian blood vessels.

1.2 TUBULOGENESIS

1.2.1 Introduction to tubulogenesis

Tubulogenesis is defined as formation of a continuous lumen. Tubular organs, such as lung, mammary glands, kidney, pancreas and blood vessel, have critical functions in gas and nutrient transport. While structure and mechanisms of tubule formation of the organs share similarity, each organ has diverse characteristic lumen network and the processes of tubule formation.

Epithelial tubes in lung, mammary glands, kidney, and pancreas are composed of cuboidal or columnar epithelial cells. Luminal membranes, or apical membranes, of epithelial cells are facing the path for gas and fluid. Basal membranes face outer side and facing with mural cells, and basolateral membranes are contacting with another epithelial cells. ECs have similar structures with epithelial cells. EC lumens clearly separates apical and basal membrane. Lumenal surface contacts with streams of blood, gas, and immune cells, and basal membranes face surrounding ECM. The obvious structural difference from epithelial cells is that ECs have narrower basolateral membrane and thinner vascular wall.

1.2.2 Mechanisms of blood vessel tubulogenesis

Models of tubulogenesis

Diverse mechanisms of tubulogenesis have been suggested in different animal models, different vascular beds, and different types of vascular formation, either de novo blood vessel

formation or angiogenesis. Vascular lumen formation has been studied for decades using variety of animal models, such as zebrafish, frog, and mouse. Various mechanisms of vascular formation in different animal models have been suggested. The heterogeneity of vessels mirrors the difference in cellular mechanisms for lumen formation. For example, while zebrafish intersomitic vessels have been suggested to form by intracellular vacuole fusion(Kamei et al., 2006), the cardinal vein of zebrafish is formed from cells that sprout off the ventral aspect of the dorsal aorta that arrange around central lumen (Herbert et al., 2009). In addition, the difference in the process of vasculogenesis and angiogenesis inherently yields different cellular mechanisms in tubule formation. During *de novo* vessel formation, as shown in the mouse dorsal aorta, ECs form a cavity between the cells by what is referred to as “cord hollowing”. This occurs when cells rearrange junctions between them and open a lumen extracellularly. In angiogenesis, an existing lumen is extended by budding of ECs from established vessels into new sprouting vessels. As genetic modification using mouse models is widely available for research and advances have been made in 3D imaging, time lapse imaging *in vitro* culture and *in vivo*, these techniques accelerated the study of vascular lumen formation, allowing us to better understand the mechanisms of vascular tubulogenesis.

Zebrafish intracellular lumen formation (cell hollowing, vacuole fusion)

In zebrafish intersomitic vessel (ISV), lumen formation via intercellular vesicle fusion was proposed (Kamei et al., 2006) **(Fig.1.2)**. Vacuole fusion as a mechanism for lumen formation was originally and primarily studied using *in vitro* 3D EC culture.(Bayless and Davis, 2002; Davis and Camarillo, 1996). In a single EC, vesicles are formed by pinocytosis from basal membrane and progressively fuse into vacuoles to form cavity in the cytoplasm. To show the vacuole fusion *in vivo*, Kamei et al. used GFP-Cdc42 labeled vacuoles in zebrafish ISVs. Vacuoles arose in individual ECs of ISVs through endocytosis, forming intracellular space. The continuous lumen formation happens by fusion of these intracellular vacuoles between adjacent

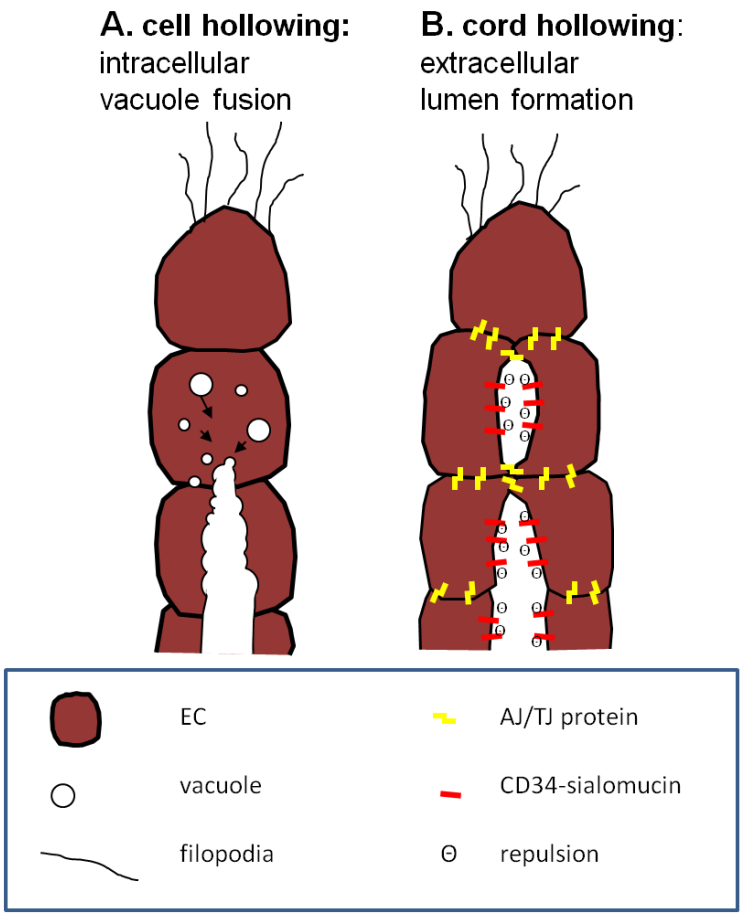

Figure 1.2 Models of lumen formation (A) Cell hollowing. Intracellular vacuoles coalesce and connect neighboring ECs to form tubules. **(B)** Cord hollowing. Extracellular lumens are formed by apical membrane repulsion. Negative charged CD34-sialomucins induce membrane repulsion and junctional proteins are removed from the lumenal membrane to open lumens.

ECs. Intravascular dye injection into the circulatory system of fish embryos, followed by live imaging, showed that ISV lumen was formed by vacuole assembly which ultimately resulted in a single tubule structure.

Zebrafish intercellular lumen formation in ISV

By contrast, it was more recently proposed that zebrafish ISVs are actually formed by intercellular vacuole fusion (Blum et al., 2008). Investigation of EC architecture in ISVs revealed that ECs are arranged in an overlapping manner, not in linear head-to-head order. This was observed with markers for adherens junctions, including VE-cadherin, and tight junctions ZO-1, which displayed overlapping ECs in ISVs. GFP- or mCherrry-expressing mosaic ECs revealed clear view of details of cell architecture in ISVs and argued against intracellular lumen formation. In addition, sections of ISVs showed lumenal space between ECs during ISV development. This work has been interpreted to mean that normally, ISV vacuoles fuse with extracellular space between ECs, not intracellularly. Together, these experiments demonstrate our evolving understanding of lumen formation, in one specialized endothelial structure. The expectation in the field is that, most likely, there will exist a number of mechanisms in different vascular beds that will be very different from one another.

Vasculogenic tubulogenesis in mouse dorsal aorta (cord hollowing)

Extracellular lumen formation as a basic mechanism has also supported by a study of vasculogenesis during mouse dorsal aortae formation (Strilic et al., 2009). During vasculogenesis, ECs undergo three processes; (1) apicobasal polarity formation, (2) junctional protein rearrangement, (3) EC cell shape change. EC precursors aggregate to form a cord. At this stage, two or three ECs are often found in mouse dorsal aortae within a single transverse section, demonstrating that the width of the cord is only a few cells wide (Strilic et al., 2009). Once the ECs aggregate and contact each other, they start to establish polarity to create an

apical side where a lumen will open. In ECs, CD34-sialomucin glycoproteins line the apical membrane and contribute to cell-cell repulsion of luminal membranes, thereby initiating lumen opening (Strilic et al., 2010) **(Fig.1.3)**. While CD34-sialomucins are accumulated in the cell-cell contact at the initiation of lumen formation stage, junctional proteins are removed from luminal side for detachment of lumenal membranes. At this point, it is unclear how this occurs, whether through endocytosis or movement of junctions to periphery of cord. Lastly, cell shape becomes altered, allowing flattening and bending of ECs, making a luminal space in the cord center. These shape changes have been proposed by our lab and that of others to occur via regulation of actomyosin contractility.

1.2.3 Molecules involved in tubulogenesis

Apical CD34-sialomucins

CD34-sialomucin family members have been shown to be preferentially expressed at the apical cell surface of lumen forming cells, and to contribute to de-adhesion of apical membranes in epithelial cells and ECs (Bryant et al., 2010; Ferrari et al., 2008; Martin-Belmonte et al., 2007; Strilic et al., 2009). In cultured epithelial cells, CD34 and PODXL, members of CD34-sialomucin family, are transferred to apical membrane by exocytosis and initiate lumen formation. A recent study in developing mouse aorta showed that CD34 and PODXL started to accumulate between cell-cell contacts of EC cords prior to lumen formation (Strilic et al., 2009). At the onset of lumen formation, negatively charged sialomucins generate repelling electrostatic fields that contribute to separation of EC lumenal membrane (Strilic et al., 2010). When negatively charged mucins are removed or neutralized, EC lumen formation was disrupted in whole mouse embryo culture. Strilic and colleagues also found that VE-cadherin deficient mutant mice failed to buildup CD34 and PODXL accumulation at EC-EC apical contacts, resulting in failure to separate EC

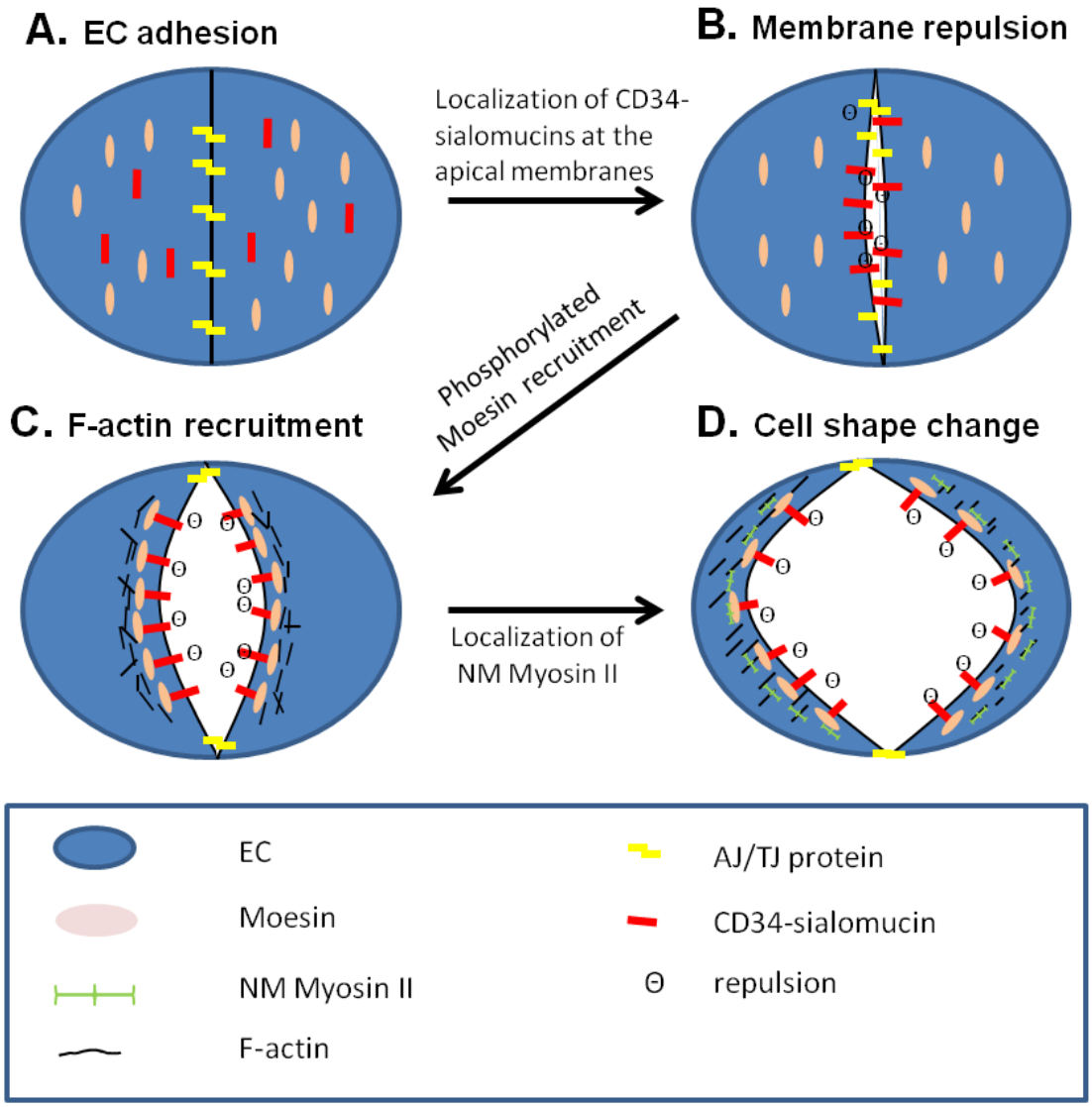

Figure 1.3 Molecular mechanism of lumen formation in developing mouse aortae. (A) ECs adhere to each other via junctions. **(B)** VE-cadherin is required for CD34-sialomucin localization to the apical membranes. **(C)** Phosphorylated Moesins and F-actins are recruited to the opening EC lumens. **(D)** VEGF-A is required for recruiting pMLC and NM Myosin II to EC apical membrane to form lumen completely and induce EC shape chnages.

membranes and to form proper lumens (Strilic et al., 2009). Apical membrane repulsion by sialomucin is thus a key step of lumen initiation to generate slits which later enlarge into functional lumens.

EC junctional molecules

In the network of blood vessels, ECs adhere via adherens junctions (AJs) and tight junctions (TJs). During vascular lumen formation, ECs undergo dynamic changes via proliferation, migration, and interaction with other ECs and ECM components, and proper regulation of adhesion and de-adhesion is required. Therefore, spatio-temporal regulation of cell junction guides vascular lumen formation. The major components of AJs are cadherin families. In ECs, VE-cadherin is one of the most well characterized adhesion molecules. VE-cadherin promotes homophilic transmembrane adhesion between ECs. VE-cadherin does not seem to be a critical protein for EC adhesion as VE-cadherin deficient mice maintain EC-EC contacts and form EC cords (Carmeliet et al., 1999). However, absence of VE-cadherin in mice leads embryonic lethality due to impaired vessel remodeling and maturation. Recent study also has shown that a number of VE-cadherin deficient embryos failed to form polarized ECs in some vessels, inhibiting proper lumen formation (Strilic et al., 2009). This indicates that VE-cadherin is also involved in polarity establishment, as well as junctional regulation.

ECM components

During vessel formations, ECs are in close contact with ECM, as well as neighboring ECs, and thus proper regulation of these contacts between ECs and its surrounding environments is important for vascular development. ECM, around most developing blood vessels, is composed of diverse proteins, including laminins, collagens, and fibronectins. One well-characterized ECM proteins known to be important for EC-ECM adhesion is fibronectin. Genetic fibronectin deficiency in mouse ECs blocked EC attachment to surrounding

mesenchyme, inhibited yolk sac vessel remodeling, and caused defects in lumen formation in the endocardium, suggesting that EC-ECM adhesion is required during vascular lumen formation (George et al., 1997; George et al., 1993).

Integrins

Important ECM adhesion proteins expressed in ECs are the integrin receptors. Integrins form heterodimeric complexes which are composed of alpha and beta subunits. Among many integrins, β1 has been reported to play important roles in EC lumen formation. In one line of experiments, an antibody, which blocks β1 integrin from binding its ligands, was injected into chick embryos, resulting in complete failure of lumen formation in the trunk dorsal aorta primordial cords (Drake et al., 1992a; Drake et al., 1992b). β1 integrin deficient mouse ECs, following ablation of using VE-cadherin-Cre^{ER} displayed defective localization of Par3 and apical vesicle transport, resulting in altered EC cell shape (ECs remained cuboidal) and blockade of lumen formation in skin arterioles (Zovein et al., 2010).

Cdc42 and the Par6/Par3/atypical PKC complex

A key family of molecules that directs fundamental cellular processes in ECs are the small Rho GTPases. In particular, Cdc42 and Rac1 have been shown to play critical roles during lumen formation, as well as in vacuole formation. When dominant negative Cdc42 was expressed in cultured HUVECs in 3D collagen matrices, vacuole formation was completely inhibited and lumen formation was blocked (Bayless and Davis, 2002; Koh et al., 2008). Cdc42 is targeted in vacuolar membranes in ECs, and regulates a cascade of downstream effectors, Pak2, Pak4, Par3 and Par6 for lumen formation (Sacharidou et al., 2010). Par3 and Par6 establish EC polarity by associating with Cdc42 and atypical PKC. Disruption of membranes of the Cdc42-Par3-Par6-PKC polarity complex inhibits lumen formation in 3D cultured ECs,

demonstrating the critical importance of GTPases, as well as basic mechanisms affecting cell polarity.

RhoA

RhoA is another GTPase, which has been linked to EC lumen formation. In cultured ECs, siRNA to RhoA has no lumen blocking effects. However, constitutively active RhoA completely blocks lumen formation in *vitro* (Bayless and Davis, 2004). RhoA was also suggested to be involved in developing vessels in mouse embryos and to be downstream of VEGF signaling (Strilic et al., 2009). Importantly, RhoA is known to activate Rho-associated protein kinase (ROCK), which in turn phosphorylates Myosin Light Chain (MLC) to activate actomyosin contractility. This Rho-ROCK activation of MLC recruits non-muscle myosin IIA (NMHCIIA) into an active Myosin II complex, which binds to the cytoskeleton and impacts internal contractility. It has been proposed that myosin II is active at the EC apical membrane, inducing cell shape change that are required for vascular lumen opening. By contrast, our lab has suggested that RhoA activity needs to be down regulated during the lumen formation, otherwise ECs remain rounded. Discoveries outlined below suggest that during lumen opening, NMHCIIA mediated cell contractility needs to be suppressed to flatten ECs via the GTPase associated molecule Rasip1 (Xu et al., 2011). Overall, the role of RhoA during endothelial lumen formation has been controversial, with some groups suggesting it is necessary, and other suggesting it must be suppressed. It is very likely that both hold true and that there are distinct temporal requirements during blood vessel lumen formation.

1.3 RASIP1

1.3.1 Introduction to Rasip1

Rasip1 identification

Rasip1 was first identified as a novel Ras GTPase interacting protein (Mitin et al., 2004). Similar to other Ras GTPase effectors, such as RalGDP and AF-6, Rasip1 possesses a Ras-associating (RA) domain, which binds to other members of the Ras GTPase family. In yeast two hybrid assays, the Ras domain of Rasip1 interacted with R-Ras, H-Ras, and Rap1A, suggesting Rasip1 may play a diverse function by interacting with different effectors. In addition, Rasip1 contains a proline rich domain, a fork-head associating (FHA) domain, and a dilute domain, however their functions have not yet been identified (Mitin et al., 2004; Xu et al., 2011). Thus, further understanding the function of Rasip1 and its domains can aid us to identify the mechanisms by which Rasip1 acts as a multifunctional GTPase effector.

EC specific protein

Rasip1 is an endothelial specific protein. It was first reported that endogenous Rasip1 was expressed in ECs, human umbilical vein endothelial cells (HUVECs) and bovine pulmonary artery endothelial (BPAE) cells (Mitin et al., 2006). Later, our lab showed that Rasip1 was exclusively expressed in all embryonic ECs during development (Xu et al., 2009). In a transcriptional gene micro array using mouse embryonic aortal ECs, Rasip1 was found to be exclusively expressed in EC and not other types of cells, and this was confirmed by *in situ hybridization* using zebrafish, frog and mouse embryos (Xu et al., 2009; Xu et al., 2011). Rasip1 is expressed in angioblasts prior to vessel formation, and throughout vascular development. To date, our lab and my work has demonstrated that Rasip1 is one of the most critical GTPase effectors found to be important for vascular development and maintenance.

1.3.2 Rasip1 as a GTPase regulator

GTPase proteins – molecular switches

GTP-binding proteins are highly conserved protein in diverse organisms, and consist of more than 100 members (Takai et al., 2001) The superfamily is classified into at least five families, including Ras, Rho, Rab, Arf, and Ran families. They act as a molecular switch as they have two interconvertible forms; GTP-bound active forms and GDP-bound inactive forms. Many upstream effectors have been identified as GTPase binding proteins to exchange between GTP and GDP-bound status, (either guanine nucleotide exchange factors, or GEFS, or GTPase-activating proteins, or GAPs), and thus control downstream events, which involve a wide variety of cell functions.

Rasip1 as a Ras effector

Rasip1 interacts with a variety of members of the Ras GTPase family members (Mitin et al., 2004). Rasip1 was first identified as an H-Ras interacting protein by a yeast two hybrid screen. Because Rasip1 possesses an RA domain, which is a characteristic domain of Ras binding in Ras effectors, Mitin and colleagues examined whether the RA domain was essential for GTPase binding. Deletion of the RA domain inhibited Ras binding, and a yeast two hybrid assay with RA domain variants showed changes in RA residues alter binding specificity, indicating that the RA domain is responsible for Ras binding. The RA domain of Rasip1 was also assessed to ask whether it is preferentially bound to the active form of Ras. When Ras was loaded with GDP or non-hydrolyzable GTP analog, the RA domain showed higher affinity for the active form of Ras rather than the inactive form in yeast two hybrid and pull down assays. In addition, in cultured cells, Rasip1 was highly co-localized with the constitutively active form of Ras at the perinuclear region, and showed no overlap with the dominant negative form of Ras. This suggests that Rasip1 is recruited by active Ras and may function at the juxta-golgi region.

Rasip1 as a RhoA modulator

Our group has proposed that Rasip1 acts as an endothelial specific modulator of Rho GTPase signaling, which in turn regulates multiple cellular parameters such as cell adhesion, polarization and cytoskeletal reorganization. Although Rasip1 does not directly interact with RhoA GTPase, we have shown that it regulates Rho signaling via interacting with Arhgap29, a Rho activating protein. This finding was recently supported by studies by another group (Post et al., 2013). Arhgap29 is a GTPase activating domain containing protein (GAP), which was shown to bind to and inactivate RhoA. The interaction between Rasip1 and Arhgap29 was identified by affinity purification and mass spectrometry, as well as and co-localization in the cytoplasm of ECs. (Xu et al., 2011). In the absence of either Rasip1 or Arhgap29, RhoA activation was upregulated, indicating that Rasip1 and Arhgap29 act together as RhoA suppressors, or alternatively, Rasip1 recruits Arhgap29 to suppress RhoA locally in vicinity to Myosin II. This resulted in increased RhoA downstream signaling, including ROCK, and pMLC, and thus activation of nonmuscle myosin IIA. Depletion of either Rasip1 or Ahrap29 in cultured ECs altered endothelial cytoskeleton contractility, and ultimately blocked *in vitro* lumen formation of ECs in 3D lumen formation assay in collagen matrices (Xu et al., 2011).

Raisip1 as a Rap1 effector

Recently, it has been reported that Rasip1 is also a Rap1 effector, which has been shown to control cell adhesion (Post et al., 2013; Retta et al., 2006; Takai et al., 2001). Rasip1 was first noted for binging to active Rap1 GTPase by a *in vitro* yeast two hybrid assay (Mitin et al., 2004), and the interaction was confirmed by *in vivo* Forster resonance energy transfer (FRET) analysis (Post et al., 2013). As a downstream effector of Rap1, Rasip1 was shown to be involved in cell spreading and endothelial barrier function (Post et al., 2013). In cell spreading assays, Rap1 activation by cAMP analog treatment or by overexpressing the active form of

Rap1 mutant increases the area of cell adhesion contact. However, siRNA mediated Rasip1 depletion blocked induced cell spreading, indicating that Rasip1 is a downstream protein of Rap1 signaling. In ECs, Rap1 activation induced Rasip1 and Arhgap29 interaction, and subsequently RhoA was suppressed by Arhgap29. This resulted in reduction of actomyosin induced tension, and increased cell spreading and endothelial barrier function (Post et al., 2013; Wilson et al., 2013). These results suggest that Rap1 is required for Rasip1 and Arhgap29 function which lead to cell adhesion and cytoskeletal alteration in ECs.

Rasip1 as a Cdc24/Rac1regultor

Interestingly, Rasip1 has a strong activation effect on Cdc42 and Rac1. As previously mentioned, Other members of RhoA GTPase family, namely Cdc42 and Rac1, were reported as essential GTPases for lumen formation (Bayless and Davis, 2002). Cdc42 and Rac1 are required for vacuole formation in 3D matrix assay, and ultimately lumen formation. In Rasip1 depleted ECs in 3D matrices, both activated Cdc42 and Rac1 GTPase levels were significantly decreased. In addition, the downstream signaling of Cdc42 and Rac1 were impaired in the absence of Rasip1. These results suggest that Rasip1 acts upstream of Cdc42 and Rac1, and is possibly involved in vacuole fusion in ECs to form endothelial lumens. However the precise mechanism by which coordination of the activity of different GTPases has not yet been discovered. Further study will help us to solidify our hypothesis that Rasip1 is an EC specific multifunctional GTPase modulator.

1.3.3 Tubulogenesis regulation by Rasip1

Rasip1 is required for vasculogenesis –in vitro and in vivo

Our lab has shown that Rasip1 is required for tubulogenesis during murine development (Xu et al., 2011). Rasip1$^{-/-}$ embryos displayed failure of blood vessel lumen formation in the dorsal aortae, the first functional blood vessels in the developing embryo, as well as throughout all tissues including the yolk sac. Rasip1 deficient mouse embryos displayed normal cord assembly, a process in which angioblasts align along the embryonic midline prior to aortae lumenization. However, after cord formation, the dorsal aortae remained lumenless. In addition, the endocardium and yolk sac vessel had discontinuous patent lumens. Due to the failure in continuous lumen formation, Rasip1 null embryo displayed severe lethality at early developmental stage. The function of Rasip1 in vasculogenesis was also tested in an *in vitro* HUVEC 3D matrix assay. In this established collagen matrix assay, cultured HUVECs ultimately develop lumens. When Rasip1 was depleted by siRNA, lumen formation was significantly decreased. When compared to control non-targeting siRNA. The Rasip1 deficient cells were able to make contacts, but they appeared unstable and would break, failing to keep viable lumens.

Rasip1 is involved in apicobasal polarity establishment

During vascular tubulogenesis, we have found that Rasip1 regulates multiple cellular processes. At the onset of lumen formation, we showed that Rasip1 contributes to the establishment of apicobasal polarity, which is a key process to determine apicobasal surfaces. Cell polarity defects in Rasip1 null ECs in mutant embryos were demonstrated by mislocalized Par3. Par3, a member of the aPKC polarity complex, was localized normally to the apical membranes of EC cords prior to lumen opening. As lumens opened, it became segregated to the lumen periphery, clearing from the apical surface. However, in the absence of Rasip1, Par3 failed to segregate from EC junctions during tubulogenesis and remained aberrantly at the apical surface. Interestingly, other than Par3, most of the apical proteins, such as CD34, PODXL, Moesin, and F-actin, were found normally localized to the apical membrane in the

Rasip1 null cord EC. Together, these observations suggested that Rasip1 was either required specifically for junctional restriction of Par3 localization, or it was required for partial establishment of cell polarity.

Rasip1 regulates adhesion protein rearrangement –EC-EC adhesion

In addition to defective apicobasal polarity, a number of junctional proteins were ectopically localized in Rasip1 null ECs. In wild-type cord EC-EC borders, after polarity establishment, both adherens junction and tight junction proteins are normally removed from the center of the cords to allow apical membrane segregation. In *Rasip1*$^{-/-}$ embryos, by contrast, ZO-1 was localized in clustered regions between ECs at the center of cord, similar to the pattern observed with Par3. In fact, *Rasip1*$^{-/-}$ ECs displayed improper localization of many tight junctions, including ZO-1 and Claudin5, as well as adherens junction, markers such as VE-cadherin, found inappropriately at the center of the cord. These junctional proteins stitch the apical membranes together and block the necessary loosening of junctions required for lumen formation. Relatively normal localization of apical proteins combined with failed segregation of apical membranes, together cause gaps between ECs, resulting in slit-like structures. However the gaps are not sufficient to form continuous and patent blood vessels, which are required for blood flow. Therefore, absence of Rasip1 causes overall failure of blood vessel patency and a block in circulation.

Rasip1 regulates EC-ECM adhesion

While the adhesion molecules ZO-1, VE-cadherin, and Claudin5 are expressed ectopically in Rasip1 deficient ECs, those same ECs displayed reduced adhesion to the surrounding ECM. ECs treated with siRasip1 showed reduced adhesion to a variety of ECMs, including collagen I, collagen IV, fibronectin. Interestingly, our lab has suggested that Rasip1 plays a role in maturation of adhesion contacts between ECs and ECM. Normally, EC-ECM

adhesion points are called focal adhesions (FAs) and they have been shown to transition between an immature, weaker state called 'focal contacts', to a much stronger state called 'fibrillar adhesions'. These different levels of maturity and strength are reflected by changes in the molecular composition of those adhesion points, where focal contacts exhibit phosphorylated paxillin (pPax) and fibrillar adhesions exhibit activated integrins. In the absence of Rasip1, focal adhesions appeared immature as pPax levels were increased, while activated β1 integrins were suppressed. Using 3D *in vitro* lumen formation assay, Rasip1 null cells temporarily adhere to the matrix but subsequently decrease contact with the matrix, retract and collapse. This is because Rasip1 depleted cells failed to develop mature focal adhesions. *Rasip1*$^{-/-}$ embryos similarly displayed weak associations between EC and ECM contacts. In wild-type embryos, ECs are tightly associated with the ECM via Fibronectin, Collagen IV, and laminin. Between the 4-6 somite stage in Rasip1 mutants, ECs failed to adhere to the surrounding mesoderm, while they remained attached to the endoderm. Together, ectopic cell-cell adhesions, as well as reduced cell-ECM contacts, resulted in failed formation of continuous lumens.

Rasip1 regulates cell contractility via RhoA inactivation

We have proposed that a key role of Rasip1 is to regulate cell contractility via interaction with Arhgap29. Arhgap29, a GTPase activating protein, suppresses RhoA activity in ECs. Findings by other groups have shown that RhoA is suppressed in EC tube formation (Bayless and Davis, 2004). Inappropriately activated RhoA causes ECs to acquire a rounded shape, as opposed to their usual flattened and elongated shape, resulting in failure of lumen formation. We propose that a cornerstone of molecular support of lumen formation is RhoA modulation, via Rasip1 and Arhgap29 regulation of the actomyosin complex. In either Rasip1 or Arhgpa29 depleted ECs, activated RhoA increased pMYPT, and pMLC, and consequently myosin IIA

activity. This indicated that Rasip1 and Arhgap29 act in concert to suppress RhoA, which results in suppression of ROCK/MLC/myosin IIA to regulate cell cytoskeleton during lumen formation.

Together, our work has shown that Rasip1 is an essential coordinator for multiple GTPase signaling during EC lumen formation. In addition, Rasip1 plays an endothelial specific roles in diverse cellular events, including cell polarity formation, cell adhesion, and cell contractility. Despite what we already know about Rasip1, precise cellular and molecular mechanisms involved in opening lumen remain to be answered. Although interaction between Rasip1 and Ras GTPases has initially identified, an EC-specific function of Rasip1 associated with Ras GTPase has not been examined. In addition, as Rasip1 is also expressed in postnatal and adult established and mature vessels, begging the question as to what its role is there. Further study of Rasip1 in vessel maintenance and angiogenesis during normal or pathological conditions is needed. Understanding Rasip1 in the context of other molecules known to be critical for blood vessel formation may yield insights into molecules that could be targeted to manipulate vessel lumen formation.

1.4 FINAL REMARKS

This introductory chapter aimed to cover our current understanding of the cellular events and the wide variety of molecules required of blood vessel development. The subjects reviewed cover only a fraction of what is known in the field of vascular development, but provides sufficient background knowledge to understand my work, which present in subsequent chapters. The work in this thesis will present my findings and contributions to a number of studies, including stepwise arteriovenous specification in developing embryo (Chapter 2), the function of Rasip1 in tubulogenesis during vasculogenesis and angiogenesis (Chapter 3) and the study of Arhgap29 as a critical regulator of placenta and cardiovascular development (Chapter 4). I hope

that the work presented in this thesis contributes to a better understanding of blood vessel development and improvement of clinical therapeutic development to treat vascular diseases.

CHAPTER 2: STEPWISE ARTERIOVEOUS FATE ACQUISITION

DURING BLOOD VESSEL DEVELOPMENT

NB: This chapter has been previously published under the title: "Stepwise arteriovenous fate acquisition during mammalian vasculogenesis" Dev Dyn. 2011Sep;140 (9):2153-65 The text has been slightly altered to suit the purpose of this dissertation.

2.1 INTRODUCTION

The cardiovascular system is the first functional organ formed in vertebrates. The ECs are the fundamental building blocks of the network of blood vessels. During blood vessel formation and maturation, ECs undergo arteriovenous (AV) differentiation, and eventually form a complex, interconnected network composed of two different types of blood vessels; artery and vein. Although arterial and venous differentiation is a critical process for formation of blood vessel network, little is known regarding arteriovenous specification in during early vascular development.

To study AV differentiation, it is essential to understand basic embryonic blood vessel anatomy. Vascular anatomy in developing embryos has been extensively studied in avian and fish model systems. Studies of quail embryos have been accelerated by QH1 antibody recognizing vasculature to analyze blood vessel anatomy (Coffin and Poole, 1988). In chick, the study of the formation and patterning of the first vessels, the dorsal aortae, has recently been established (Reese et al., 2004). In zebrafish, vasculature anatomy has been described in details due to embryonic transparency and vascular reporters such as Fli1-GFP (Isogai et al., 2001; Lawson and Weinstein, 2002). While vascular development in mouse embryo has been

studied for decades (Coffin et al., 1991), spatiotemporal analysis of embryonic blood vessels has only been recently provided (Walls et al., 2008).

Recent studies using chick, quail and zebrafish have revealed the underlying mechanisms that modulate AV differentiation. There are two distinct ideas arising from these studies. 1) Angioblasts are predetermined for artery or vein fate prior to blood vessel formation. 2) AV identity is plastic and is determined by cues in its environment, such as hemodynamic flow. A study supporting the first idea was performed in chick embryo. Yolk sac blood island ECs were shown to express AV markers before blood vessel plexus formation (Herzog et al., 2005). Another study performed with zebrafish demonstrated that angioblasts are restricted to one of the artery or vein fate, and this decision is guided by Notch pathway (Lawson et al., 2002; Zhong et al., 2001). Other studies have encouraged the other idea. Angioblasts in chick embryo are highly plastic for arterial-venous determination as ECs achieve their cell fate after the onset of blood flow (le Noble et al., 2004). These studies suggested that AV fate is partially determined in EC precursors, and it is also plastic and influenced by hemodynamic flow.

In this chapter, I show that mouse embryonic vessels differentiate and establish arterial or venous fate in a step-wise manner during blood vessel development. The dorsal aortae, the first intraembryonic vessels initiate arterial specification before complete circulation occurs, while other vessels remain undifferentiated. These first vessels gradually express a subset of arterial genes. By contrast, the first veins establish their fate later than the first arteries. The arteriovenous specification does not require hemodynamic flow, but the flow affects maintenance of select arterial genes. Together, the data presented here provides a subset of arterial and venous markers during early blood vessel development, and demonstrates that arteriovenous fate is progressively acquired.

2.2 RESULTS

2.2.1 Stepwise formation of major vessels

To characterize the anatomy of the embryonic blood vessels, arteries and veins, I used *Flk1-LacZ* mouse line to allow visualize ECs (Shalaby et al., 1995). Flk1 (VEGFR2) is a tyrosine kinase receptor for VEGFA and is expressed in all ECs (Yamaguchi et al., 1993). This mouse was used to visualize angioblasts from their initial aggregation into the primary vascular plexus, and to their subsequent remodeling and patterning. Here, I focused on analyzing intraembryonic vessels that were identified based on their relative anatomical locations and morphology.

Formation of the first artery – dorsal aortae

During mouse vascular development, angioblasts emerge first in the extraembryonic yolk sac. At 0 somite stage (0s), or embryonic day 7.75 (E7.75), scattered angioblasts were detected in the extraembryonic yolk sac, but not within the embryo proper **(Fig. 2.1 A)**. Hours later, at 1s, two parallel tracts of angioblasts are distinguishable in the embryo, which are dorsal aortae primordium. Another noticeable feature is a crescent of angioblasts along the developing anterior intestinal portal (AIP) termed the 'cardiac crescent' **(Fig. 2.1 B,C)**. These angioblasts at the cardiac crescent (CC) are precursors of the endocardium, or heart ECs. At 2s, pre-aortic angioblasts become more cohesive cords, which did not form appreciable internal lumens at this stage **(inset, Fig. 2.1 D)**. By 5s, aortic cords form the first patent embryonic vessels, the dorsal aortae, which displayed expanded and continuous lumens **(inset, Fig. 2.1 E,F)**.

Embryo turning

By 8s, cardiac crescent angioblasts undergo morphological changes to form the primitive heart tube and the associated sinus venosus, which is the inflow tract for blood **(Fig. 2.1 G)**. The dorsal aortae remained two paired vascular tubes, which extended anteriorly into the cranial

mesoderm and posteriorly to the tail and allantois. At 9s, the embryo initiated turning **(Fig. 2.1 H,I)**. Before this turning, the embryo was cup shaped with its ventral side facing outside. During this embryonic morphogenetic transformation, the embryo turned towards its right, as the AIP and caudal intestinal portal (CIP) began to constrict towards the future umbilical cord **(Fig. 2.1 K-L)**. By this process, the embryo changes its posture allowing its abdominal side to contract.

Formation of vitelline vein

Interestingly, the veins appeared shortly after aortae formation. Just posterior and lateral to the cardiac crescent, two short tracts of angioblasts appear along the yolk sac-embryo interface at the future location of the sinus venosus and anterior vitelline veins **(Fig. 2.1 E,F)**. While the dorsal aortae form complete patent tubes extended from the heart to the allantois, the vitelline veins are comprised of blind-ended vessels. At this early embryonic stage, these partial vessels were the first and only distinguishable veins. The progressive extension of the vitelline vein primordium was observed at the onset of turning. Pre-vitelline angioblasts aligned at positions ventrolateral to the dorsal aortae at 2-8s **(Fig. 2.1 D,E,G,H, blue arrowheads).** Scattered angioblasts appeared to be recruited into the forming vessels, posterior to the sinus venosus and at the border of the embryonic and yolk sac tissues **(Fig. 2.2 A-C)**. Between 6-10s, the ventral view of embryo showed extending vitelline vein from the sinus venosus to the caudal allantois. After turning, at 13s, the vitelline vein appeared as more cohesive and established vessel **(Fig. 2.1 K, Fig. 2.2 D-F)**.

Formation of cardinal vein

Prior to turning, a wide flat endothelial tube was observed lateral to the sinus venosus, at the expected position of the common cardinal vein, at 8s **(Fig. 2.2 B,C)**. Following turning, angioblast cords were distinguished and positioned laterally along each flank of the embryo **(Fig.**

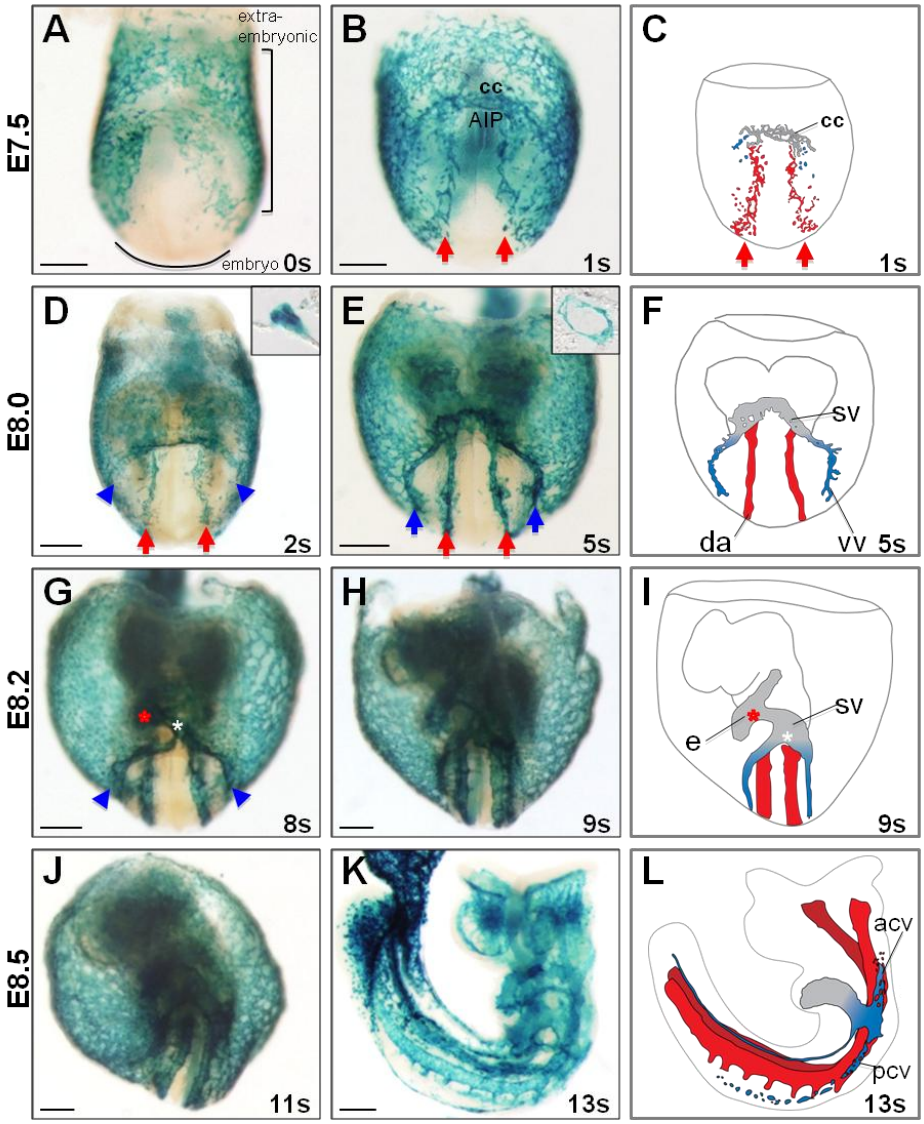

Figure 2.1. Progressive formation of first embryonic vessels: dorsal aortae and vitelline vein primoria. β-galactosidase staining of *Flk1-LacZ* embryos from E7.5-E8.5 and cartoon schematics representing major arteries and veins during vasculogenesis. **(A)** *Flk1* expression at 0s is restricted to vessels of the extraembryonic tissues or yolk sac. **(B,C)** At 1s, angioblasts began to align and coalesce into the paired dorsal aortae (red arrows), as well as the cardiac crescent. **(D)** At 2s, the dorsal aortae form cords that lack a lumen (inset). **(E,F)** At 5s, the paired aortae are lumenized (inset) and the vitelline veins (blue arrows) have begun to coalesce posterior to the cardiac crescent and sinus venosus. At this stage, the heart begins to beat weakly. **(G)** By 8s, the primitive heart tube, or endocardium (red asterisk), and sinus venosus (white asterisk) have formed. **(H,I)** At 9s, the embryo is initiating turning and the paired aortae are in closer proximity. Vitelline vein cords extending from sinus venosus are longer. **(J-L)** After the embryo completes turning, vitelline vein cords extend to the tail, while the anterior and posterior cardinal veins begin to appear. Acv, anterior cardinal vein; aip, anterior intestinal portal; cc, cardiac crescent; da, dorsal aortae; e, endocardium; pcv, posterior cardinal vein; sv, sinus venosus; vv, vitelline vein. Scale bars = 200μm

2.1 K,L). Interestingly, unlike the aortae, the cardinal vein never transitioned through a cord phase, but instead initially presented as a loose plexus, appearing to arise from the coalescence of scattered angioblasts. At 14s, a loose but narrow plexus extended anteriorly from this vessel into the head **(Fig. 2.2 D)**, and by 16s, the posterior cardinal vein appeared to extend from the common cardinal vein towards the tail **(Fid. 2.2 E)**. By 20s, both the anterior and posterior cardinal veins were distinguishable established vessels, running the length of the anteroposterior axis, albeit extensively interconnected to the flank vascular plexus **(Fig. 2.2 F)**. This spatio-temporal analysis of initial blood vessel formation demonstrates a step-wise anatomical emergence of arteries and veins, where the aortae form first, then the vitelline veins, and finally the cardinal veins.

2.2.2 Stepwise expression of arterial genes and venous genes

To investigate AV differentiation in the early vascular development, we performed β-galactosidase staining or in situ hybridization to assess expression of known AV markers (Eichmann et al., 2005; Rocha and Adams, 2009) in E8.0-9.5 embryos. Comparison of early vessel formation to AV marker expression with the anatomical observations will demonstrate whether the fate of angioblasts is specified before they aggregate into vessels.

Expression of arterial marker at E8.0

We first examined the expression of the arterial markers *EphrinB2*, *Cx40*, *Cx37*, *Hey1*, *Hey2*, *Nrp1*, *Notch1*, *Notch4*, *Dll4* and *Jag1* during emergence of angioblasts at E8,0 (4-5s). Surprisingly, ECs of the paired dorsal aortae at this stage lacked most of standard arterial markers assayed, including *Ephrin B2*, *Cx40*, *Hey2*, *Nrp1*, *Notch1*, *Notch4,* or *Jag1* **(Fig. 2.3 A,B,E,F,G,H,J)**. Only weak *Cx37*, *Hey1*, and robust *Dll4* were detected in the forming dorsal aortae **(Fig. 2.3 C,D,I)**. It is interesting that although the dorsal aortae were clearly patent

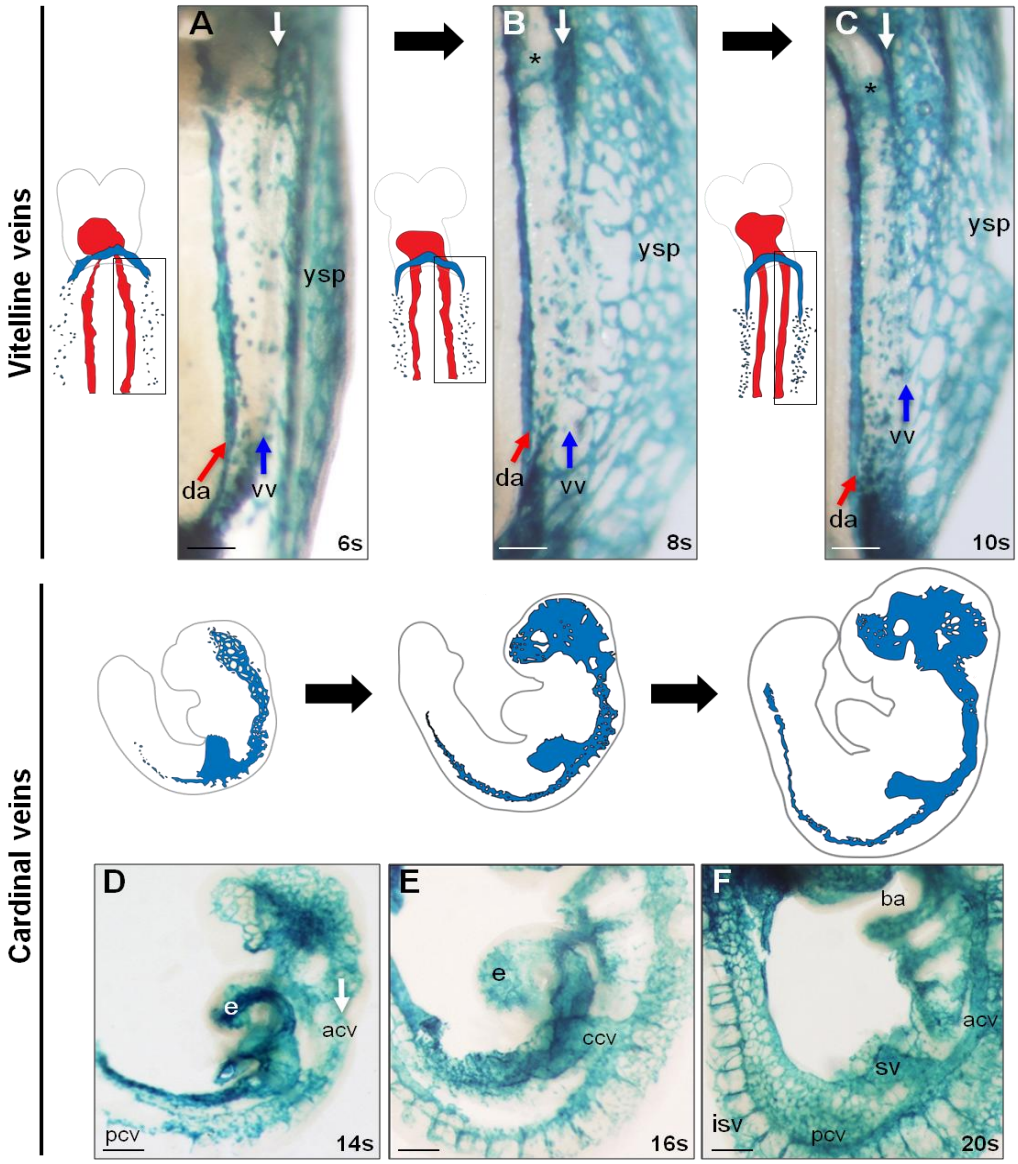

Figure 2.2. Vitelline and cardinal vein formation follows that of the dorsal aortae. β-galactosidase staining of *Flk1-LacZ* embryos, at stages indicated. Schematics depict major vessels. Arteries, red; veins, blue. **(A-C)** The vitelline veins form lateral to the dorsal aorta and along the edge of the yolk sac plexus. At 6s, there are a few scattered angioblasts posterior to the vitelline "blind-ended" vessels (white arrow). However, by 10s more angioblasts have emerged and the vitelline vein has formed more posteriorly (blue arrow), thus lengthening. **(D-F)** Following turning, the anterior and posterior cardinal veins can be seen beginning to form as loose, lateral plexus-like vessels, connected to the sinus venosus via the common cardinal veins. At 14s, the anterior cardinal vein is distinguishable from the heart to the head, and at 16s, both the anterior cardinal and posterior cardinal veins are longer and sprout intersomitic vessels. Acv, anterior cardinal vein; ba, branchial arch; da, dorsal aortae; ccv, common cardinal vein; e, endocardium; isv, intersomitic vessel; pcv, posterior cardinal vein; sv, sinus venosus; vv, vitelline veins; ysp, yolk sac plexus; *, forming Duct of Cuvier. Scale bars = 100 µm (A-C) and 200 µm (D-F).

vessels by the 4-5s stage **(Fig 2.1 E)**, most arterial markers tested failed to be detected in aortic endothelium at this stage. Also it is surprising that many of the arterial markers, including *Ephrin B2, Cx40*, *Hey2*, *Nrp1*, *Notch1*, *Notch4,* or *Jag1* were expressed in the cardiac crescent including the sinus venosus.

Expression of arterial marker at E8.25

Just a few hours later, at E8.25 (7-8s stage), a set of arterial markers became detectable in the dorsal aortae, while others still remained weak. *EphrinB2*, *Cx40*, *Nrp1*, *Notch1*, *Notch4* initiated expression in dorsal aortae **(Fig. 2.3 A',B',F',G',H')**. Transverse sections of the E8.25 aortae revealed expression in ECs **(Fig. 2.3 a-d,f-i)**. In contrast, Hey2 and Jag1 lacked EC expression at this stage **(Fig. 2.3 E',J', e,j)**. Surprisingly, many reported arterial markers, such as *Ephrin B2*, *Cx37, Hey1, Nrp1,* and *Jag1*, were also expressed in the sinus venosus, a region that is supposed to express venous markers **(Fig. 2.3 A',C',D',F',J')**. This suggested that sinus venosus ECs may not yet have acquired venous identity at this stage, as they exhibit a partial arterial feature. In addition, we found that most standard arterial markers examined were not restricted to arterial endothelium, or the dorsal aortae. Some of those were also present in other ECs including sinus venosus, endocardium, and yolk sac.

Expression of arterial marker at E8.5

Shortly after, at E8.5 (9-11s) during embryonic turning, some arterial markers finally became arterial specific. *Ephrin B2, Cx40, and Cx37* were robustly expressed in the aortae **(Fig. 2.3 A'-C'')**. By contrast, *Hey1, Nrp1, Notch1, Notch4* and *Dll4* expression were down-regulated in the aortae **(Fig. 2.3 D'',F''-I'')**, while *Hey2* and *Jag1* were never expressed in the aortae by this stage **(Fig. 2.3 E'',J'')**. Of note, many of these markers were also down-regulated in the sinus venosus over time. This may suggest that ECs of the sinus venosus are initially ambiguous in their AV fate, displaying markers of both fates, and only secure their venous

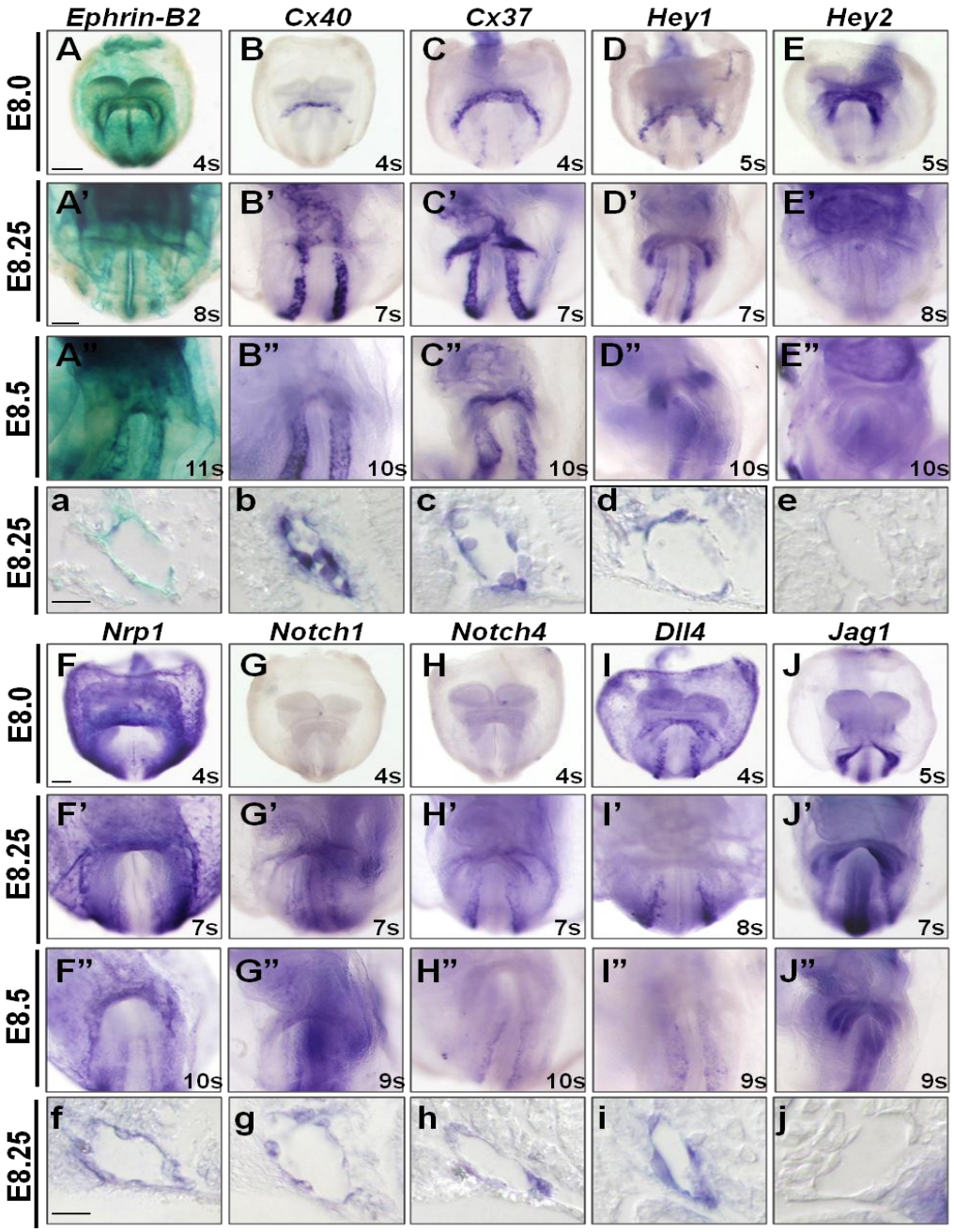

Figure 2.3. Step-wise initiation of arterial gene expression in dorsal aortae prior to turning. *in situ* hybridization or β-galactosidase staining of established arterial markers from E8.0 to E8.5, as indicated. **(A-J)** During early vasculogenesis (4-5s), *Cx 37, Hey1,* and *Dll4* are the first arterial genes expressed in the forming dorsal aortae (red arrows). *Ephrin-B2, Cx40, Hey2, Nrp1, Notch 1/4,* and *Jag1* are not detected in endothelium. **(A'-J')** At E8.25 (7-8s), additional arterial genes have initiated, including *Cx40* and *Notch 1/4*. **(A"-J")** Dorsal aortae expression is robust using *Ephrin-B2, Cx40,* and *Cx37*. *Hey1, Notch4 and Dll4* expression become downregulated. **(a-j)** Transverse sections through E8.25 embryos reveal the presence or absence of expression in ECs of dorsal aortae. Somite stage for each embryo given at bottom right. Scale bars = 200µm (A-J); 100µm (A'-J'); 25µm (a-j).

identity later. Together, our observations demonstrate that step-wise arterial differentiation during vasculogenesis can be detected with a subset of established arterial markers.

Expression of venous marker at E8.0

To examine onset of venous specification, we investigated β-galactosidase staining and in situ hybridization for known venous markers. At E8.0 (4-5s), *EphB4, Nrp2*, and *Flt4* expression was detected weakly in the inflow tracts of the sinus venosus **(Fig. 2.4 A,C,E)**, but most of venous markers examined were expressed in non-endothelial tissues. *CoupTFII, Nrp2,* and *APJ* were strongly detected in somites and lateral plate mesoderm **(Fig. 2.4 B,C,D)**. Surprisingly, although *Flt4* is known for a venous marker, it was also enriched in the dorsal aortae as well as in the vitelline vein **(Fig. 2.4 E)**. These results revealed that venous specification initiates after arterial specification compared to arterial specification.

Expression of venous marker at E8.25

As the vitelline and cardinal veins developed poorly compared to arteries at E8.25 (7-8s), based on the analysis of vein anatomy, venous markers do not change their expression profile dramatically by this stage. Expression of *EphB4* was increased marginally in sinus venosus **(Fig. 2.4 A')**, and *Nrp2* and *Flt4* were expressed more prominently in vitelline vein angioblasts **(Fig. 2.4 C',E')**. The transverse sections of the embryo at this stage demonstrated an absence of venous markers in the dorsal aortae **(Fig. 2.4 a-d)**, except for *Flt4* **(Fig. 2.4 e)**.

Expression of venous marker at E8.5

By E8.5 (9-10s), as vitelline vein extends prominently **(Fig. 2.2 C)**, many of the venous markers became distinguishable in the pre-vitelline vein, at the sinus venosus and along the interface of the embryonic and yolk sac **(Fig. 2.4 A''-E'')**. *EphB4* expression was more robust at this stage **(Fig. 2.4 A'')**, and *Flt4* expression in dorsal aortae was significantly decreased **(Fig.**

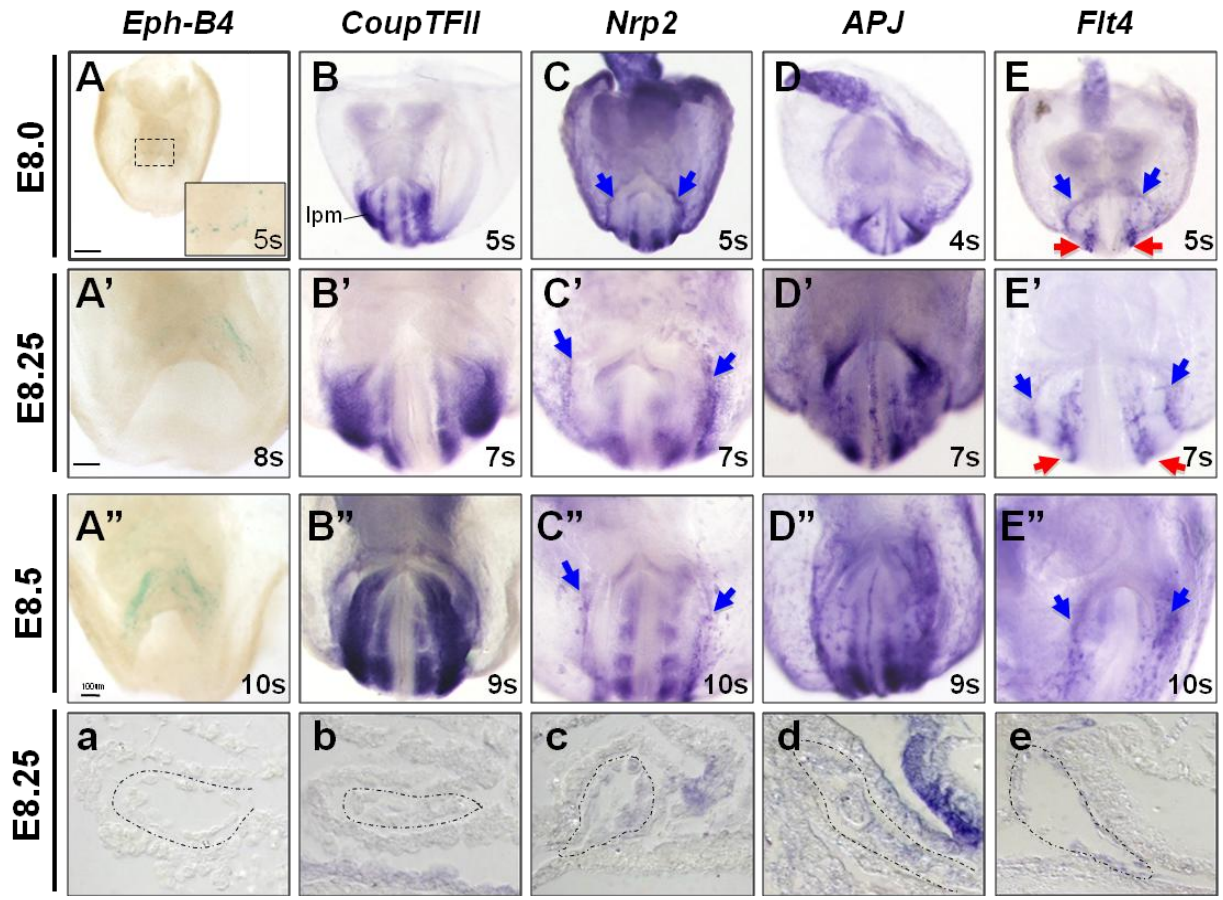

Figure 2.4. Venous gene expression is largely absent from endothelium prior to E8.5. *in situ* hybridization or β-galactosidase staining of established venous markers from E8.0 to E8.5, as indicated. **(A-E)** At E8.0 (4-5s), expression of venous markers was not observed in distinguishable veins. *EphB4* displayed punctate expression along the sinus venosus (inset) while *CoupTFII, Nrp2*, and *APJ* were expressed in the somites and lateral plate mesoderm (lpm). *Flt4* and *Nrp2* were observed in the vitelline vein primordia (blue arrows) while *Flt4* was also observed at the dorsal aortae (red arrows). **(A'-E')** At E8.25 (7-8s), venous expression remained relatively similar for all markers examined, except EphB4, which marked more cells in the sinus venosus. **(A"-E")** At E8.5, vitelline vein expression can be identified using venouse markers, *Nrp2* and *Flt4* (Blue arrows). **(a-e)** Transverse sections through E8.25 embryos reveal the presence of absence of venous expression in ECs (outlined) of the sinus venosus. Scale bars = 200μm (A-E); 100μm (A'-E")

2.4 E''). We confirmed that *Nrp2, APJ* and *Flt4* were expressed in early vitelline angioblasts **(Fig. 2.5 A-C)**.

Expression of venous marker after turning

Expression of venous markers were detected at these later embryonic stages, as the cardinal vein initiated taking shape soon after vitelline vein was formed **(Fig 2.2 D-F)**. Expression of *APJ* and *Flt4* were detected at the forming cardinal and sprouting intersomitic veins **(Fig. 2.5 D-F)** near the common cardinal vein, at the level of the heart along the axis, and extended anteriorly and posteriorly following turning. *EphB4-LacZ* expression was observed much later in the common cardinal vein **(Fig. 2.5 G)**, and expanded along the forming cardinal veins over time **(Fig. 2.5 H)**. By 20-22s, *EphB4-LacZ* could be observed along most of the anterior cardinal vein and the nascent posterior cardinal vein.

Ambiguous arteriovenous fate in early vessels

To examine AV vessel identity with greater resolution and with access to more internal vessels, we examined the earliest AV markers identified above for which antibodies were available. We assessed CX40, Nrp1 and Nrp2 expression in Flk1-EGFP embryo **(Fig. 2.6)**. These markers readily distinguished arteries from veins in established vascular beds, with CX40 and Nrp1 in arteries and Nrp2 in veins as previously reported (Ema et al., 2006).

Ambiguous vein fate at E8.25

We then examined establishment of AV fate in E8.25 primary vascular plexus. CX40 was primarily restricted to the dorsal aortae **(Fig. 2.6 A-A'')**, as expected. Similarly, Nrp1 was expressed in aortic ECs **(Fig. 2.6 B-B'')**. Interestingly, we found low levels of CX40 **(Fig. 2.6 A,A')** and Nrp1 **(Fig. 2.6 B,B')** expression in secondary (smaller) blood vessels (white arrows), including the paired 'head veins' (blue arrows). In addition, ECs of the sinus venosus also

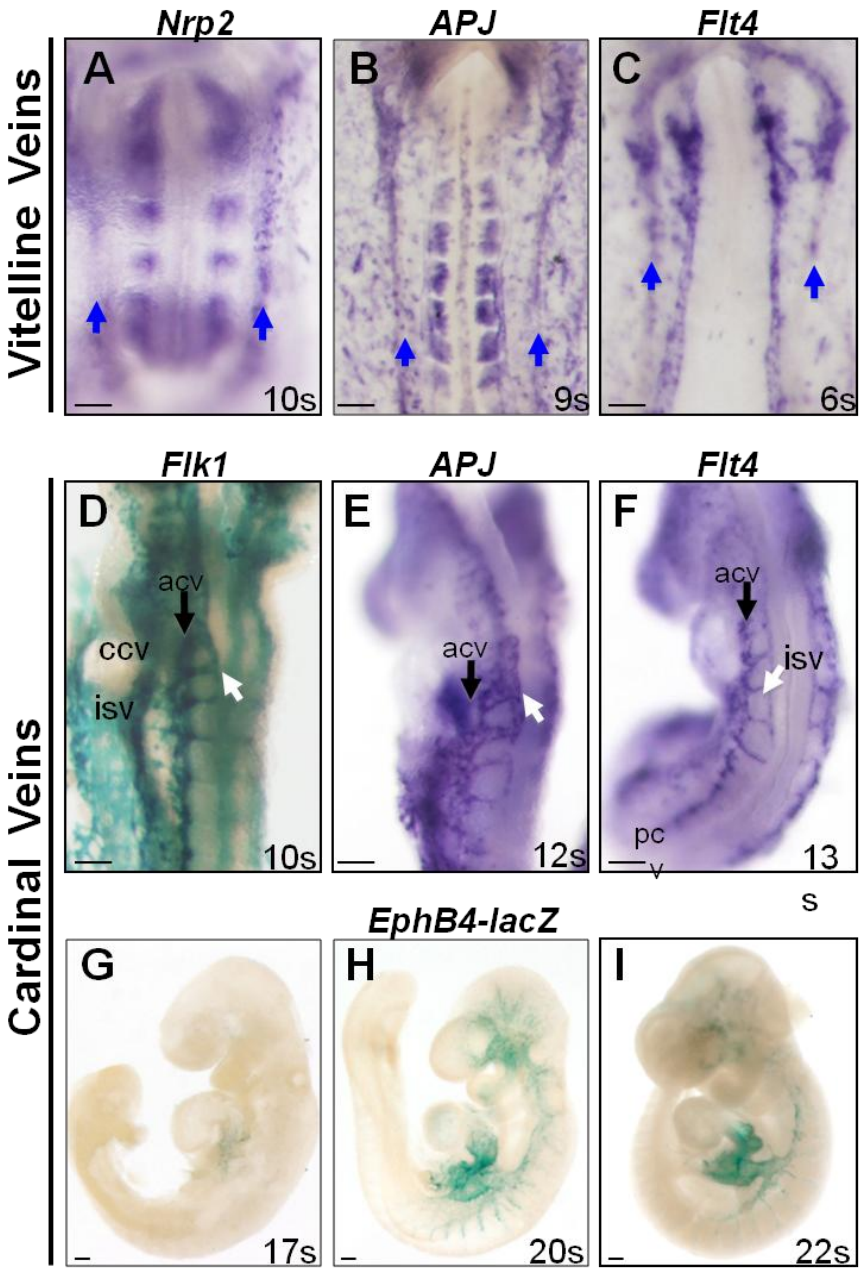

Figure 2.5. Step-wise initiation of venous gene expression in forming vitelline and cardinal vein. *In situ* hybridization or β-galactosidase staining of *Flk1-LacZ* and *EphB4-LacZ* embryos, at somite stages indicated. **(A-C)** *In situ* hybridization with *Nrp2, APJ*, and *Flt4* show positive staining in forming vitelline veins (blue arrows). **(D)** *Flk1-LacZ* embryo, focusing on the developing anterior cardinal vein (black arrow) and sprouting intersomitic veins (white arrow). In this forming vessels, both *APJ* **(E)** and *Flt4* **(F)** initiate expression during turning, as angioblasts aggregate and form cords. **(G-I)** *EphB4-LacZ* expression initiated in ECs of the sinus venosus. Expression expanded first in the anterior cardinal vein (H), and then the posterior cardinal vein (I), as they formed and became established. acv, anterior cardinal vein; ccv, common cardinal vein; isc intersomatic vessels; sv, sinus venosus. Scale bars = 100µm.

expressed low levels of both arterial proteins (as seen in **Fig. 2.3**). Together, it suggests that early veins exhibit ambiguous AV identity and have not yet stabilized their venous identity at this point. By contrast, the venous marker Nrp2 was expressed in the sinus venosus endothelium **(Fig. 2.6 C,C'')**, as expected, and was not expressed within the ECs of dorsal aortae. Together, these observations suggested that the AV identity of the first veins is at first promiscuous early embryo at E8.25, as they express arterial markers inappropriately.

Stabilized vein fate at E9.5

One day later, similar analysis was performed at E9.5, when arteries and veins are formed completely after turning. CX40 was robustly and exclusively expressed in the dorsal aortae, with no trace detected in veins **(Fig. 2.6 D-D'')**. Similarly, Nrp2 endothelial expression was restricted to the head veins **(Fig. 2.6 F-F'')**. By contrast, Nrp1 was strongly expressed in the dorsal aortae but still displayed low levels in the head vein of the perineural vascular plexus (PNVP) **(Fig. 2.6 E-E'')**, suggesting that veins at this stage still possessed some level of ambiguity in their AV fate. These data revealed that arteriovenous identity became solidified, and demonstrated the step-wise and progressive restriction of fate involved in the establishment of initial vessel identity, which occurs earlier in arteries than in veins.

2.2.3 Role of flow on arteriovenous identity

In vitro model of 'flowless' vessels: embryonic explants

As AV differentiation appeared to initiate prior to, or concurrent with, the known onset of blood flow, I examined whether AV marker expression depend on hemodynamic flow. Explants studies were carried out to assess arterial fate in the absence of blood flow. To generate "flowless" embryonic explants, 5s embryos were dissected, and anterior and posterior halves of

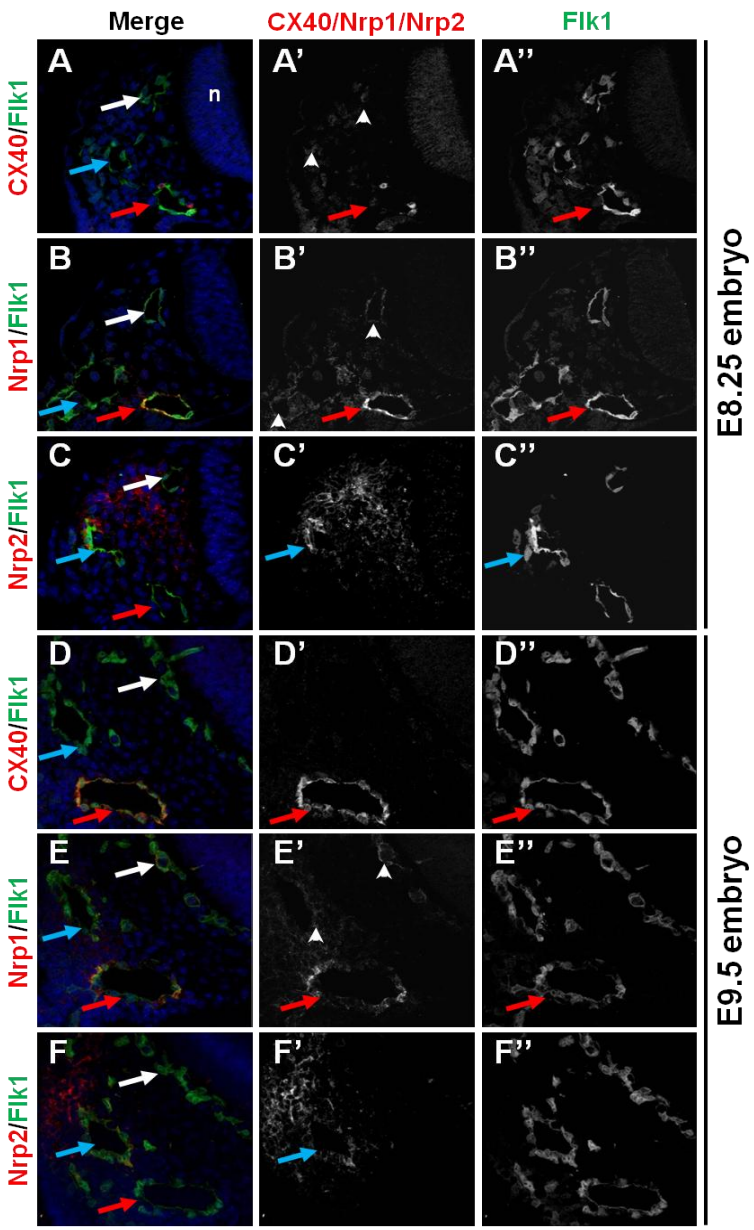

Figure 2.6. Step-wise acquisition of arteriovenous fate in early vessels. Co-immunofluorescence for *Flk1* and arterial markers, at E8.25 **(A-C)** or E9.5 **(D-F)**. Single channels for either *Cx40, Nrp1,* or *Nrp2* **(A'-F')** or for endothelial *Flk1* **(A"-F")**. Note expression of the arterial markers *Cx40* **(A)** and *Nrp1* **(B)** in dorsal aortic ECs, but also sinus venosus and vessels of the head/PNVP (white arrowheads) (A',B') at E8.25. *Nrp2*, by contrast, is strongly expressed in the sinus venosus, and head /PNVP vessels, but not in the dorsal aorta **(C,C')**. By E9.5, *Cx40* (one of the two arterial markers assayed) had become restricted to the aorta **(D)**. *Nrp1*, however, was still expressed in the venous ECs of the sinus venosus and the head/PNVP (white arrowhead) **(D,D')**. *Nrp2*, like *Cx40*, was restricted its expression by E9.5 and exhibited expression only in the venous ECs of the sinus venosus. White arrows point to vessels of the head/PNVP; blue arrows point to sinus venosus; red arrows point to dorsal aorta. Nuclei counterstained with DAPI.

these were isolated **(Fig. 2.7 A,B)**. These embryonic halves were then cultured for 10 or 18 hours. At 5s, arterial fate had been specified in the dorsal aortae, as assessed using *CX40* and *Dll4* **(Fig. 2.7 C)**, which both display early, robust and largely specific arterial expression at this early stage.

Using 5s *Flk1-LacZ* embryos as controls, at time 0, the dorsal aortae were lumenized vessels both in the anterior and posterior portions of the embryonic axis **(Fig. 2.8 A,D)**. After 10 hours in culture, both the dorsal aortae and cardiac crescent largely maintained their morphology in culture **(Fig. 2.8 B,E)**. Following 18hours in culture, however, the aortae broke up into endothelial pockets **(Fig. 2.8 C,F)**. This was accentuated in the posterior explants **(Fig. 2.8 F)**.

Using the embryonic explant experiments, arterial fate was assessed in the cultured embryo and found that *Cx40* was dramatically downregulated after 10 hours, and extinguished by 18 hours **(Fig. 2.8 A'-C')**. In the posterior region, *Cx40* expression was largely gone in aortae after 10 hrs, although it remained expressed at low levels in yolk sac vessels **(Fig. 2.8 E')**. However, after 18 hours, *Cx40* was completely undetectable **(Fig. 2.8 F')**. By contrast, *Dll4* remained robustly expressed after 10 hours, in both anterior and posterior aortae, and only slightly diminished after 18 hours **(Fig. 2.8 A''-C'',D''-F'')**. Using the same experimental conditions, we also tested venous fate in the ''flowless'' vessels of cultured embryonic explants. In the explant cultures, *EphB4-LacZ* embryo explants exhibited no detectable positive cells in the sinus venosus at the onset of culture or later (data not shown).

These results support that flow is not required for arterial specification but rather for the expression of subsets of AV markers. While flow is clearly required for maintenance of certain arterial markers, such as *Cx40*, it is not required for others, such as *Dll4*. From these experiments, however it is unclear what role blood flow plays in venous differentiation as

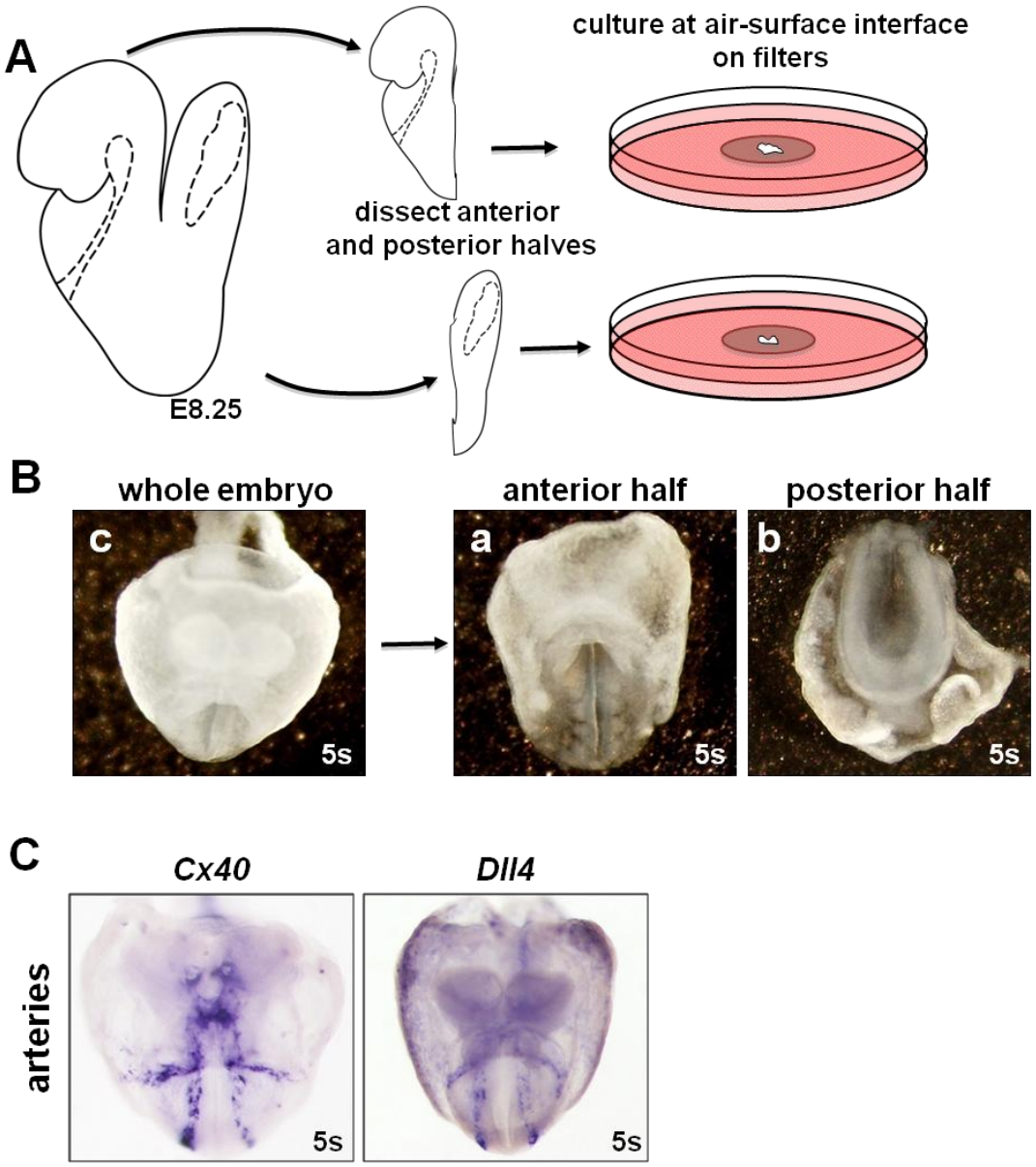

Figure 2.7. Explant procedure and controls. Schematic of explant procedure. **(A)** 5s embryos were bisected and each half was grown on a filter, at the air-surfaced interface. **(B)** Brightfield images of the whole embryo **(a)** , isolated anterior **(b)**, and posterior **(c)** halves. **(C)** *Cx40* and *Dll4* are expressed in the dorsal aortae at 5s in unmanipulated embryos.

measurable venous marker expression initiates later than the developmental timeframe covered in these experiments.

In vivo model of 'flowless' vessels: Rasip1 null embryos

To test whether blood flow was required for arterial specification *in vivo*, expression of arterial genes, *Cx40* and *Dll4,* was assessed in *Rasip1* null embryos which were previously reported lack all vascular lumens, and consequently lack blood circulation (Xu et al., 2011). These embryos displayed normal angioblast specification, as *Flk1*-expressing angioblasts were present and normally distributed, however they failed to undergo the normal cord-to-patent vessel transition and appeared as cords rather than tubes, as previously described (Xu et al., 2011).

Cx40 expression was detected in Rasip1 null embryo dorsal aortae at early stages E8.25, but in a faint and discontinuous manner **(Fig. 2.9 A,B)**. As development proceeded, expression of *Cx40* rapidly declined. By E9.0, no trace of *Cx40* presented in the lumenless dorsal aortae in the Rasip1 mutant, although low levels of expression could be seen in the vitelline artery **(Fig. 2.9 C,C',D,D')**. This corroborated the *in vitro* "flowless" explant experiments. Interestingly, again similar to the explants, we observed relatively normal or increased levels of *Dll4* expression in *Rasip1*$^{-/-}$ aortic cords **(Fig. 2.9 E-H')**. This is in agreement with the increase in *Dll4* expression previously observed in flowless mouse models (Jones et al., 2008).

Together, these data show that at least one arterial gene, *Cx40*, appeared to depend on blood flow, while another one, *Dll4*, was expressed regardless of blood flow status, These results support the contention that flow is not required for initial arterial specification, but is required for expression of the full range of arterial genes, suggesting differentiation and maintenance of arterial fate in blood vessels depends on hemodynamic flow.

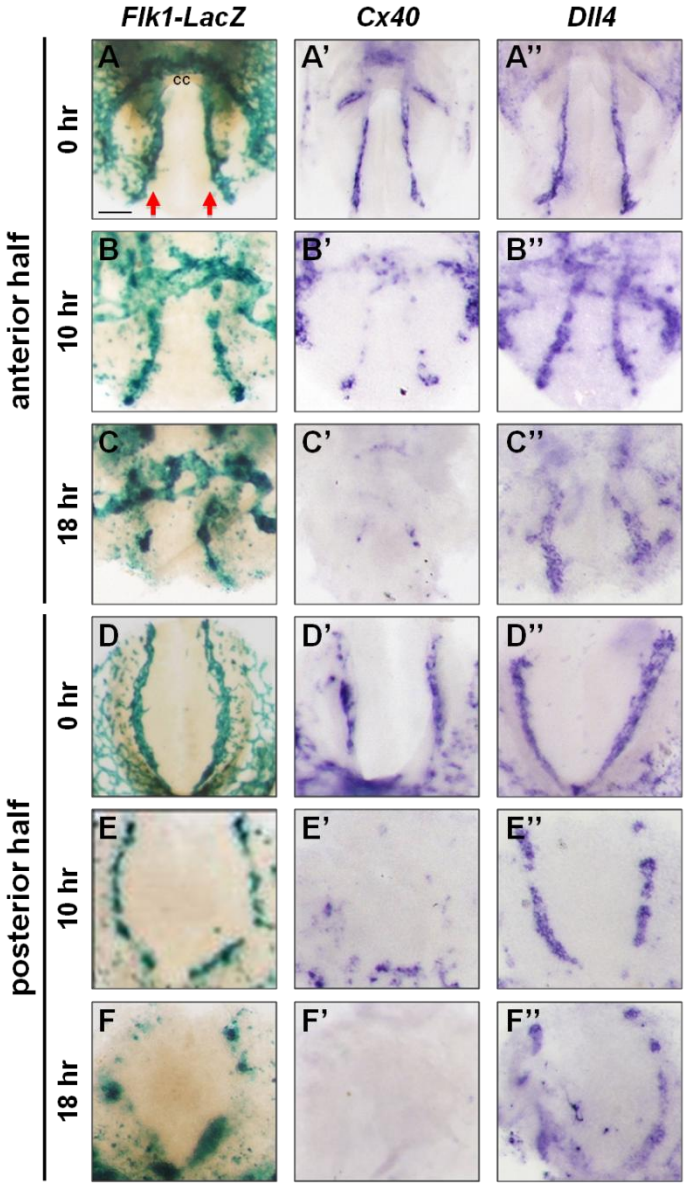

Figure 2.8. Blood flow is required for arterial expression of *Cx40*, but not *Dll4*. β-galactosidase staining and *in situ* hybridization on cultured explants show that disruption in flow reduces expression of *Cx40*, but not *Dll4*. Explants were cultured for 10 or 18 hr. **(A-A")** At 5s, the dorsal aortae were clearly outlined using *Flk1-LacZ* and the arterial markers *Cx40* and *Dll4*. **(B-B")** After 10hr, the dorsal aortae were still clearly outlined and distinguishable using *Flk1* and *Dll4*. However, *Cx40* expression decreased significantly. **(C-C")** After 18hr, dorsal aortae expression was still visible using markers *Flk1* and *Dll4*. However, *Cx40* expression was almost completely absent in the aortae. In explants containing posterior portions of the embryos, similar trends were identified. **(D-D")** At 5s, expression of *Flk1*, *Cx40*, and *Dll4* was robust in the paired aortae. **(E-E")** After 10hr in culture, *Flk1* and *Dll4* continues to be expressed in the vessels. However, *Cx40* expression was relatively low and had diminished more rapidly than in the anterior portion. **(F-F")** After 18 hr in culture, *Flk1* and *Dll4* expression remained, albeit the vessels appeared discontinuous. However, *Cx40* expression was completely lacking. cc, cardiac crescent; red arrows point to dorsal aortae. Scale bar = 100μm.

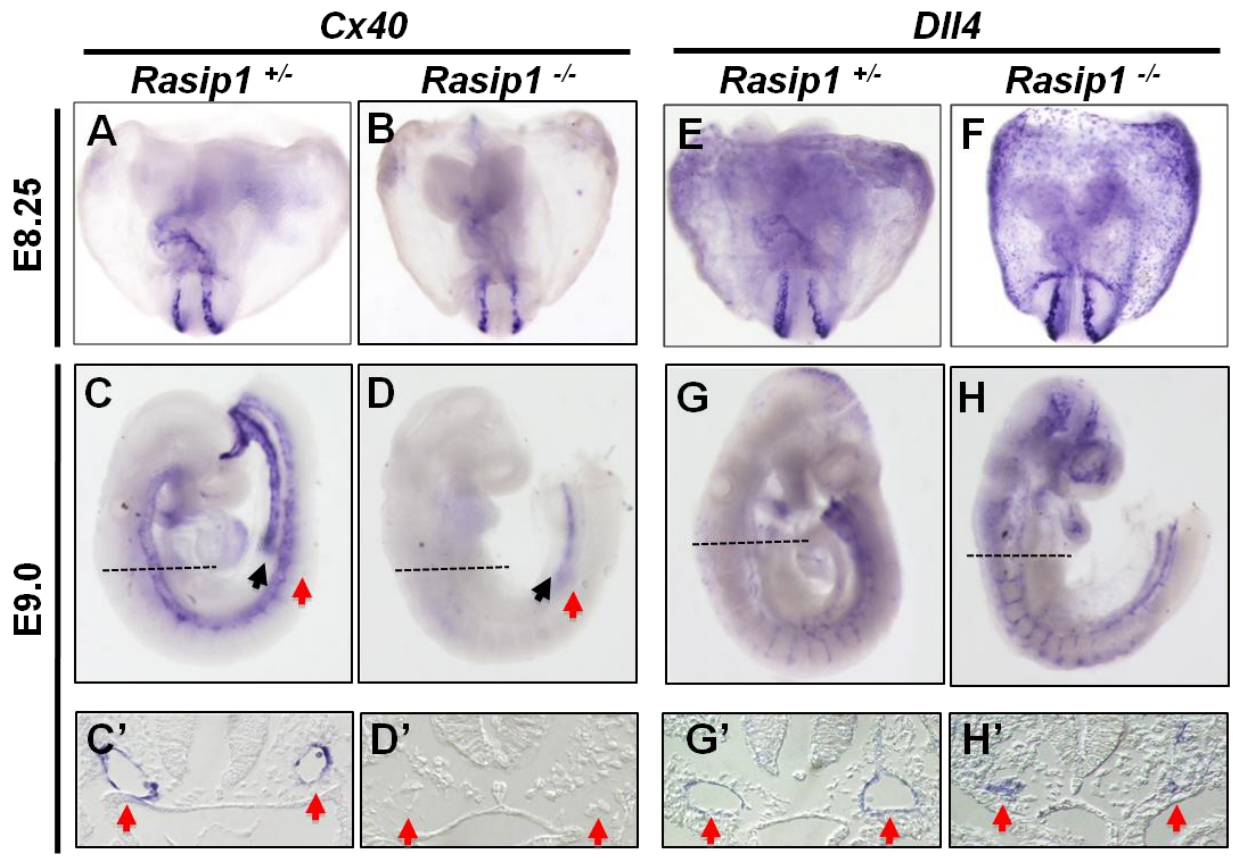

Figure 2.9. Dependence of select arterial gene expression on blood flow. To test the dependence of arterial specification on flow, we analyzed arterial gene expression using in situ hybridization on E8.25 and E9.0 Rasip1 null embryos, which lack vascular lumens and blood flow. Expression of Cx40 was robust in the aortae of *Rasip1* $^{+/-}$ at E8.25 **(A)** and E9.0 **(C,C').** However, Cx40 expression in the *Rasip1* $^{-/-}$ was fainter and discontinuous at E8.25 **(B),** and subsequently downregulated by E9.0 **(D,D')**. Whole **(C,D)**, and transverse sections **(C',D')** of E9.0 embryos. In contrast, *Dll4* expression is not downregulated in Rasip1$^{-/-}$ aortic cords at E8.25 compared to Rasip1 $^{+/-}$ **(E,F)** and expression continues at E9.0 **(G,G', H,H').** Whole **(G,H)**, and transverse sections **(G',H')** of E9.0 embryos. Red arrows, aorta; black arrows, vitelline artery. Striped lines represent plane of section for **(C',D',G',H').**

2.3 DISCUSSION

In this chapter, spatio-temporal analysis demonstrates that initial murine artery and vein formation and differentiation take place in step-wise manner. A variety of mutants have been identified as having vascular remodeling defects, causing embryonic lethality, however exact vascular defects has not been described, likely due to the complexity and rapid changes of the embryonic vasculature and to lack of useful AV markers. While murine vascular anatomy during early development was described in a number of studies (Walls et al., 2008), AV fate acquisition of the early vessel was not well characterized. The work presented in this chapter is thus the first examination of AV marker expression profile during initial embryonic vessel development, which establishes a baseline for future studies of mouse embryos with disrupted vascular development.

2.3.1 Step-wise formation of major embryonic vessels

To assess AV fate, the anatomy of the artery and vein was investigated during rapid vasculature remodeling in early mouse embryo. The precursors of ECs emerge as scattered at E7.5 and aggregate to form the first vessels as previously shown (Drake and Fleming, 2000). In this study, it was observed that the first vessels are formed in progressively and from dorsal aortae and vitelline veins, and then cardinal veins. The dorsal aortae appeared as solid cords, and then quickly transformed to form lumens and completely established the tube by 5s. Surprisingly, at this time point, the vein primordium at the sinus venosus remained short in length and blind-ended. After the formation of the first artery, the veins quickly take shape during embryonic turning and extend towards the tail, suggesting that a functional embryonic circulation loop is not completed at early stages. Although the heart initiates beating at E8.0 (Lucitti et al., 2007), formation of closed circulation loop is accomplished by E9.0.

2.3.2 Step-wise arteriovenous specification

By investigating the AV marker expression in earliest stages of embryonic vasculogenesis, it was shown that expression of most standard AV markers does not coincide with the emergence of artery and vein, but occurs in step-wise manner. Few standard AV markers are initially expressed in early vessels right after they are formed, and this subset incrementally grows over time. It was noticed that arteries solidify their fates slightly earlier than veins do, likely as the consequence of their earlier formation. In addition, co-expression of AV markers in early vessels suggests that the pre-mature vessels contain ambiguity in AV fate, which resolves as the vessels become established. Together, this study provides a toolkit of markers that are useful for identifying the first arteries and veins, as well as resolving the timing of their specification (onset of AV identity) and differentiation (functional AV identity). These tools will be critical for analysis of vascular mutant mouse embryos at the early stages described here.

2.3.3 Role of flow in maintenance of arteriovenous identity

The role of flow on vascular development has been discussed in many literatures in the field. Sheer stress and stretch, caused by local flow conditions, are sensed by ECs that line vessels and these physical forces drive morphological and transcriptional changes within these cells (le Noble et al., 2004). It has been shown that plasma circulation in mouse embryos begins as early as the 3 somite (3s) stage (Lucitti et al., 2007). At this stage, the heart myocardium has begun to beat, and generates primitive erythroblast movement through the vascular plexus. It is clear from anatomical observations that the intraembryonic circulatory loop has not been completed. The main arteries have formed by 5s, but there are no veins to close the circuit.

Given that the heart begins to beat prior to a complete circulatory loop, it is postulated that vessels at this time experience pulsative pressure from plasma due to the heartbeat, and it is possible that this pressure influences vascular lumen formation, remodeling, and maintenance.

To examine whether blood or plasma flow played a role in early AV fate, we assessed AV markers examined in the presence or absence of hemodynamic flow using *in vitro* embryo explants and *in vivo* Rasip1 null mouse. It was shown that Cx40 expression depends on flow, as *Cx40* expression is initiated, but decreased when flow is abrogated. On the other hand, Dll4 expression was not affected by hemodynamic flow. These results suggest that some arterial genes depend on flow, while others do not, indicating that partial arterial specification is not affected by flow, but maintenance does require flow for arteries to become established. By contrast, hemodynamic flow is likely not required for vein formation, as most venous markers initiate in pre-venous angioblasts, prior to vein tube formation of blood flow. The timeline and molecular signature of arteries and veins provided by this study will provide tools to examine the role of blood flow.

2.3.4 Summary

The data shown in this study suggests new findings to understand initial vascular development: (1) arteries form prior veins, and both emerge via progressive formation of blind-ended vessels, (2) AV fate establishment occurs in a stepwise manner, and (3) hemodynamic flow is required for some, but not all, arterial gene expression suggesting that arterial specification does not depend on flow, but full differentiation does.

During vasculogenesis, primary vascular plexus initiates to take shape in a stepwise manner, first arteries - the dorsal aortae - and then later, the veins - the vitelline and the cardinal veins. The artery formation and specification occurs early, prior to the establishment of blood

flow, but concurrent with the onset of pulsative pressure from the heartbeat. The expression of a subset of arterial genes occurs during aortic cord formation, at the onset of vascular lumen formation, but prior to embryonic circulation. These findings suggest that AV specification is driven by a cell intrinsic program, rather than by hemodynamic cues. However, in the absence of hemodynamic flow, some, but not all arterial gene expression is extinguished, suggesting that some aspects of AV differentiation/maintenance depend on cell extrinsic factor such as the mechanical force of blood flow. While classical work has demonstrated this to be true in the chick yolk sac (le Noble et al., 2004), the data presented in this chapter is the first such analysis in mammalian embryos and intraembryonic blood vessels. Furthermore, this study defines both spatiotemporal molecular signature of developing arteries and veins, as well as the selective dependence of certain arterial markers on blood flow. This work will instruct future studies of the cardiovascular system and provide greater resolution to studies of mammalian vasculogenesis.

CHAPTER 3: RAS INTERACTING PROTEIN 1 IS REQUIRED FOR VASCULOGENESIS AND ANGIOGENESIS

3.1 INTRODUCTION

Formation of a functional blood vessel network is essential for cardiovascular system function. During network formation, ECs, the building blocks of blood vessels, undergo "tubulogenesis", which involves cellular and molecular events to open a central cavity that allow blood flow to provide oxygen and nutrients to tissues. During early development, de novo vessel tubulogenesis, termed 'vasculogenesis', happens via EC assembly around embryonic day 8 (E8.0). EC progenitors, or angioblasts initiate aggregation to form a linear cord structure, followed by opening of a central lumen. Then, new blood vessels sprout from pre-existing blood vessels, which is called 'angiogenesis'. The growing blood vessels expand lumens and remodel to form vascular network for functional circulatory system. The mechanisms underlying formation of a functional lumen during blood vessel development is still not completely understood.

Until recently, little was known about vascular lumen formation in mammalian blood vessels. While lumen formation has extensively been examined in epithelial in vitro systems (Datta et al., 2011) and more recently *in vivo* (Kesavan et al., 2009) examination of lumen formation in ECs was largely carried out in culture. Indeed, HUVECs were used in 3D collagen matrices to identify entire cascades of molecules required for lumen formation (Bayless and Davis, 2002; Koh et al., 2008). A landmark study by Lammert and colleagues opened the door for examination of blood vessel lumen formation when this group noted that the classical VEGF

mouse mutant displayed vessels lacking lumens in portions of the dorsal aortae (Strilic et al., 2009). In this study, it was shown that a cascade of molecules worked together to coordinate cell behaviors to drive opening of a central blood carrying lumen. One component was the negatively charged glycoprotein (CD34) sialomucin podocalyxin (PODXL) localizes at the apical side of ECs at the onset of lumen formation in mouse embryo aorta and provides electrostatic repulsion of luminal membranes initiating lumen opening (Strilic et al., 2009). In addition, vascular cadherin (VE-cad), a cell adhesion molecule that must be removed from the apical surface for lumen opening, was shown to be essential to proper formation of vessels as VE-cadherin null mutants fail to form proper lumens. While ECs open a central cavity through a de-adhesion process, adhesion of ECs to the peripheral ECM as well as to each other plays critical roles for tubulogenesis. One study showed that loss of b1-integrin in embryonic ECs leads to loss of cell polarity and a block of lumen formation in arterioles (Zovein and Iruela-Arispe, 2009), In addition, ECs sustained connections via adherens junction (AJ) and tight junction (TJ) to maintain a sheath of ECs. Further identification of important regulators of vascular lumen formation is thus a critical next step.

Ras interacting protein Rasip1 was identified in our laboratory as required for blood vessel formation in the early embryo (Xu et al., 2011). In this study, Rasip1 was shown as an endothelial specific factor expressed in growing blood vessels throughout embryonic development and into post-natal stages, and was found to be critical for normal vasculogenesis as global deletion of Rasip1 results in complete vascular failure. Rasip1 null ECs exhibit disrupted polarity and mislocalization of junctional complexes, as well as loss of adhesion of ECs to ECM. The ultimate result was discontinuous vascular tubes, which blocked blood flow and ultimately led to early embryonic lethality. Depletion of Rasip1 in ECs cultured in 3D matrices similarly led to failure of lumen formation and disruption of Rho GTPase activity, with Cdc42 and Rac1 activity being severely reduced and RhoA activity being elevated. Similar 2D

cultures showed that in the absence of Rasip1, b1-integrin expressing adhesion contacts failed to mature properly. Rasip1 was initially identified in a yeast two-hybrid screen, as preferentially bound to the GTP bound form of Ras (Mitin et al., 2004) and has more recently been identified as a Rap1 effector controlling cell adhesion and junctions during blood vessel stabilization (Post et al., 2013; Wilson et al., 2013). Rasip1 was found to be a binding partner of Rho GTPase-activating protein 29(ArhGAP29) (Xu et al., 2011). Together these findings revealed Rasip1 was critical to normal assembly of ECs into cohesive functional vessels, but questions still remain open as to how it is effecting coordination of cell behaviors and regulation of GTPase activity.

Here, I show that Rasip1 is critical to lumen maintenance during development, embryonic vessel growth and angiogenesis. Using different ubiquitous or inducible endothelial Cre driver lines, I ablated expression of Rasip1 at different developmental time points. I found that deletion of Rasip1 from the onset of embryogenesis using *Sox2-cre* phenocopied our original global Rasip1 knockout (Xu et al., 2011). However, here I show that Rasip1 is not only required during the cord-to-tube transition that occurs during early vasculogenesis, but it is also required during embryogenesis for blood vessel lumen maintenance and remodeling. This requirement, however, does not last into adulthood, as Rasip1 is dispensable in established adult blood vessels. Interestingly, I found that Rasip1 is also required for angiogenic sprouting in both the growing retinal vasculature and in one model of adult angiogenesis. Together, this work extends and confirms our original findings, and it suggests Rasip1 may be a useful target for development of anti-angiogenic therapies.

3.2 RESULTS

3.2.1 Rasip1 is essential to initial blood vessel lumen formation

Sox2-Cre Rasip1 deletion results in vasculogenesis defects

The Rasip1 global null (*Rasip1*$^{-/-}$) mouse embryo was previously shown to fail to form functional vascular tubes during initial blood vessel formation around E8.5 (Xu et al., 2011), resulting in 100% lethality. To investigate the role of Rasip1 at later stages of blood vessel development and in established adult vessels, I generated a conditional Rasip1 (*Rasip1*$^{fl/fl}$) mouse, which lacks Exon3 in *Rasip1* locus **(Fig. 3.1 A)**. We acquired a commercially available knockout construct and carried out homologous recombination in mouse embryonic stem cells to generate live mice bearing the conditional allele, which contained a cassette containing both an inserted LacZ gene and a neomycin cassette. *LacZ* reporter gene revealed EC specific expression of Rasip1 in E8.5 embryo **(Fig. 3.1 B,C)**,confirming proper insertion. When the *Rasip1LacZNeo*$^{fl/+}$ was bred with a line containing the a *Flk1-EGFP* transgene allowing EC visualization. *Rasip1LacZNeo*$^{fl/fl}$ embryos displayed defective (narrower) dorsal aortae cords at E8.5, indicating this mouse line partially recapitulated the global *Rasip1* knockout **(Fig. 3.1 D,E)**. To confirm Rasip1 deletion, *Rasip1*$^{fl/fl}$ was crossed with a *Sox2-Cre* driver line (Hayashi et al., 2002) to delete *Rasip1* ubiquitously, and embryos were examined for defects in forming vessels. This global ablation of Rasip1 displayed identical vascular tubulogenesis failure as that seen in the Rasip1 global null mouse (Xu et al., 2011). *Rasip1*$^{fl/fl}$*;Sox2-Cre* mouse showed efficient deletion of Rasip1 expression in ECs at E8.5 embryos, and in the absence of Rasip1, PECAM and Endomucin positive ECs did not develop vascular lumens **(Fig. 3.1 F-G")**. By E8.75, *Cx40* expression in *Rasip1*$^{fl/fl}$*;Sox2-Cre* was significantly decreased, indicating failure of vascular tubulogensis **(Fig. 3.1 H,I)**, and failure of flow induced *Cx40* expression (see Chapter 2).

Rasip1*$^{fl/fl}$*;Tie2-Cre shows variable vasculogenesis defects

To investigate the function of Rasip1 in vascular development subsequent to initial vasculogenesis, *Rasip1*$^{fl/fl}$ was crossed to the *Tie2-Cre* driver line, in which Cre recombinase is

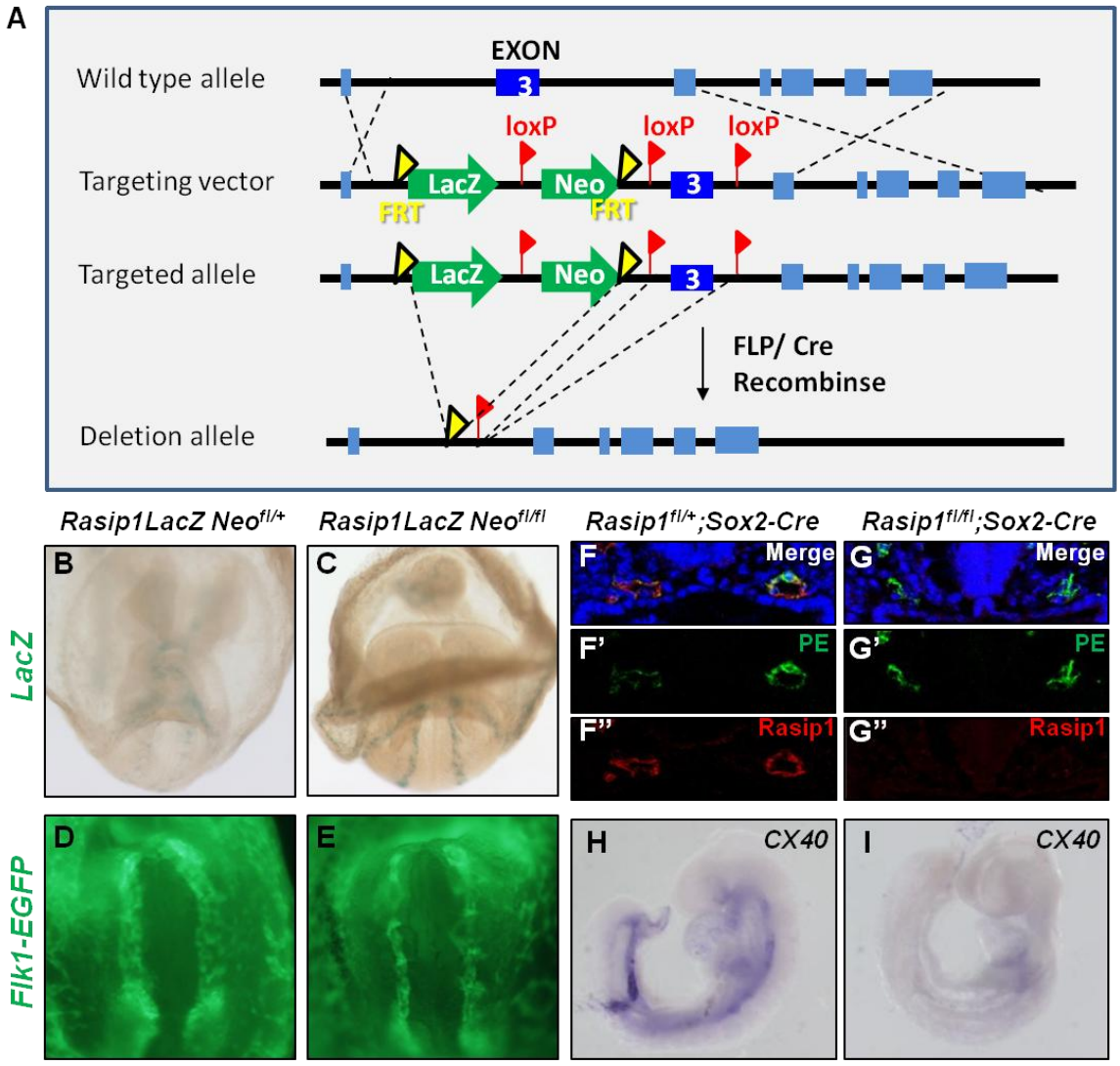

Figure 3.1. Generation of conditional Rasip1 mouse. (A) Rasip1 gene targeting strategy to delete Exon3 for generation of conditional Rasip1 mouse. (B-C) LacZ alelle expression in ECs. (D-E) ECs, visualized by using *Flk1-EGFP* mouse line, reveals tubulogensis defect in *Rasip1LacZNeo*$^{fl/fl}$. (F-G'") *Rasip1*$^{fl/fl}$*;Sox2-Cre* mutant are lack of Rasip1 in PECAM and Endomucin expressing ECs, and failed to form patent blood vessel lumen at E8.5. (H-I) In situ hybridization with *Cx40* reveals lack of blood flow at E8.75 in *Rasip1*$^{fl/fl}$*;Sox2-Cre*.

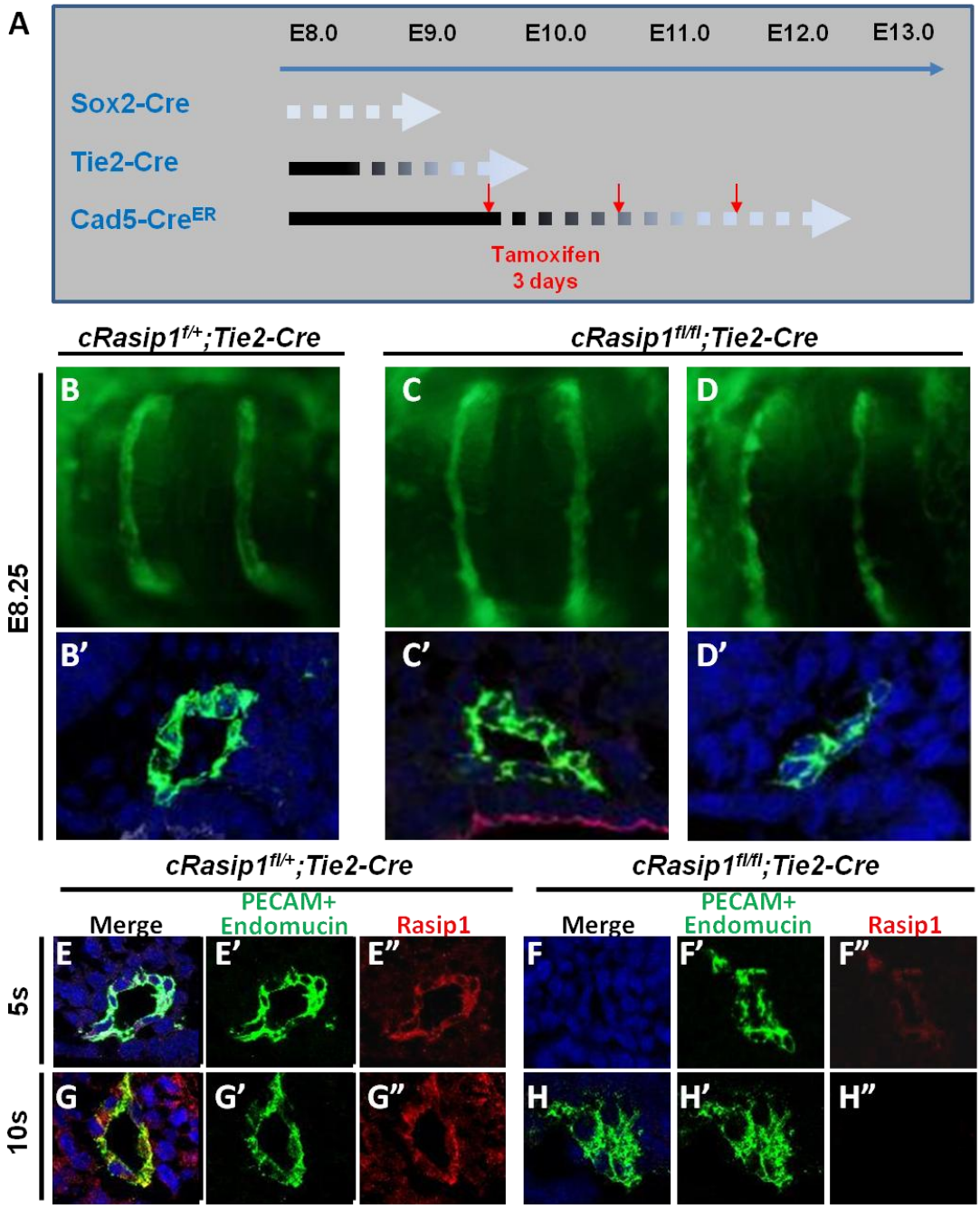

Figure 3.2. Delayed deletion of Rasip1 in *Rasip1$^{fl/fl}$;Tie2-Cre* results in delayed vasculogenesis defect. (A) Schematic diagram showing Rasip1 deletion in different Cre mice. **(B-D)** *Rasip1$^{fl/fl}$;Tie2-Cre* embryo display variable phenotype of tubulogenesis defect in dorsal aortae. ECs were visualized by using *Flk1-EGFP* allele. **(B'-D')** Transverse sections of embryo show dorsal aortae . ECs were shown by PECAM and Endomucin immunostaining. **(E-H")** Sections of dorsal aortae at indicated stages. At 5s, Rasip1 presents in lower level in *Rasip1$^{fl/fl}$;Tie2-Cre*. By 10s, Rasip1 is completely removed in ECs.

A

Somite	Lumen	No Lumen
5-6	1	1
9-14	3	5
22	0	1

B

Somite	Rasip1	No Rasip1
5-6	3	0
9-12	1	4
22	0	1

Table 3.1. *Rasip1$^{fl/fl}$;Tie2-Cre* embryos show variability in lumen defect and Rasip1 expression in dorsal aortae ECs. (A) The number of embryos in which lumen presents or absents in indicated somite stages. **(B)** The number of embryos in which Rasip1 protein presents or absents in indicated somite stages.

expressed in an endothelial specific manner from angioblasts during early development (Kisanuki et al., 2001). I found that not all *Rasip1$^{fl/f}$;Tie2-Cre* embryos displayed tubulogenesis defects at E8.5 **(Fig. 3.2 B-D')**, which was different from *Sox2-Cre* driven and global *Rasip1* null mouse. ECs, visualized with *Flk1-EGFP*, showed that some of the *Rasip1$^{fl/fl}$;Tie2-Cre* embryos displayed comparable width of the dorsal aortae **(Fig. 3.2 B,C)**, and sections of embryos revealed that those aortae had open lumen **(Fig. 3.2 B',C')**. By contrast, some of the *Rasip1$^{fl/fl}$;Tie2-Cre* embryos displayed thinner ECs in dorsal aortae and yolk sac, and closed cord EC in the transverse sections of the embryos (**Fig. 3.2 D, D',** data not shown). I found that 33% of the *Rasip1$^{fl/fl}$;Tie2-Cre* embryos examined displayed open lumen at E8.25-E8.75 **(Table 3.1 A)**. .

Rasip1 deletion is delayed in Rasip1$^{fl/fl}$;Tie2-Cre

The variable phenotype led me to investigate efficiency of Rasip1 protein deletion in ECs by immunofluorescence staining. Cre expression was clearly detected in early angioblasts, suggesting gene deletion by Cre expression initiated in EC precursors, however we wanted to verify this directly. Unexpectedly, low level of Rasip1 protein was detected in PECAM and

endomucin positive ECs in *Rasip1$^{fl/fl}$;Tie2-Cre* embryo at 5s, indicating that the remained Rasip1, which in turn likely helped drive relatively normal lumen formation in *Rasip1$^{fl/fl}$;Tie2-Cre* embryos **(Fig. 3.2 E-F")**. By 10s, however, Rasip1 protein appeared to be more clearly absent and was mostly not detectable in ECs by immunostaining **(Fig. 3.2 G-J")**. By 13s, the majority of mutants displayed defective vascular tubes (**Table 3.1 A,B)**, and embryos showed lethality.

Rasip1 is required for embryonic vessel maintenance

Rasip1$^{fl/fl}$;Tie2-Cre embryos displayed severe vascular defects from late E8.75. PECAM whole mount staining of embryos revealed that Rasip1 deficient dorsal aortae had a constricted appearance and discontinuous lumens **(Fig. 3.3 A,B)**. In addition, arterial endothelial fate was affected as *connexin 40 (CX 40)* gene expression, which is dependent on normal blood flow (Chong et al., 2011), was absent in dorsal aortae of *Rasip1$^{fl/fl}$;Tie2-Cre*, likely due to discontinuity in forming vascular tubules **(Fig. 3.3 C,D)**. 100% of *Rasip1$^{fl/fl}$;Tie2-Cre* mutant embryo growth was delayed grossly by E9.0 **(Fig. 3.3 E,F)**. Discontinuous and constricted vascular lumens in aortae were shown in the transverse section through the trunk of the embryos **(Fig. 3.3 G,H)**. To examine whether *Rasip1$^{fl/fl}$;Tie2-Cre* embryos had functional blood vessels, we assessed blood circulation by injecting fluorescent Isolectin B4 (IB4) into the pumping heart of E9.5 mice. Injected IB4 in the wild type embryos rapidly traveled through the dorsal aortae and reached to caudal tail **(Fig. 3.3 I)**. By contrast, IB4 in the *Rasip1$^{fl/fl}$;Tie2-Cre* mutant embryos failed to circulate properly down to the dorsal aortae and remained in the heart even though it was pumping at normal rates and strength (as per visual observation), suggesting blocked blood circulation **(Fig. 3.3 J)**.

These results show that blood vessel failure in *Rasip1$^{fl/fl}$;Tie2-cre* mutant embryos are distinct from that in *Rasip1$^{-/-}$* global mutant embryos, which fail to initiate lumen formation. *Rasip1$^{fl/fl}$;Tie2-Cre* embryos, in which residual Rasip1 protein remains due to inefficient Rasip1

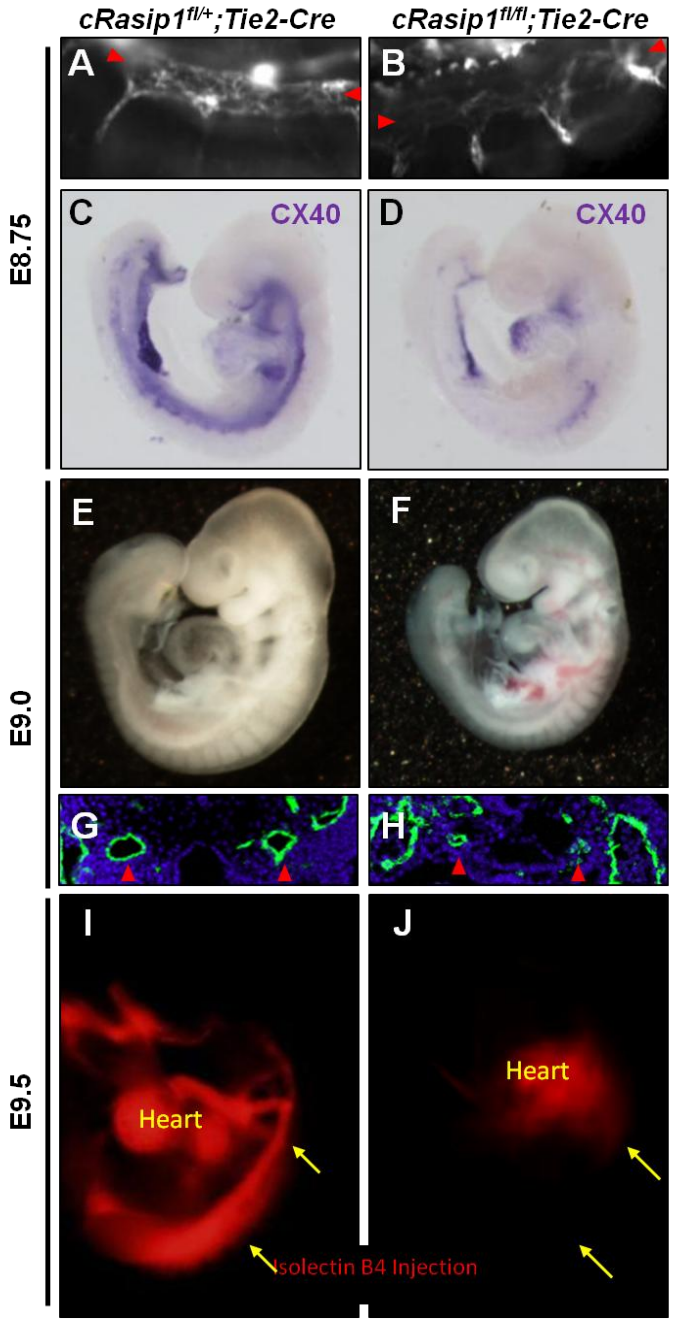

Figure 3.3 ***Rasip1$^{fl/fl}$;Tie2-Cre*** **displays discontinuous vessels and lack of blood flow. (A-B)** Whole mount PECAM staining in embryos at E8.75. While patent lumens in dorsal aortae were seen in *Rasip1* heterozygous littermate, discontinuous lumens were observed in the absence of Rasip1. **(C-D)** Whole mount *in situ* hybridization with *Cx40*. *Cx40* expression, which is dependent on blood flow, is significantly decreased in Rasip1 mutants**. (E-F)** Growth retardation becomes obvious in Rasip1 depleted embryo from at E9.0. **(G-H)** Transverse sections of embryos showed constricted lumens in PECAM positive dorsal aorta ECs. **(I-J)** Isolectin B4 injection was performed into pumping hearts to visualize dorsal aortae with patent lumen. Although the heart was beating in *Rasip1$^{fl/fl}$;Tie2-Cre*, Isolectin B4 did not go through the dorsal aorta, indicating lack of blood flow.

removal prior to the lumen initiation stage, are able to undergo tubulogenesis. Previous literature suggests this delay in Cre recombinase accumulation in the *Tie2-Cre* driver line ECs and we confirm this finding (Kisanuki et al., 2001). However, following Rasip1 complete depletion (which occurs over time as Cre accumulates in Tie2 expressing ECs, by approximately E8.75), ECs fail to maintain lumens and collapse, indicating Rasip1 is required to maintain open vascular lumens during development.

Rasip1 recruits pMLC to EC contacts

To address the reason why Rasip1 depletion caused collapse of lumens, I have investigated molecules involved in tubulogensis, including apical and junctional proteins, and cell contractility regulators. To open vascular lumen, it has been shown that VE-cadherin is involved in polarity establishment (Strilic et al., 2009). Apical sialomucins are recruited at the EC-EC contacts, likely via VE-cadherin, and make small slits between EC-EC membranes by repulsion. Moesin and F-actin are subsequently recruited to sialomucins to facilitate lumen formation. VEGF-A signaling elevates ROCK activity to activate MLC, and in turn, pMLC recruits nm-Myosin II to alter cell shape. As lumen formation is impaired in the absence of Rasip1, I have examined whether these molecules are properly recruited to EC-EC contacts in *Rasip1$^{fl/fl}$;Tie2-Cre* mice during lumen opening at E8.0 **(Fig. 3.4)**. As expected, only low level of Rasip1 protein was detected by immunostaining in PECAM and endomucin expressing dorsal aortae ECs **(Fig. 3.4 A",B")**. PODXL, which is a lumen initiation molecule, was located properly at the apical lumen in both control and Rasip1 deficient ECs **(Fig. 3.4 C",D")**. As previously shown in *Rasip1$^{-/-}$* mice (Xu et al., 2011), junctional proteins were similarly located at apical and junctional EC contacts, indicating that the junctional molecule likely blocked lumen opening or lumen maintenance **(Fig. 3.4 a,b,c,d,e,f)**. Strikingly, pMLC, which is activated by RhoA/ROCK signaling and regulates cell actomyosin contractility via nm-Myosin II, failed to be recruited to the EC junctions in the absence of Rasip1 **(Fig. E",F")**. These results suggest that Rasip1 is

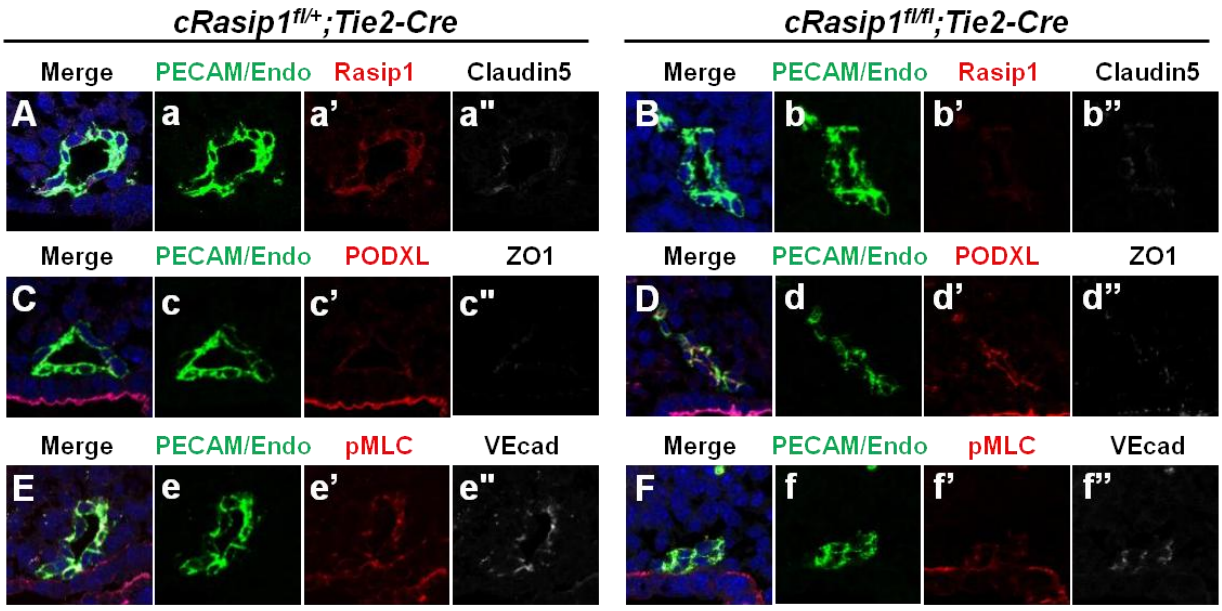

Figure 3.4. Impaired recruitment of pMLC at cell junctions in absence of Rasip1. Transverse sections of embryonic dorsal aortae ECs at E8.0 were examined by immunostaining with indicated antibodies. **(A-B,a',b')** The level of Rasip1 is decreased in PECAM and endomucin positive ECs in *Rasip1$^{fl/fl}$;Tie2-Cre.* **(C-D,c',d')** PODXL was normally localized to apical membrane of Ecs in Rasip1 mutant and control ECs. **(E-F,e',f')** Rasip1 deficient ECs failed to recruit pMLC to apical/junctional EC contacts. Tight juntions (a",b",c",d") and adherens junction (e",f") were seen at EC-EC junctions, however they were not completely segregated from lumenal membranes.

critical for activated pMLC recruitment to the EC contacts and for junction protein rearrangement during lumen formation, but not for apical sialomucins recruitment.

Rasip1 is required for vessel maintenance during later embryonic development

Because *Rasip1$^{fl/fl}$;Tie2-Cre* mutant embryos die by E10.5, we crossed the Rasip1 conditional allele to *Cad5-Cre^{ER}* driver line (Monvoisin et al., 2006), which expresses Cre recombinase under the control of VE-cadherin promoter in an inducible manner. To test whether Rasip1 is required in later development, we induced gene deletion at E9.5 by tamoxifen gavage, and looked at vascular defects at E12.5 **(Fig. 3.2 A)**. *Rasip1$^{fl/fl}$;Cad5-Cre^{ER}* embryos showed growth retardation compared to wild-type littermates, and hemorrhage was evident **(Fig. 3.5 A,B)**. Superficial vascular plexus were visualized with whole mount PECAM staining on limbs **(Fig. 3.5 C,D)**. Limb vasculature appeared thin and disconnected plexus in *Rasip1$^{fl/fl}$;Cad5-Cre*^{ER} embryo, indicating that Rasip1 is required for vessel maintenance after lumen formation **(Fig. 3.5 E,F)**.

3.2.2 Rasip1 is dispensable for blood vessel maintenance

To examine whether Rasip1 is required in adult mouse blood vessels, long after they are established, Rasip1 was deleted in 8 week old mice using inducible *Cad5-Cre^{ER}*. Tamoxifen was applied every other day for two weeks to effectively delete Rasip1. Following tamoxifen regimen, Rasip1 deletion was confirmed by polymerase chain reaction (PCR) using genomic DNA to detect the exon3-deleted allele **(Fig. 3.6 A)**. To confirm the deletion of exon3 by Rasip1 transcripts, exon2 and exon3 loci were examined. While exon2 was detected in *Rasip1$^{fl/fl}$;Cad5-Cre^{ER}*, exon3 was significantly reduced **(Fig. 3.6A)**. To confirm whether Rasip1 protein was depleted, western blot analysis was performed with lung tissues where Rasip1

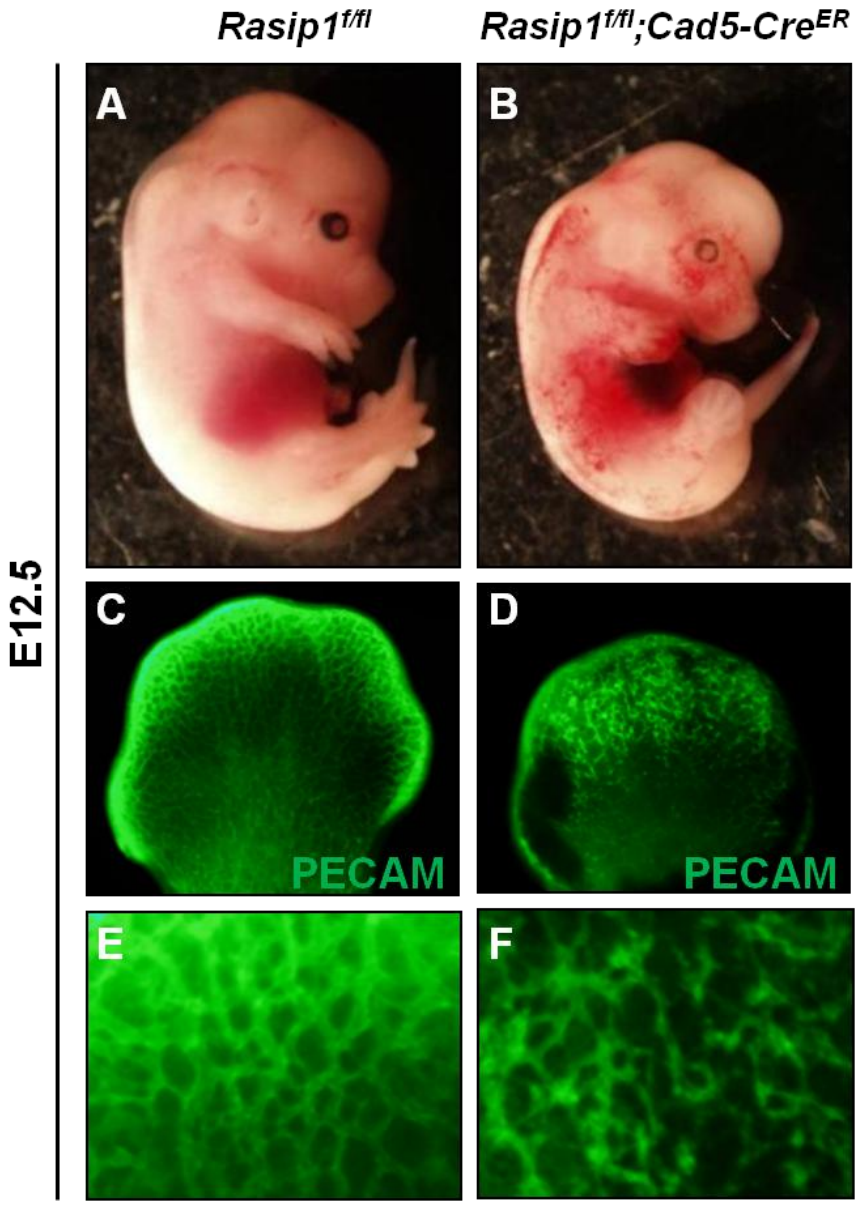

Figure 3.5. Rasip1 is required for embryonic blood vessel maintenance and lumen formation during late embryonic development. (A-B) Following tamixifen induction, Rasip1deficient *Rasip1$^{f/fl}$;Cad5-Cre^{ER}* embryos display gross retardation and hemorrhage. **(C-F)** Whole mount immunofluorescence for PECAM. In the absence of Rasip1, limb vasculatures fail to form lumens.

protein is most abundant. As expected, Rasip1 level was decreased in Rasip1 deficient lung (Mitin et al., 2004) **(Fig. 3.6 A)**. To visualize the Rasip1 deletion efficiency, *Rasip1$^{fl/fl}$;Cad5-Cre^{ER}* mice were bred with *Rosa26-Tomato* reporter mice. After tamoxifen induction, most of the ECs, examined in *Cad5-Cre^{ER}* mice, expressed tomato fluorescence in aortae **(Fig. 3.6 B)**. In addition, when immunofluorescence staining was performed for Rasip1 in the endothelium, lining the adult dorsal aorta, Rasip1 was not detected in *Rasip1$^{fl/fl}$;Cad5-Cre^{ER}* ECs **(Fig. 3.6 C,D)**.

Rasip1$^{fl/fl}$;Cad5-Cre^{ER} mice were grossly normal and healthy after tamoxifen regimen and Rasip1 deletion (data not shown). To examine whether Rasip1 depletion causes any defects in blood vessels, ear skin vessels were immunostained with PECAM **(Fig. 3.6 E,F)**. Rasip1 depleted vasculature appeared normal and indistinguishable from control vessels. The number of proliferating ECs in Rasip1 depleted aortae, marked with phospho-histone H3, was comparable with that in the control mice **(Fig. 3.6 G)**. It is likely that Rasip1 removal in ECs does not affect cell proliferation, cell death, or appearance.

3.2.3 Rasip1 is required in angiogenesis

Rasip1 is required for neonatal retinal vessel outgrowth

To study whether Rasip1 is required for blood vessel growth via angiogenesis *in vivo*, I examined retinal vessel growth in postnatal mice. Rasip1 was deleted ubiquitously, using inducible *Cagg-Cre^{ER}* driver line (Hayashi and McMahon, 2002), as Rasip1 is exclusively expressed in ECs in all tissues, including retina. I confirmed the EC-specific expression of Rasip1 using *in situ* hybridization, showing restricted expression of Rasip1 in retinal blood vessels **(Fig. 3.7 B).** Following tamoxifen treatment, Rasip1 was deleted, and retinas were analyzed at postnatal day (P) 6 **(Fig. 3.7 A)**. Vessels were visualized using isolectin B4 staining

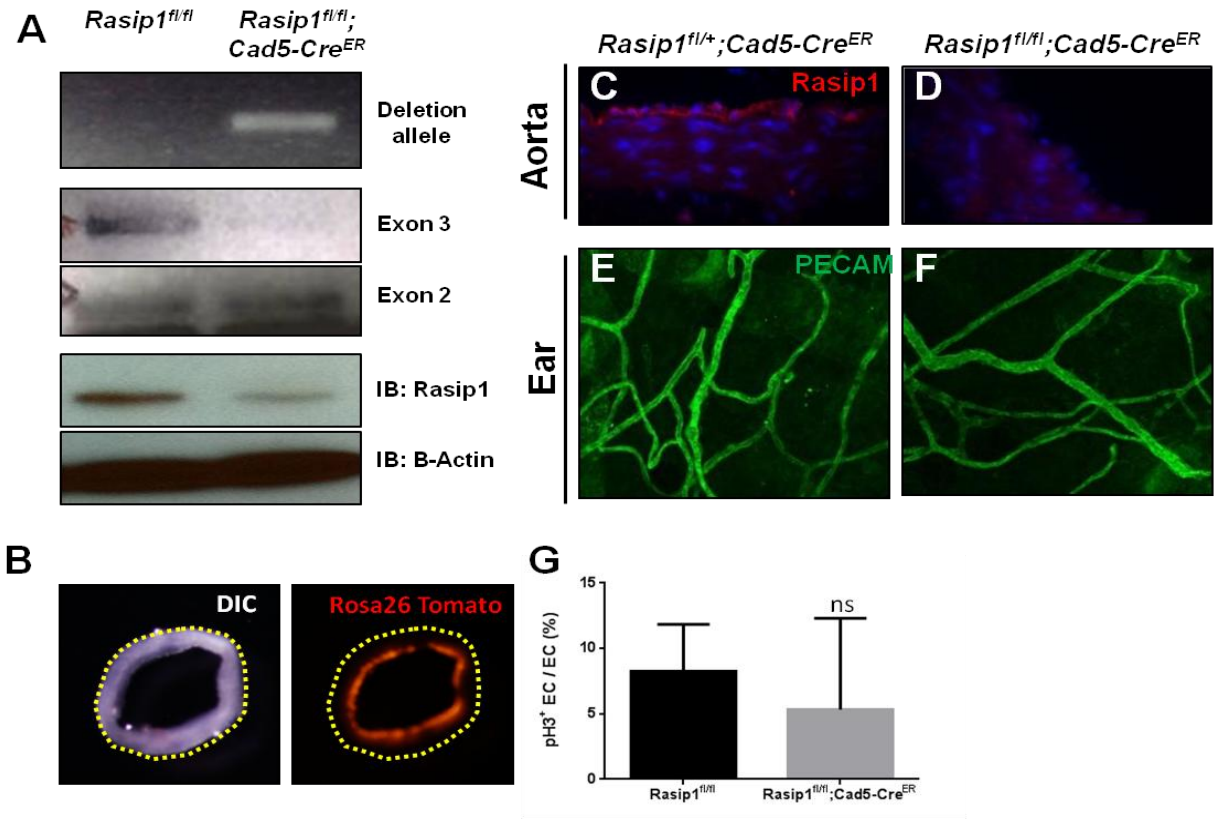

Figure 3.6. Rasip1 is dispensable for adult blood vessel maintenance. (A) Deletion of Rasip1 was confirmed by detecting floxed locus in deletion allele, lack of exon 3 in Rasip1 transcript, and Western blot analysis **(B)** Rosa26-Tomato allele was used to visualize Rasip1 deficient ECs in mouse aortae. **(C-D)** Rasip1 depletion is shown using immunofluorescence. **(E-F)** *Rasip1* deficient blood vessels in ear are morphologically normal compared to the control vessels. **(G)** Quantification of EC proliferation in aortae ECs.

(Fig. 3.7 D-N), and efficiency of Cre recombinase, following tamoxifen application, was examined using *Rosa26-tomato* reporter allele. Following tamoxifen application, not all ECs were tomato positive **(Fig. 3.7 C)**, indicating that there are ECs containing Rasip1.

To assess the requirement of Rasip1 in angiogenesis, neonatal retinal vessels were examined to determine if they are defective in vessel growth, remodeling, and lumen formation. Firstly, it was noted that Rasip1 depleted retinas showed significant decrease in blood vessel growth compared to control retinas **(Fig. 3.7 D,E)**. The quantification showed 23% reduction in vessel growth when the distance between optical stalk and vascular tip was measured **(Fig. 3.7 F)**. To determine whether reduced outgrowth in Rasip1 deficient vessels is resulted from decreased proliferation of ECs, BrdU incorporation assay was carried out. The number of BrdU positive ECs in Rasip1 mutant was similar to that in control **(Fig. 3.7 G-I)**, suggesting that Rasip1 deletion did not affect EC proliferation. It has been known that angiogenesis correlates with formation of angiogenic sprouts and filopodia at growing tip cells. The number of filopodia and sprouts were not affected by Rasip1 deletion **(Fig. 3.7 J-L)**. However, it was noted that Rasip1 depletion led to increased vascular density at vascular front with elevated number of ECs **(Fig. 3.7 M,N)**. In the growing retinal vascular plexus, Rasip1 deficient vessels displayed higher density of vascular front area by 18.5% (P value =0.0025) **(Fig. 3.7 I)**. The vessel outgrowth was likely reduced in the absence of Rasip1 due to failure in vessel remodeling.

Rasip1 deficiency cause unstable vessel plexus and elongated vessels

In addition to increased density, retinal vessels displayed unstable and poorly organized plexus in Rasip1 deficient retinas. Rasip1 deficient plexus often displayed thin vessels at the periphery of the vascular front, as shown in the embryonic Rasip1 depleted dorsal aortae. To examine vessel stability in Rasip1 deficient plexus, type IV collagen was used to visualize EC track, as basement membrane of blood vessels persist after ECs disappear. Many of Collagen

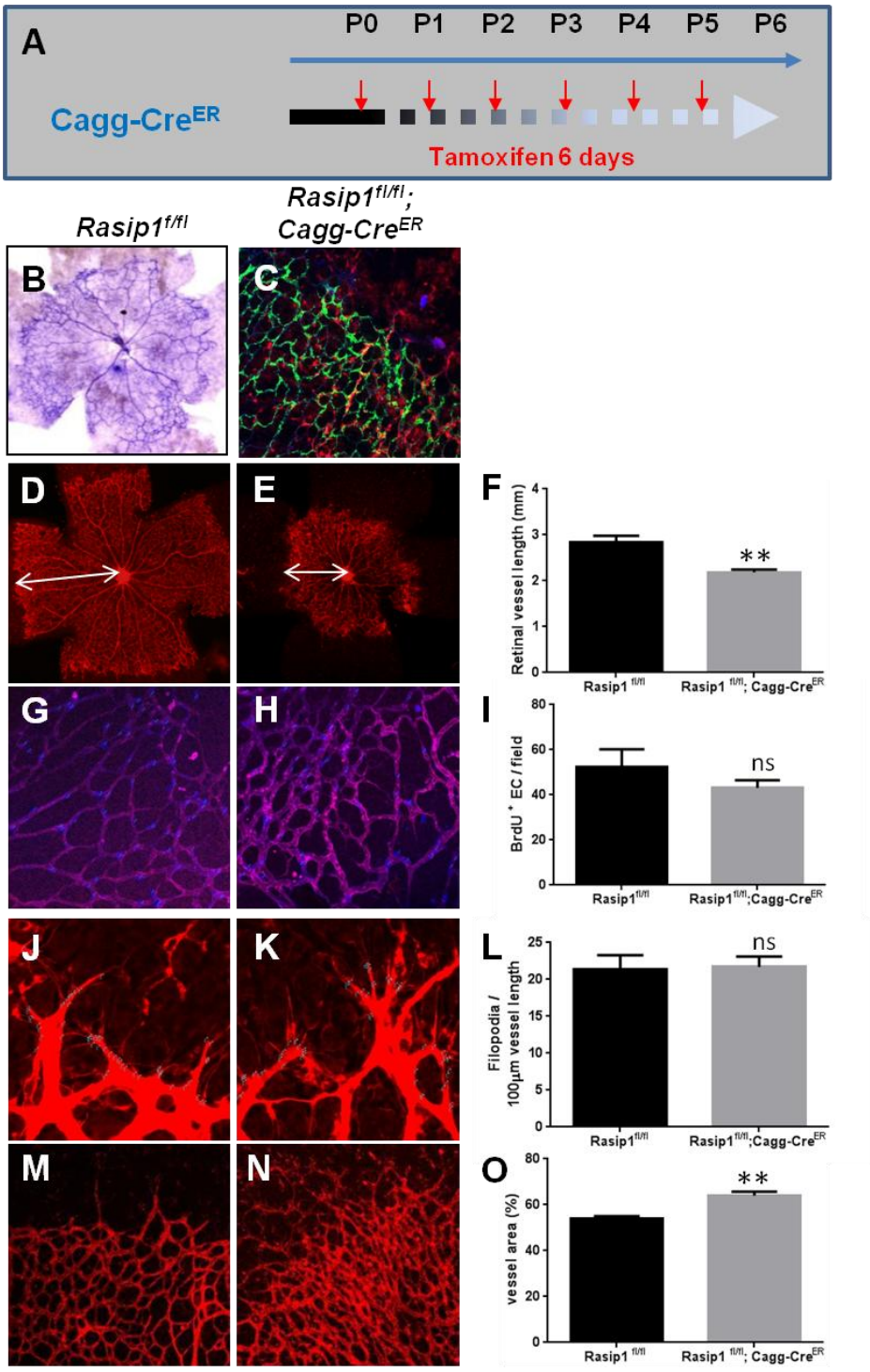

Figure 3.7. Rasip1 is essential for retinal vessel outgrowth. (A) A diagram for tamoxifen induction into the pups for Rasip1 ablation. **(B)** *In situ* hybridization with Rasip1 probe. **(C)** Tamoxifen efficiency was shown with Rosa26-Tomato reporter. **(D-O)** Isolectin B4 staining of whole mount P6 retinas. Quantification of distance between optical stalk and tips (D-F), BrdU positive ECs (G-I), number of filopodia protrusions (J-L), vascular area at vessel plexus margins (M-O). *P<0.05, values represents mean ± s.e.m.

IV positive area in Rasip1 mutant did not co-localize with IB4 positive blood vessels in vascular front, where thin sprouts exist **(Fig. 3.8 A-C)**. This revealed blood vessel basement track left by retracting tip vessels, indicating failure in stabilization of remodeling vessels in the absence of Rasip1. In addition, at the sprouting vascular front, Rasip1 depleted tip cells showed elongated and thin sprouts which failed to anastomose with neighboring vessels. In wild-type vessels, all the sprouts formed well-organized vascular network by anastomosis process, which makes a bridged connection between two neighboring sprouts. In Rasip1 deficient vessels, however, elongated and thin sprouts were seen frequently. Those sprouts were protruding but did not form branch with neighboring sprouts **(Fig. 3.7 D,E)**. The number of elongated sprouts was significantly increased in Rasip1 deficient sprouts, indicating failure in anastomosis **(Fig. 3.7 F)**.

Rasip1 depleted vessels fail in proper lumen formation

During vasculogenesis, Rasip1 was identified as a critical factor for lumen formation. To examine whether Rasip1 has the same function for lumen formation during angiogenesis, fluorescein isothiocyanate (FITC)-dextran was injected into the vascular lumens by perfusion. Dextran was traveling through the lumenized vessels in the retinal plexus, and most of the vessels were containing dextran in their lumen in wild-type **(Fig. 3.8 G)**. In contrast, dextran containing lumens were reduced in Rasip1 depleted vessels, indicating decreased lumen area, and all the thin and elongated sprouts displayed lack of dextran perfusion **(Fig. 3.7 H)**. In Rasip1 depleted vessels, dextran was seen in many vessels, indicating that Rasip1 depleted vascular plexus had open lumen, likely due to the incomplete Rasip1 depletion in the ECs **(Fig. 3.7 C)**. Quantification of the dextran perfused area in growing vessels showed 72% reduction in the mutants **(Fig. 3.7 I)**. All together, these data suggest that Rasip1 is required for proper lumen formation and vascular plexus remodeling.

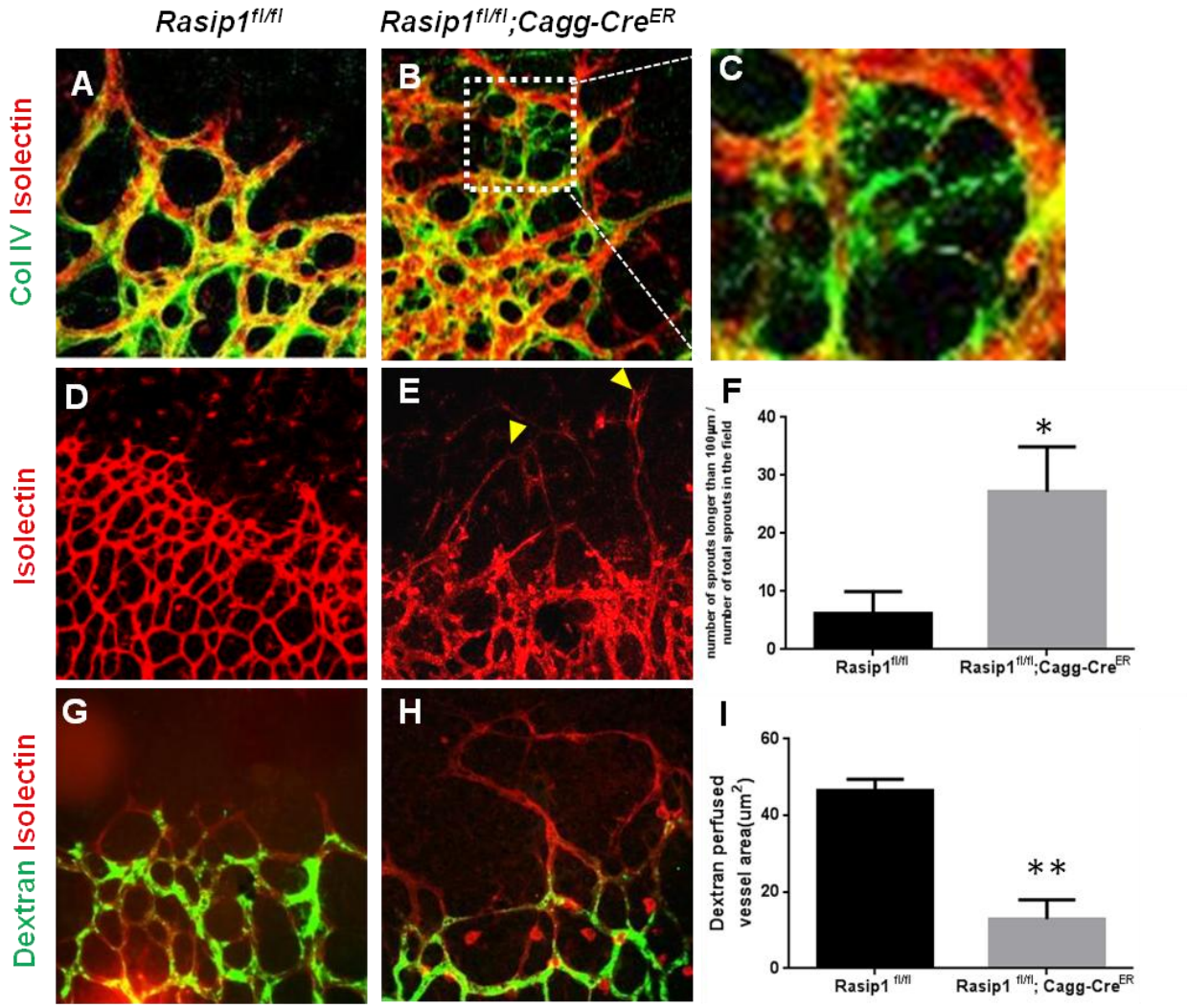

Figure 3.8. Rasip1 is required for retinal blood vessel remodeling and lumen formation. (A-C) Whole mount immunofluorescence for Isolectin B4 and Col IV. Col IV positive areas without vessel were detected in *Rasip1$^{fl/fl}$;Cagg-Cre^{ER}* indicating vessel regression is increased in the absence of Rasip1. **(D-F)** Elongated sprouts (yellow arrowheads) were seen in *Rasip1$^{fl/fl}$;Cagg-Cre^{ER}*. The numbers of prouts longer than 100μm were quantified. **(G-I)** FITC-dextran was perfused into retinal vessel intralumen. Quantification of dextran perfused area shows that lumenal space is decreased in the absence of Rasip1. *P<0.05, values represents mean ± s.e.m.

Rasip1 is required for adult angiogenesis

To investigate whether Rasip1 is required for angiogenesis in adult mice *in vivo*, like in neonatal retinal vessels, I performed an assay for subcutaneous blood vessel growth called directed *in vivo* angiogenesis assay (DIVAA) in *Rasip1$^{fl/fl}$;Cad5-Cre^{ER}* mice. In this assay, we implanted silicon tubes (called angioreactors) containing basement membrane extract (BME) mixed with fibroblast growth facter-2 (FGF-2), and vascular endothelial growth factor (VEGF) into tamoxifen treated mice and control mice subcutaneously **(Fig. 3.9 A)**. After two weeks of vessel growth, angioreactors were taken out from the mice. ECs expressing Cre recombinase were visualized by using *Rosa26-Tomato* reporter mice. Vessel growth were seen in angioreactors **(Fig. 3.9 B-C)**, and Tomato labeled ECs revealed that Rasip1 depleted ECs decreased vessel invasion into the angioreactor **(Fig. 3.9 B'-C')**. When ECs, invaded into the angioreactors, were analyzed based on EC numbers in the angioreactors using FITC-lectin, the number of ECs in the angioreactors in *Rasip1$^{fl/fl}$;Cad5-Cre^{ER}* mice were significantly reduced compared to that in control mice **(Fig. 3.9 D)**. These results suggest that Raip1 is required for FGF/VEGF-induced angiogenesis in adult vessels.

Intracellular localization of Rasip1

To gain an insight of molecular and cellular function of Rasip1 in ECs, intracellular localization of Rasip1 and Rasip1 mutants was investigated in cultured ECs **(Fig. 3.10 A)**. Rasip1 has characteristic domains: Proline rich(PR) domain, Ras associating (RA) domain, forkhead associated domain(FHA), and dilute domain (Mitin et al., 2004). To examine the functions of them, it was tested whether absence of domains affects proper Rasip1 localization. Rasip1 is known for its scattered punctae localization at juxta golgi region in cytoplasm (Mitin et al., 2004; Xu et al., 2011), so we postulated that Rasip1 may be involved in vesicles and function in vesicular transport. Various versions of GFP-tagged Rasip1 mutants were generated

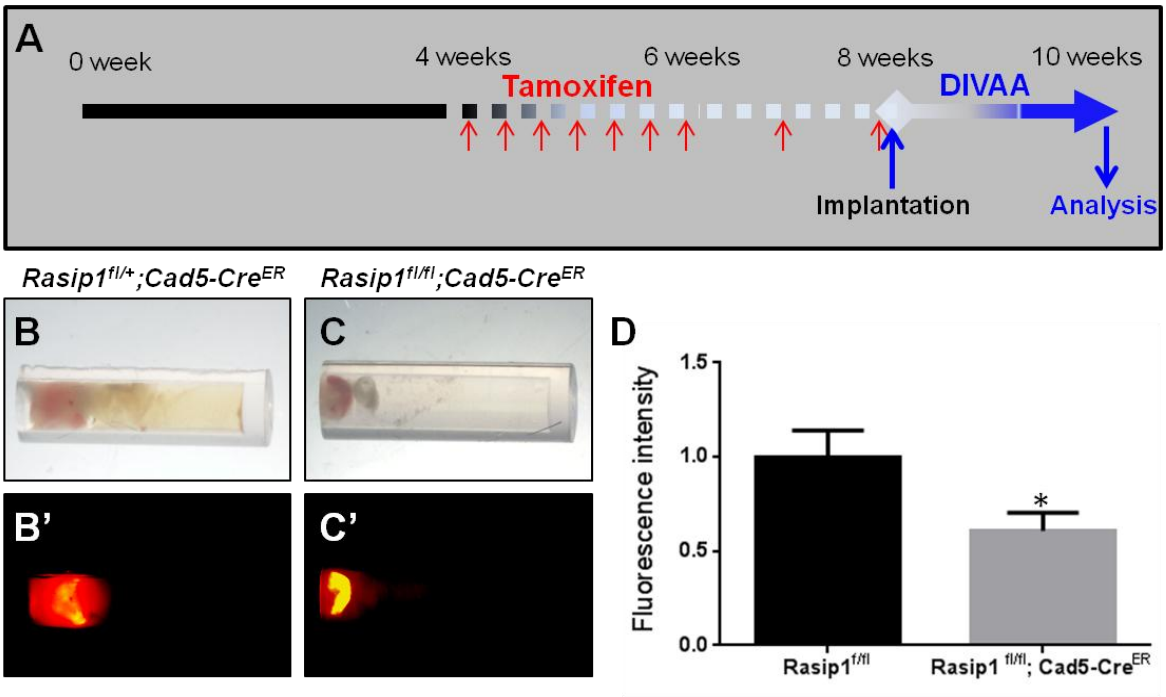

Figure 3.9. Rasip1 is required for angiogenesis in adult subcutaneous vasculature. (A) Schematic diagram of Tamoxifen induction and DIVAA experiment. (B-C) Invaded ECs into DIVAA angioreactor. (B'-C') Rosa26-Tomato reporter allele shows ECs in angioreactor. (D) Fluorescein-Lectin detection of EC in angioreactor. The fluorescent intensity was measured and normalized to the control. *P<0.05, n=15, values represents mean ± s.e.m.

(by Ke Xu in lab and provided by Natalia Mitin). GFP control proteins were seen smoothly distributed in the cytoplasm **(Fig. 3.10 a)**, and GFP-Rasip1 full length proteins localized as punctae in the cultured ECs **(Fig. 3.10 b)**. Interestingly, PR domain deletion caused smoothened localization and punctae pattern was not observed, indicating that PR domain is responsible for vesicle localization of Rasip1 **(Fig. 3.10 c)**. Another interesting feature was dilute domain. In the absence of dilute, mutant positive vesicles were aggregated and not fused properly, resulting in a grape shape **(Fig. 3.10 d)**. These suggest that dilute domain may be required for vesicle fusion. When only dilute domain was overexpressed in ECs, bigger vesicles were formed, indicating that dilute domain targets to vesicles, but is not able to transport. **(Fig. 3.10 e)**. All together, each domain of Rasip1 examined is responsible for proper Rasip1 localization and may function in vesicle transport.

Transient localization of Rasip1at EC-EC contacts during EC tube formation assay

It was previously demonstrated that Rasip1 is required for angiogenesis in matrigel tube formation assay (Xu et al., 2009), and tubulogenesis in mouse aortae (Xu et al., 2011). Therefore, it was thought that Rasip1 may function at EC-EC contacts to make EC plexus on matrigel or open lumen in aortae ECs respectively. To test this, Rasip1 localization was examined in HUVECs during matrigel tube formation assay **(Fig. 3.10 B)**. Interestingly, Rasip1 was localized transiently to cell-cell junctions. In an isolated single cell, before tube formation, Rasip1 was randomly seen in the cytoplasm **(Fig. 3.10 f)**. ECs then initiated aggregation on matrigel, and Rasip1 was highly enriched at cell-cell contacts in two EC and multiple EC aggregates **(Fig. 3.10 g,h)**. Later, when ECs formed plexus network, Rasip1 was dissociated from the cell contacts and seen in a scattered manner in cytoplasm **(Fig. 3.10 i)**. The dynamic localization change of Rasip1 implicates that Rasip1 transiently function at EC-EC adhesion to regulate the tube formation process.

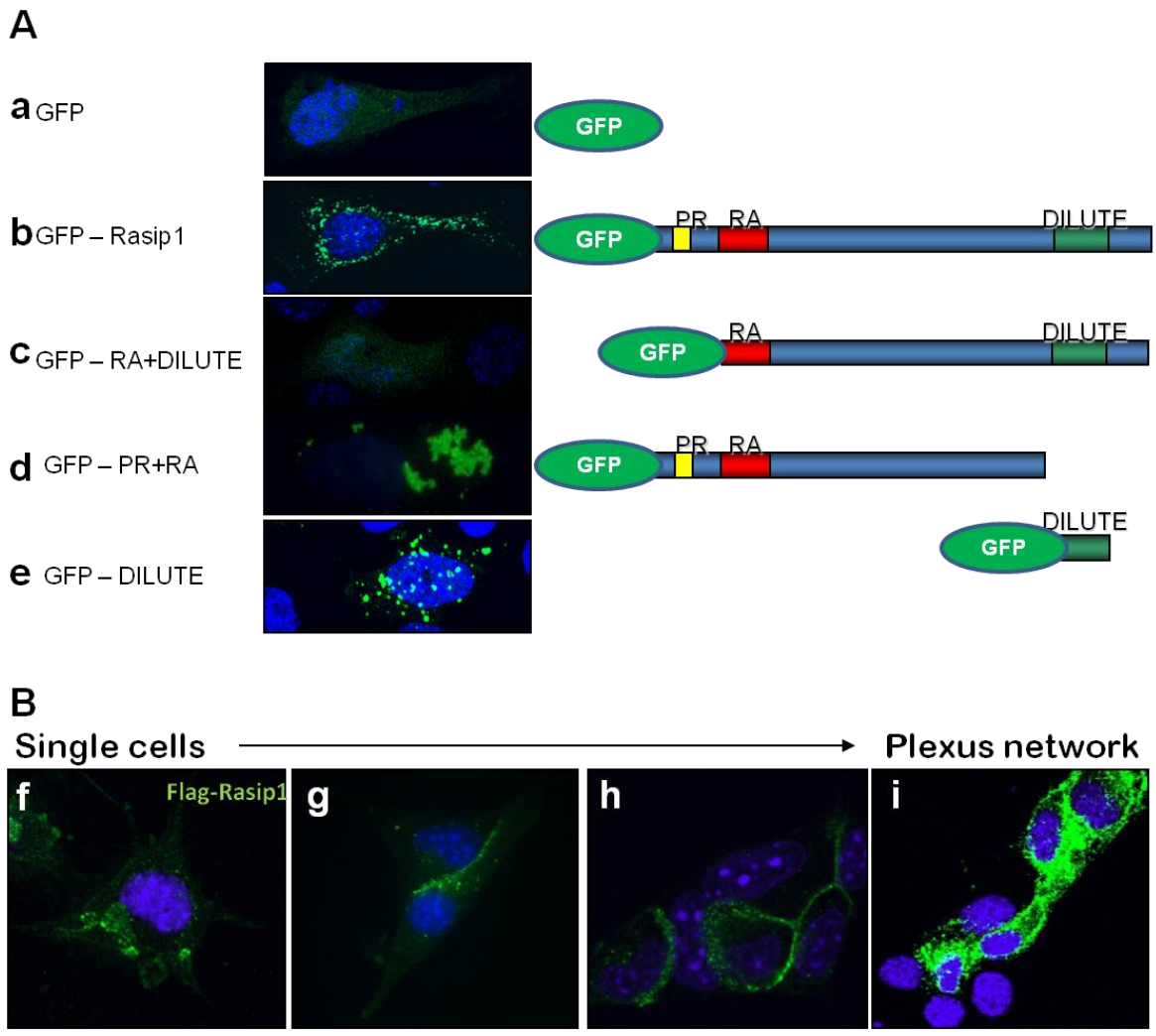

Figure 3.10 Localization of Rasip1 and Rasip1 mutants in cultured ECs. (A) Rasip1 domain deletion variants shows different intracellular localization pattern. **(B)** Rasip1 transiently associates with cell-cell contacts during matrigel tube formation assay.

3.3 Discussion

3.3.1. Rasip1 is essential for lumen formation during vasculogenesis

Rasip1 is required for lumen formation

It was previously identified that Rasip1 is critical for vascular tubulogensis (Xu et al., 2011), and this idea has been challenged by Wilson *et al*., who proposed that Rasip1 is not required for de novo lumen formation, as patent lumen was observed in Rasip1 knockout mice. Here, I confirmed that Rasip1 is essential for lumen formation by using independently generated conditional Rasip1 mice, supporting the first observation. From conditional Rasip1 mice, *Sox2-Cre* driven universal Rasip1 null mice were generated, which phenocopied tubulogenesis defect. Rasip1 requirement for lumen formation was also confirmed by using *Tie2-Cre* driver mice. Although *Tie2-Cre* transgenic mouse has been reported as early Cre expressing mouse line in endothelium (Kisanuki et al., 2001), complete Rasip1 removal was seen to be delayed. Despite its early expression of Cre recombinase, Rasip1 was not completely eliminated in ECs until E8.5, and this led *Rasip1$^{fl/fl}$;Tie2-Cre* to initiate tubule formation, as opened lumens were seen in 5-6s embryos. These results support the previous proposal that Rasip1 is essential for vasculogenesis.

Rasip1 is required for pMLC recruitment

In recent studies, it has been proposed that mouse aortic lumen formation occurs by cell polarity establishment, followed by relocalization of junctional proteins and cell shape changes during embryonic vasculogenesis (Strilic et al., 2009). Based on this extracellular lumen formation mechanism, VE-cadherin is required for recruiting CD34-sialomucins to the cell-cell contact sites during mouse aortae vasculogenesis (Strilic et al., 2009). CD34-sialomucins further localize F-actin and non-muscle myosin II to the lumenal membranes. To investigate whether Rasip1 is involved in these sequential vasculogenesis steps, Rasip1 depleted mouse

aortae were assessed. In the absence of Rasip1, VE-cadherin and PODXL localized properly to the EC junctions, however it was noted that pMLC was not recruited. This result is opposed to a previous report that Rasip1 knockdown increases RhoA activity via loss of Arhgap29 interaction, consequently elevates ROCK/pMLC/NMHCIIA signaling in *in vitro* lumen formation assay (Xu et al., 2011). As *in vitro* assay is performed with whole EC lysates from the vasculogenesis assay, it is therefore hypothesized that Rasip1 may control pMLC spatially at EC junctions. Further investigation is required to understand precise Rasip1 function in pMLC regulation at EC contacts.

3.3.2. Rasip1 is dispensable in adult vessel maintenance

The notion of active signaling for vascular maintenance has been demonstrated (Murakami, 2012), since vascular maintenance has received attention as clinical treatments for vascular diseases has failed due to interruption in vessel integrity. I have been shown that signaling pathways, including VEGF, Tie2, and Notch signaling, regulate junction stabilization and vessel integrity. Interruption of these pathways resulted in vascular abnormalities and malformations, and caused severe clinical conditions. As Rasip1 is critical for embryonic tubulogenesis, it was expected that Rasip1 deletion in adults would cause severe vascular problems. However, Rasip1 deficient mice appeared healthy and lived for a long term without any chronicle health conditions. Proliferation, cell death, and morphological appearance were not affected by absence of Rasip1. From these data, Rasip1 is seemed to be dispensable in established and quiescent vessels. Previously, it was demonstrated that Rasip1 is required for maintenance of EC permeability in cultured ECs (Post et al., 2013). Rasip1 regulates Rap1 induced RhoA activity, and in turn formation and contraction of stress fibers, attached to VE-cadherin based AJs. Rasip1 depletion caused irregular and highly dynamic junctions, resulting in increased cell permeability. Although unchallenged Rasip1 deficient adult mice did not display

any defects, it is possible that depletion of Rasip1 causes decreased EC permeability, and further investigation is required.

3.3.2. Rasip1 is required for angiogenesis

Following vasculogenesis, blood vessels expand via angiogenesis, which happens through activation of quiescent ECs, sprouting, proliferation, anastomosis, and lumen formation. As angiogenic process occurs in many pathologic conditions, angiogenesis has been extensively studied to treat diseases. Consequently mechanisms, signaling pathways, and different molecules regulating angiogenesis have been revealed. In previous study, potential Rasip1 function in angiogenesis was tested *in vitro* by using matrigel tube formation assay and wound healing assay. From these assays, Rasip1 depletion inhibited EC tube formation and cell motility, suggesting that Rasip1 is likely required for angiogenesis (Xu et al., 2009).

To examine angiogenic role of Rasip1 *in vivo*, we used two different model systems; neonatal retinal vessel angiogenesis, and adult subcutaneous vessel angiogenesis. In the first model, it was shown that Rasip1 deficient retinal vessels displayed various angiogenic defects; significantly reduced vessel outgrowth, higher vascular density, elongated vessels at the tips and unstable vessels. Interestingly, elongated vessels often found in Rasip1 depleted sprouts, which failed to make connections with neighboring sprouts. The same phenotype was previously reported in macrophage specific Notch1 deficient mice. In the study, it was shown that macrophages interact with Dll4 positive tip cells and activate Notch signaling to promote anastomosis (Outtz et al., 2011). It is, therefore, speculated that impaired Notch signaling possibly caused failure in anastomosis via macrophages in Rasip1 depleted retina, resulting in elongated vessels.

Previously Rasip1 has been shown to play a critical role in lumen formation (Xu et al., 2011). Therefore, it was thought that Rasip1 possibly functions in angiogenic lumen formation,

and tubulogenesis would be blocked in the absence of Rasip1. To test this, fluorescence labeled dextran was injected into control and Rasip1 deficient intravessels to visualize lumens. Dextran was detected in both control and Rasip1 mutant mice, but in the absence of Rasip1, the retinal vessels displayed perturbed lumens at newly growing vascular tips, indicating that Rasip1 is required for angiogenic lumen formation. In the Rasip1 deficient vessels, existing lumen was possibly formed due to inefficient Rasip1 deletion.

3.3.4. Summary

In this study, Rasip1 was established as a critical factor regulating tubulogenesis during vasculogenesis and angiogenesis *in vivo* by using Rasip1 conditional knockout mouse. During embryogenesis, Rasip1 deficiency caused failure in lumen formation, as previously shown (Xu et al., 2011). Rasip1 is also required for embryonic lumen maintenance after initiation of lumen formation, as Rasip1 deficiency caused discontinuous blood vessels in embryos. However, quiescent adult vessels remained intact in the absence of Rasip1, suggesting that Rasip1 is dispensable for established vessel maintenance. During angiogenesis, Rasip1 depletion caused significant reduction in angiogenesis partially due to failure in vessel remodeling. Rasip1 removal was also affected angiogenesis in adult, as shown in DIVAA experiment. However, when Rasip1 was depleted in the adult, when most blood vessels are established, it did not cause any defects on blood vessel lumen maintenance. Together, these findings suggest that Rasip1 is critical for angiogenesis during developing vasculature, but not for maintenance of stable vasculature.

Angiogenesis research has received clinical attention with numerous new findings, tools, and methods. Despite rapid progress, many basic questions have remained to be answered. Further study of Rasip1 as an essential factor for angiogenesis and tubulogenesis will lead us to better understand the mechanism of angiogenesis and lumen formation. In addition, taking the

advantage of dispensability, Rasip1 has a great potential as a key for clinical therapies to treat vascular diseases.

Chapter 4. ARHGAP29 IS REQUIRED FOR PLACENTA AND CARDIOVASCULAR DEVELOPMENT

Here, I will discuss my preliminary findings regarding the role of the Rasip1 binding partner Arhgap29. Our lab identified this RhoA inhibitory protein as associating with Rasip1 in endothelial cells.

4.1 Introduction

Arhgap29 identification as a Rho GTPase effector

Arhgap29, Rho GTPase protein activating protein 29, was originally identified as a RhoA GTPase effector (Saras et al., 1997). As a member of Ras-like GTPases, Rho GTPases functions as molecular switches, cycling between active GTP-bound and inactive GDP-bound states. RhoA is negatively regulated by Rho GTPase activating proteins, called RhoGAPs. These effectors catalyze the intrinsic GTPase activity of G proteins, and in this case, shift Rho to a GDP-bound state. As a RhoGAP, Arhgap29 was found to be responsible for GTP hydrolysis activity with a preference for Rho over Rac and Cdc42. Arhgap29, together with Ras interacting protein 1 (Rasip1), was identified as a Rho signaling regulator in endothelium (Xu et al., 2011). Depletion of Arhgap29 in cultured ECs increased active RhoA/ROCK/Myosin II signaling, resulting in modified cell architecture and contractility, as well as blocking lumen formation.

Arhgap29 identification as a Rap1/2 GTPase effector to regulate RhoA

Arhgap29 also regulates Rap GTPase signaling, and was first reported as a Rap2 effector (Myagmar et al., 2005). Arhgap29 was identified by yeast two hybrid screening performed with Rap1 as bait. Ahrgap29 was specifically bound to the active form of Rap2 via its ZPH region, but not dominant negative or GDP bound inactive Rap2. Furthermore, Myagmar et al. demonstrated that Arhgap29 inactivated Rho GTPase signaling to regulate the actin cytoskeleton under the control of Rap2 signaling pathway. Inactivation of RhoA by Arhgap29 caused loss of actin stress fibers in Arhgap29 over-expressing fibroblasts. In addition to Rap2, Rap1 has recently been noted as one of the Arhgap29 regulators (Post et al., 2013). Together with Rasip1, Arhgap29 functions in downstream of the Rap1 pathway to modulate Rho signaling and actin dynamics.

Arhgap29 expression in heart, placenta, and cleft palate

While *in vitro* studies of Arhgap29 demonstrated that it regulates the cell cytoskeleton via GTPase signaling, its functions *in vivo* remain unknown. A few publications describing Arhgap29 expression profiles in human or mouse tissues provide insights into Arhgap29 functions. The mRNA transcripts of Arhgap29 were first detected by northern blot analysis from human tissues, including heart, placenta, skeletal muscle, and pancreas (Saras et al., 1997). It was also identified as an early cardiac expressed gene by transcriptional profiling from mouse embryonic stem cells (Miller et al., 2008). By using a transgenic mouse line expressing GFP under the control of cardiac gene, Nkx2-5, cardiac cells were isolated from embryos at E7.5-9.5. Arhgap29 was one of the genes most highly expressed in the GFP positive cardiac cells, the cardiac crescent and surrounding tissues at E7.5 by *in situ* hybridization. At E8.5, and E9.5, Arhgap29 expression was enriched in the branchial arches, inflow and outflow tract, and other tissues. Craniofacial expression of Arhgap29 was also found by *in situ* hybridization in the developing embryo between E10.5 and E14.5 (Leslie et al., 2012). Mutation in Arhgap29 protein coding exons causes nonsyndromic cleft lip with or without cleft palate (NSCL/P), a common birth

defect. In addition, our lab reported Arhgap29 expression in mouse dorsal aortae at E8.5 (Xu et al., 2011). We proposed that Arhgap29, together with Rasip1, controls EC contractility via RhoA signaling, resulting in tubulogenesis of mouse aortae. These studies indicate that Arhgap29 expression is detected in various tissues and may have various roles as embryos develop.

In order to study function of Arhgap29 *in vivo*, I generated Arhgap29 genetic models of ablation in mice. Strikingly, Arhagp29 deficient embryos displayed failure of allantois-chorion fusion, and cardiovascular defects. Arhgap29 expression patterns were correlated with the sites of defects, as Arhgap29 transcripts were detected in allantois, blood vessels and heart. Here, I suggest that the Arhgap29 is likely involved in cell adhesion and RhoA regulation in chorioallantois and cardiovascular tissues.

4.2 Results

4.2.1 Arhgap29 is required for chorioallantois fusion

Generation of conditional Arhgap29 knockout mice

Arhgap29 has been studied *in vitro* to understand its functions and its mechanism of action as a Rho GTPase regulator, however its role *in vivo* had not been examined yet. As broad and diverse expression of Arhgap29 has been reported, we generated a conditional knockout mouse to study loss of function for Arhgap29 in different types of tissues *in vivo*. The targeting vector was designed to remove *exon 4* and *exon 5*, which results in elimination of Arhgap29 expression **(Fig. 4.1 A)**. A targeting vector acquired from the EUCOMM KOMP consortium was injected into ES cells, and I screened recombined ES cells by Southern blot analysis. The ES cells containing targeted allele were determined by probes detecting 5’ arm and 3’ arm **(Fig. 4.1 B)**. The ES cells with targeted allele were injected into blastocysts and

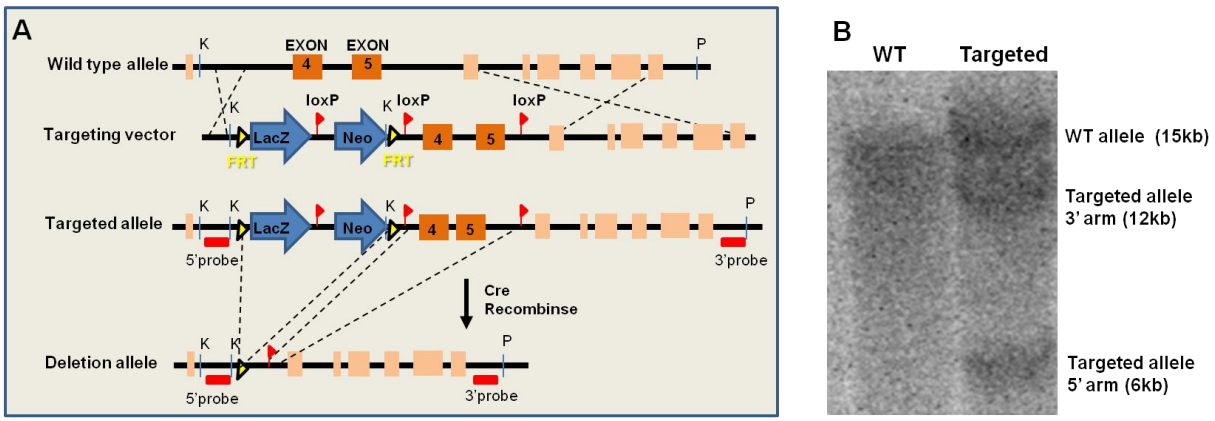

Figure 4.1. Generation of conditional Arhgap29 knockout mouse. (A) Diagram showing the vector for generation of conditional *Arhgap29* knockout allele. Exon 4 and 5 will be deleted by homologous recombination. **(B-C)** Confirmation of the targeted allele in ES cells by **(B)** Southern blot, and **(C)** PCR with gDNA. K, KpnI cutting site; P, PstI cutting site.

Arhgap29Neo/LacZ$^{fl/fl}$ mice were subsequently obtained. The targeted allele in the mouse was confirmed by polymerase chain reaction (PCR) with genomic DNA **(Fig. 4.1 C)**. β-galactosidease (LacZ*)* staining was performed to confirm cassette integration and examine the Arhgap29 expression profile, however unfortunately no LacZ expression was detected in embryos (data not shown), likely due to gene disruption.

Arhgap29$^{-/-}$ *mice display embryonic lethality*

To generate a *Arhgap29* global null mouse, *Arhgap29Neo/LacZ*$^{fl/fl}$ mice were bred with Sox2-Cre (Hayashi et al., 2002). This breeding allows Arhgap29 expression to be ablated ubiquitously and generate a null allele. Heterozygous *Arhgap29* mice were viable and no defects were detected from embryogenesis through adulthood. By contrast, *Arhgap29*$^{-/-}$ pups were not obtained, therefore I investigated whether *Arhgap29* null embryos are embryonic lethal. Embryo lacking Arhgap29 looked relatively normal, and were not distinguishable from wild-type or heterozygous littermate to stage E8.5 **(Fig. 4.2 A,B)**. However, at E9.0, *Arhgap29* null

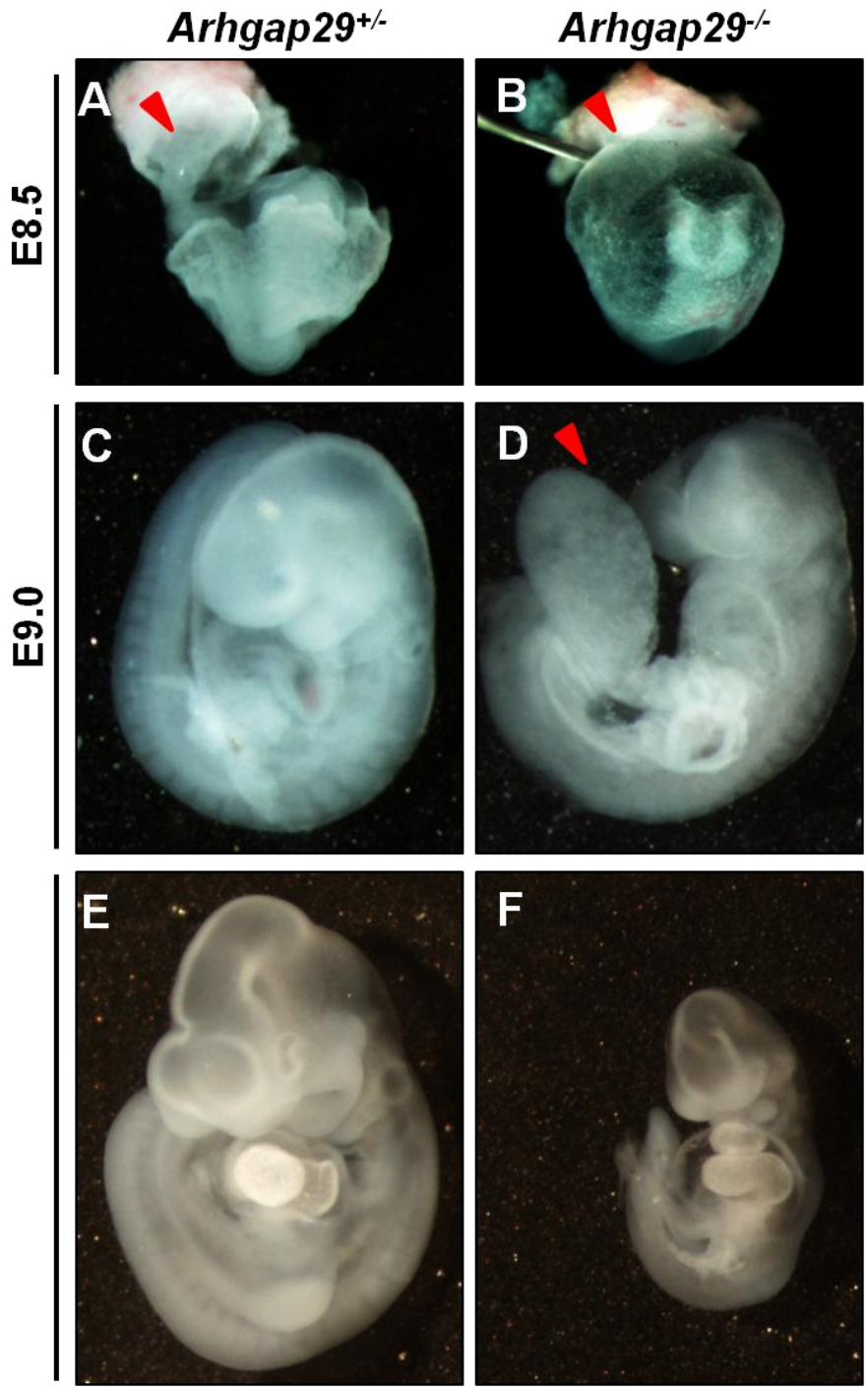

Figure 4.2. In *Arhgap29*$^{-/-}$, allantois fails to fuse to placenta during embryonic development. (A-B) Wholemount of E8.5 littermate mouse embryos. *Arhgap29*$^{-/-}$ is indistinguishable from its heterozygous littermate. **(C-D)** E9.0 littermate mouse embryos. *Arhgap29*$^{-/-}$ embryo displays delayed growth, and swollen sac of allantois. **(E-F)** E9.75 embryo litermates. *Ahrgap29*$^{-/-}$ is significantly smaller that the heterozygous and has edema around heart .

embryos displayed gross growth retardation **(Fig. 4.2 C,D).** By E9.75, the size of *Arhgap29* null embryos were significantly smaller than Arhgap29 heterozygous littermates and obvious edema around heart was observed **(Fig. 4.2 E,F)**. The ratio of the number of *Arhgap29*$^{-/-}$ embryos were met the expected Mendelian frequency (25%), but decreased after E9.0 (**Table 4.1**, data not shown), indicating embryonic lethality.

Arhgap29$^{-/-}$ *embryos show chorio-allantois fusion defects*

To find the cause of lethality, *Arhgap29* embryos between E8.5 and E9.75 were analyzed. Surprisingly, I noticed that the allantois of *Arhgap2* $^{-/-}$ embryos were larger and swollen at E9.0 **(Fig. 4.2 D)**. The allantois is the precursor of the umbilical cord and is used for nutrient and gas exchange between the embryo and the mother (Arora and Papaioannou, 2012). In the mouse, the allantois emerges from posterior of the embryo then approaches and fuses with the chorion at 4-6 somites. The fusion is completed by E8.75, and the chorio-allantoic plate is formed. The vasculature of the allantois grows into the chorion and placenta, and remodel to form umbilical vessels. By E9.0, the allantois normally attaches to the chorion to develop the placenta. However, in *Arhgap29* $^{-/-}$ embryos, the allantois was isolated and not connected to the placenta. Therefore, I speculated lack of chorio-allantois fusion led to embryonic lethality in Arhgap29 null embryos due to lack of essential nutritional resources.

Expression of Arhgap29 in the allantois

The defective fusion between allantois and chorion suggests that Arhgap29 may function in these tissues. Domains of Arhgap29 expression have been previously reported in several studies. Arhgap29 expression has been reported to be present in human placenta (Saras et al., 1997), in addition to cardiac and craniofacial tissue during mouse development (Leslie et al., 2012; Miller et al., 2008). However the precise site of expression in the allantois during development has not been reported or shown. To investigate its expression in allantois, *in situ*

Embyonic day	Arhgap29$^{+/+}$	Arhgap29 $^{-/+}$	Arhgap29 $^{-/-}$	total
E9.0	2	10	4	16
	13%	63%	25%	
E9.75	1	6	1	8
	13%	75%	13%	
Mendelian ratio	25%	50%	25%	100%

Table 4.1. The number and percentile of genotypes of *Arhgap29*$^{-/-}$ embryos. Among the investigated embryos, the ratio of *Arhgap29*$^{-/-}$ met the expected mendelian ratio, however, it is decreased later at E9.75.

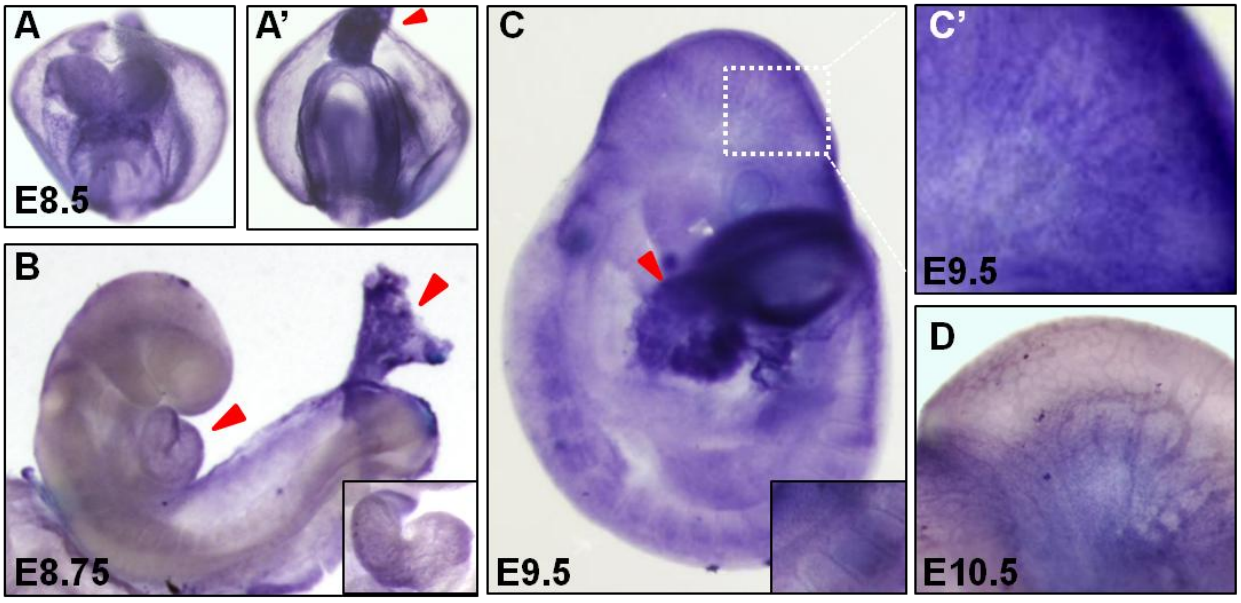

Figure 4.3. *Arhgap29* expression was detected by *in situ* hybridization. (A-A') Anterior and posterior view of whole mount embryos. At E8.5, *Arhgap29* is detected widespread, but strongly in **(A)** heart and **(A')** allantois. **(B)** At E8.75, the expression is noted in allantois, heart (inset), and somites. **(C,C')** At E9.5, *Arhgap29* presents at the distal tip where umbillical vessel forms. Vasculature expression is seen in (inset) intersomatic vessels and **(C')** head. **(D)** Expression of *Arhgap29* becomes more specific in the head vessels at E10.5.

hybridization was performed in the mouse embryo between E8.25 and E10.5. As predicted, strong expression of Arhgap29 was observed in the allantois at E8.25 and E8.75, and at E9.5 **(Fig. 4.3 A',B,C)**, confirming that Arhgap29 is indeed present in the allantois where it is required for allantois fusion.

Cardiovascular expression of Arhgap29

To gain insights into Arhgap29 function in other tissues, I investigated the expression pattern of Arhgap29 in the embryo. Arhgap29 was expressed in a widespread manner, however, the expression was stronger in the cardiac crescent and neural tube at E8.5 **(Fig. 4.3 A)**. Its cardiac expression was consistent with previous reports (Miller et al., 2008). At E8.75, Arhgap29 expression was more restricted to allantois, heart and somites **(Fig. 4.3 B, inset)**. At E9.5, vascular expressions became apparent in the head and intersomitic vessels. **(Fig. 4.3 C,C')**, and at E10.5, it was more restricted to the vasculature in the head **(Fig. 4.3 D)**. These data suggest that Arhgap29 has a critical role in the allantois, but the function of Arhgap29 is not restricted to the allantois as the expression was found in other tissues. These observations led me to study the function of Arhgap29 in the vasculature and heart.

4.2.2 Depletion of Arhgap29 leads defects in cardiovascular development

Allantois culture shows vascular remodeling defect in Arhgap29$^{-/-}$

In vitro studies of Arhgap29 have demonstrated that it modulates cell architecture via control of RhoA activity in EC cultures, resulting in EC lumen formation and decreased cell permeability (Post et al., 2013; Wilson et al., 2013; Xu et al., 2011). To examine the vascular function of Arhgap29, I performed allantois culture and examined vascular behavior *ex vivo*. Allantois culture experiments have been developed as a model system to understand vessel

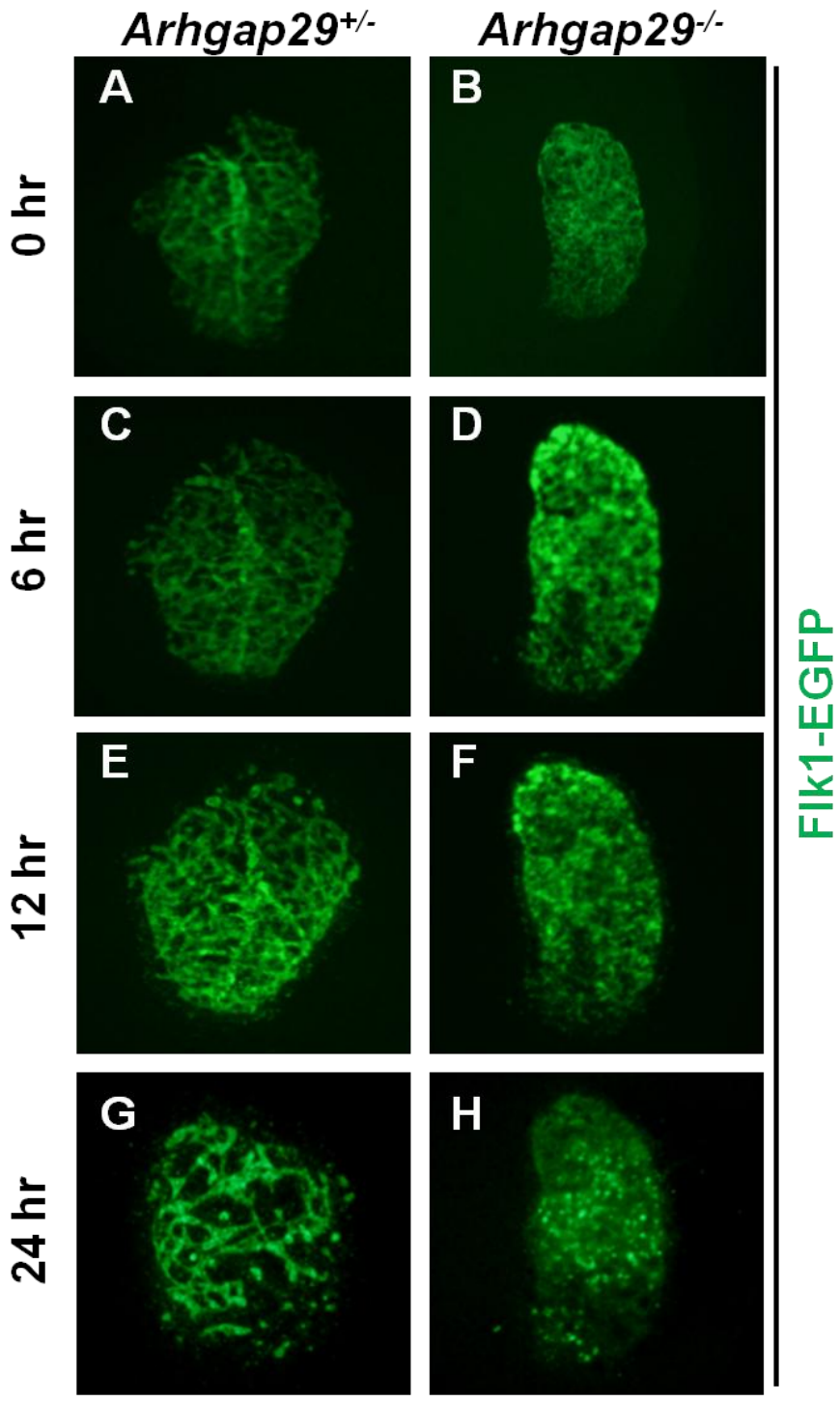

Figure 4.4. *Arhgap29* deficient ECs failed in blood vessel remodeling during allantois culture. (A,C,E,G) *Arhgap29*$^{+/-}$ allantoic vessels reorganize the structure during culture for 24hr. **(B,D,F,H)** *Arhagp29*$^{-/-}$ allantoic vessels fail to remodel vascular plexus and remain punctuate.

formation as it has advantages to study blood vessel development (Arora and Papaioannou, 2012). The allantois consists of mesodermal cells that differentiate into ECs, and mesenchyme, both surrounded by ECMs. Therefore, the allantois is a great tool to study vasculogenesis and angiogenesis in vitro. To visualize ECs in the explants, a *Flk1-EGFP* allele was introduced in the *Arhap29*$^{-/-}$ mice. Allantoises were isolated from embryos at E8.5, and cultured on a filter for 24 hours. The remodeling vascular plexus was observed every 6 hours. In the heterozygous allantois, the vascular plexus was well organized with a wide vessel in the center at time point 0 **(Fig. 4.5 A)**. Over the course of explant culture, the existing allantois plexus became remodeled **(Fig. 4.5 C,E,G)**. *Arhgap29*$^{-/-}$ allantoises displayed a lack of organized vascular hierarchy from the beginning of the culture, although a vascular plexus did exist **(Fig. 4.5 B)**. In contrast to *Arhgap29*$^{+/-}$ allantois cultures, the ECs in *Arhgap29* deficient allantoises failed to undergo remodeling during culture and the existing plexus was disassembled, resulting in scattered endothelial punctate structures **(Fig. 4.5 D,F,H)**. Although further investigation is required to understand the exact role of Arhgap29 in allantois vasculature, these data suggest that Arhgap29 is required for EC remodeling in allantois.

Arhgap29*$^{-/-}$ *embryos show vascular defects

Data from our lab suggested that Arhgap29 functions in RhoA regulation via Rasip1 in ECs to open lumen during vasculogenesis in mouse aortae (Xu et al., 2011), and vascular expression of Arhgap29 was observed in these cells **(Fig. 4.3)**. Therefore I examined whether Arhgap29 displayed vascular defects in the embryonic aortae and developing vessels. At 8.75, vasculature was visualized by Flk1-EGFP, blood vessels looked grossly normal by size and morphology in aortae and yolk sac **(Fig. 4.5 A,B)**. By contrast, as previously described, allantois defects were apparent by visualizing the vasculature. In *Arhgap29*$^{+/-}$ embryos, the allantois was fused and blood vessels were intercalated into the placenta **(Fig. 4.5 A)**. By contrast, allantoises of *Arhgap29*$^{-/-}$ embryos formed swollen sac, and were not connected from the placenta **(Fig. 4.5**

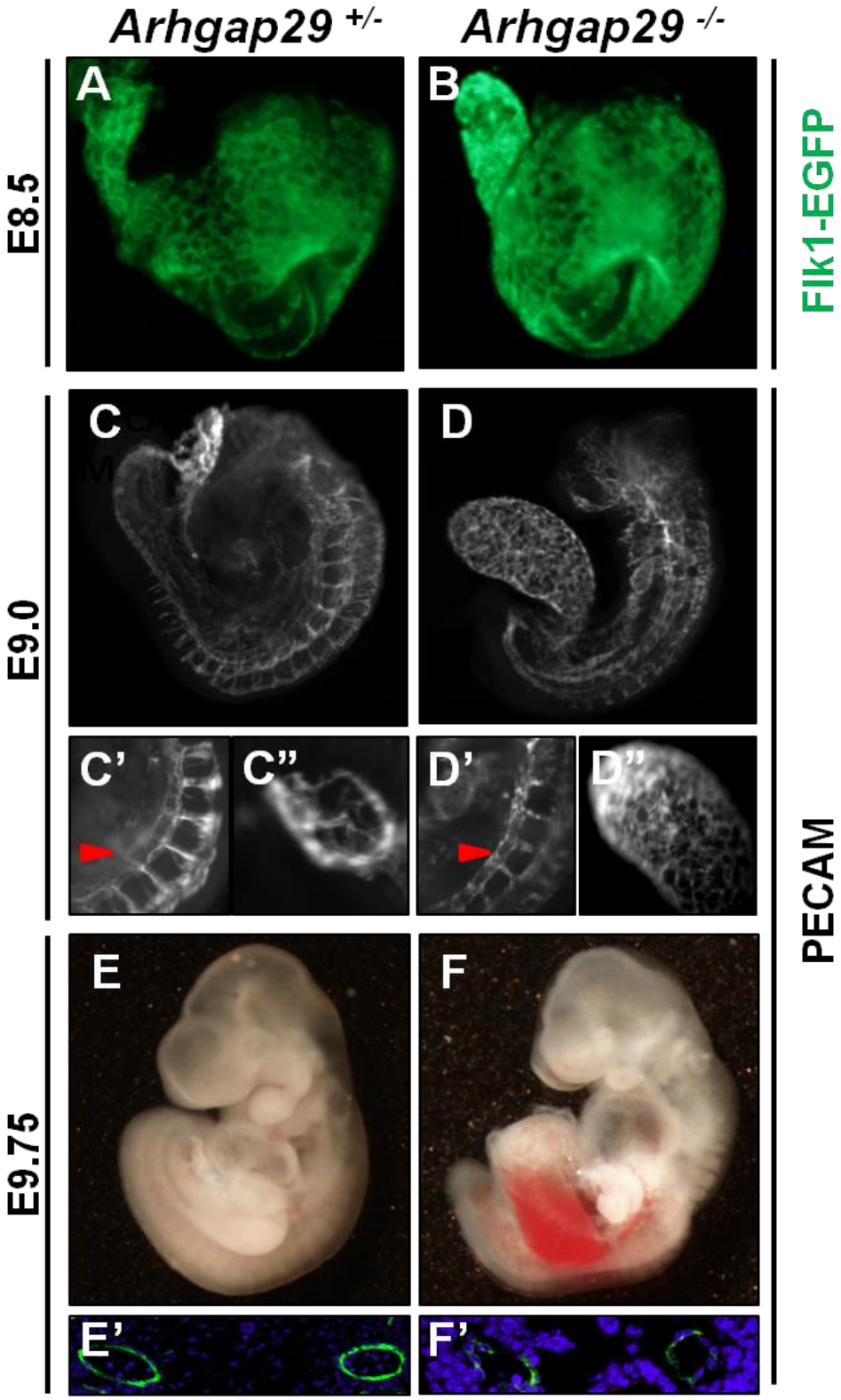

Figure 4.5. Arhgap29 depletion leads to cardiovascluar defects during embryonic development. (A,B) At E8.5 the vasculature in *Arhgap29*$^{-/-}$ appeared morphologically normal in yolk sac, and aortae. A sac of allantois is noted in *Arhgap29*$^{-/-}$. **(C-D'')** At E9.0, *Arhgap29*$^{-/-}$ embryos display **(C',D')** narrower vessels in aortae and **(C'',D'')** underdeveloped vessels in allantois. **(E-F')** Whole mount embryo shows delayed growth at E9.75. **(E',F')** The section of embryo reveals constricted aortae in the absence of Arhgap29.

B).

By whole-mount PECAM immunostaining at E9.0, the control embryos displayed patent lumen in the aortae, intersomitic vessels, and the allantois vascular plexus **(Fig. 4.5 C-C")**. In the *Arhgap29*$^{-/-}$ embryos, the aortae appeared to open lumen, but these were more narrow than the those of control embryos **(Fig. 4.5 D,D')**. In addition, the vasculature in the allantois was thin and lacked of vessel hierarchy **(Fig. 4.5 D")**, as seen in E8.5 allantois culture. At E9.75, hemorrhaging was obvious in the location of umbilical vessels in *Arhgap29*$^{-/-}$ embryos. **(Fig. 4.5 E,F)**. Transverse sections revealed that the PECAM positive vessels have opened lumens although they are constricted **(Fig. 4.6 E',F')**. These results suggest that Arhap29 deficiency causes failure in embryonic blood vessels.

SMA expression in increased in Arhgap29*$^{-/-}$ *heart

As *Arhgap29* was reported as a cardiac gene in the early mouse embryo (Miller et al., 2008), and its cardiac expression was detected in the embryo by *in situ* hybridyzation **(Fig. 4.3 A,B)**, I examined the heart to see whether *Arhagp29*$^{-/-}$ embryos displayed any defects in the absence of Arhgap29. In transverse sections of the embryos, *Arhgap29* $^{-/-}$ mutants were grossly smaller than the heterozygous control due to growth retardation, including the heart **(Fig. 4.6 A,B)**. By immunostainig for PECAM and endomucin, the aortae were narrower than those in controls, as shown before **(Fig. 4.5 E',F')**, however the endocardium, which lines the inner surface of the myocardium, was grossly normal. Because Arhgap29 inactivates RhoA which regulates the actin cytoskeleton, removal of Arhgap29 was expected to cause increased actin bundling and stress fiber formation. Therefore, I examined expression of smooth muscle actin (SMA), an actin isoform expressed in cardiac tissue, using immunostaining. Surprisingly, the level of SMA was significantly elevated in myocardium, likely due to removal of Arhgap29, a RhoA inactivator. **(Fig. 4. 6 A,B)**. This data suggests that Arhgap29 may have an essential role

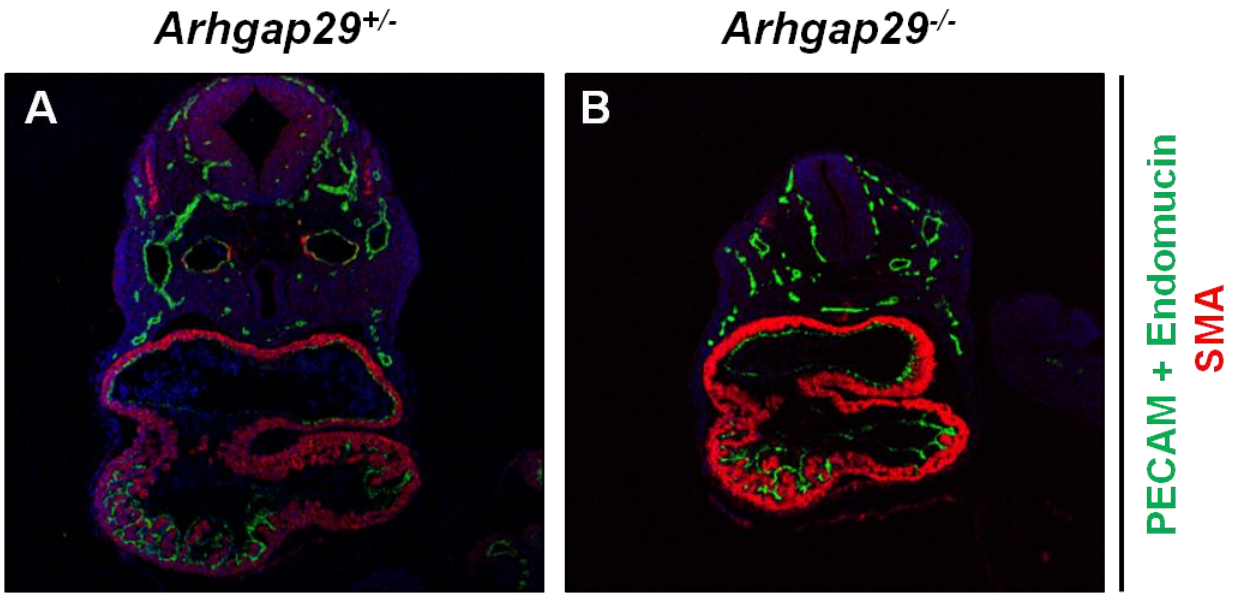

Figure 4.6. SMA is increased in heart of Arhgap29$^{-/-}$. (A,B) PECAM and endomucin expressing vessels in the heart appeared normal in *Arhgap29*$^{-/-}$. However, In the absence of Arhgap29, the myocardium expresses abnormally elevated level of SMA.

in myocardium by regulating actin dynamics.

4.3 Discussion

4.3.1Arhgap29 is required for chorioallantois development

In this chapter, it was shown that Arhgap29 is critical for allantois attachment to the chorion within the placenta. The allantois is an embryonic precursor tissue for umbilical vessels that are formed and required for nutritional supply to the embryo from the maternal placenta. Despite its significance during development, the study of allantois development has not been the center of attention. In this chapter, Arhgap29 is identified as one of the critical factors for chorioallantois fusion, initiating connection between mother and embryo. In the absence of Arhgap29, the embryo fails to undergo allantois to chorion attachment, which at least in part leads cardiovascular lethality.

The mechanisms of chorioallantoic fusion still remained unknown, however, a few reports have demonstrated that the interaction between vascular cell adhesion molecule 1 (VCAM-1), and its counter receptor, α4 integrin, are together critical for allantois-chorion fusion (Kwee et al., 1995; Yang et al., 1995). During the allantois-chorion fusion, VCAM-1 is expressed in the distal tip of allantois, and α4 integrin is present in the chorion, where fusion occurs. In the absence of either molecules, mouse embryo failed to undergo fusion, resulting in swollen allantois sac formation and embryonic lethality. Another study showed that FoxO1, a transcription factor, is required for placenta development (Ferdous et al., 2011). FoxO1 deficiency leads chorio-allantois fusion defects in the embryo by regulation of VCAM-1 gene expression. As a critical factor for allantois-chorion attachment, it is possible that Arhgap29 is involved in regulation of α4 integrin – VCAM-1 interactions.

It is likely that Arhgap29 regulates attachment of allantois by controlling cell adhesion. Our lab showed that Arhgap29 is required for proper adhesion between ECs and ECM (Xu et al., 2011). Arhgap29 depleted ECs displayed reduced adhesion to ECM proteins, including fibronectin, collagen I, collagen IV, laminin, and fibrinogen. In addition, focal adhesions were immature, and activated β1 and β3 integrin was reduced in the absence of Arhgap29, resulting in reduced adhesion. In addition, Arhgap29 is downstream of Rap1 signaling, which is known for integrin-mediated adhesion (Post et al., 2013). Rap1 was reported to increase integrin affinity, resulting in increased cell adhesion (Retta et al., 2006). As a Rap1 effector, Arhgap29 may be involved in cell adhesion, and it will be interesting to study how Arhgap29 regulates adhesion molecules.

4.3.2 Depletion of Arhgap29 leads defects in cardiovascular development

It was previously reported that Arhgap29 is expressed in the heart and endothelium (Miller et al., 2008; Xu et al., 2011), and I also showed that it is expressed in cardiac tissue and the vasculature in developing embryo by in situ hybridization **(Fig. 4.3)**. This suggests that Arhgap29 functions in those tissues. In this chapter, I demonstrated that Arhgap29 deficiency led to failure in cardiovascular development by showing that ECs of *Arhgap29* null embryos failed to undergo remodeling during allantois culture, and the endothelium in the *Arhap29* null embryos displayed constriction in blood vessels after E9.0.

Our lab showed Arhgap29 may function together with Rasip1 in lumen formation during vasculogenesis (Xu et al., 2011), and I found that Arhap29 null mice showed cardiovascular failure. Therefore, I expected that Arhgap29 may be involved in tubulogenesis. To assess the function of Arhgap29 in ECs, conditional Arhgap29 mutants were bred with *Tie2-Cre*, which is an early endothelial specific Cre mice (Kisanuki et al., 2001). However, endothelial knockout of

Ahrgap29 did not affect vascular development. *Ahrgap29$^{fl/fl}$;Tie2-Cre* mice were viable and no defects were detected in the embryo through adulthood. I speculate that it is possible that the function of Arhgap29 in ECs is redundant with other GAPs. Many GTPases are reported to be important for endothelial development function, and a variety of GTPase effectors, such as GTPase activating proteins. Therefore, the absence of Arhgap29 in ECs may not cause dramatic effects because other GAPs may work in its place.

The defect that the *Arhgap29* knockouts did not phenocopy the Rasip1 nulls, with respect to vascular defects, suggests two possible reasons for cardiovascular failure in Arhgap29 null embryos. 1) Cardiovascular failure in Arhgap29 null is caused by lack of allantois-chorion attachment, resulting in lack of nutrition or exchange of gas and wastes, and overall wasting of embryos. 2) Intraembryonic Arhgap29 deficiency in other tissues causes vascular failure, as Arhgap29 expression was broadly detected, such as heart and somites. To find causative factors of vascular failure will require further study and conditional knockout in various tissues will be a useful tool.

Although endothelial deficiency of Arhagp29 did not cause direct and measurable endothelial failure, the vascular function of Arhgap29 remains to be understood. Despite unknown functions of Arhgap29 during development, Arhgap29 may have critical role in the endothelium in adulthood, which has not been investigated yet. The endothelial function of Arhgap29 was suggested by in vitro experiments (Post et al., 2013; Wilson et al., 2013), but not evident *in vivo*. As a Rap1 effector, Arhgap29 affected endothelial barrier function by regulating Rho signaling. Arhgap29 depletion in cultured ECs resulted in reduced electrical impedance, which represents junctional resistance. In addition, knockdown of Arhgap29 caused increased incidence of irregular junctions and stress fibers, indicating increased junctional remodeling and reduced EC stability. In order to study the exact function of Arhgap29 in endothelium *in vivo*, it

will be interesting to investigate whether Arhgap29 is required for vascular permeability, vascular homeostasis, or angiogenesis in adults.

The expression of Arhgap29 transcript in heart led me to investigate heart development in *Arhgap29* null mice. In the absence of Arhgpa29, it is known that RhoA activity is increased and mediates actin assembly. It is also known that RhoA induces Rho kinase pathway, and subsequently increase SMA expression in myofibroblasts via translocation of the transcriptional coactivator, myocardin-related transcription factor A (MRTF-A) into the nucleus (Zhao et al., 2007). Using immunohistochemistry to detect SMA in myocardium, significant elevation of SMA was observed in *Arhgap29*$^{-/-}$ embryos. It is likely caused by Arhgap29 deletion, which resulted in increased of RhoA activity. This data indicates that Arhgap29 has a critical role in myocardial development, and further study is required to understand its function.

It is also possible that Arhgap29 regulates VCAM-1 and α4 integrin interaction in heart as well as in the allantois, as they are expressed in both allantois and heart (Kwee et al., 1995; Yang et al., 1995). VCAM-1 was detected in the distal tip of allantois, where Arhgap29 is present, and in the myocardium during the development. Its counter receptor, α4 integrin, is expressed in chorion and epicardium. It was shown that both VCAM-1 and Arhgap29 are expressed in distal tip of allantois, suggesting Arhgap29 may regulate VCAM-1. Expression of Arhgap29 in chorion has not been investigated yet. Its precise expression in the heart needs to be examined to determine the relation of Arhagp29 and α4 integrin. It was reported that VCAM-1 deficient embryos displayed lack of epicardium at E11.5, and α4 integrin null embryos showed a epicardium-myocardium attachment defect. To study Arhgap29 function in VCAM-1 and α4 integrin interaction in heart development, it will require investigation of *Ahrgap29*$^{-/-}$ embryos at later stages as the epicardium develops and covers myocardium after E10. Because *Arhgap29* null embryos display defects earlier than E10, analysis of heart development is precluded and

cardiac specific conditional knockout mice will be required to better understand its function in heart development.

In conclusion, it was demonstrated that Arhgap29 is critical for placenta development, and possibly functions in the endothelium and heart. Arhgap29 absence causes a striking failure of allantois-chorion attachment, which leads to failure of maternal and fetal connection during embryonic development. This suggests that Arhap29 may be important during human pregnancy and therapeutics targeting this molecule should be examined carefully. In addition, the results presented here suggest the possible function of Arhap29 in adhesion regulation during development in placenta, and possibly in heart. Although further studies are required to study mechanisms of Arhap29 function, the works presented here will guide future studies.

Chapter 5. SUMMARY, FUTURE DIRECTIONS, AND CONCLUSIONS

The studies in this dissertation cover a wide range of topics of cardiovascular development: from characterization of vascular development, to specific molecules involving in cardiovascular function. Each chapter provides new findings and insights for understanding of cardiovascular development. In this chapter, potential future directions for each chapter will be discussed.

5.1 Chapter2:Stepwise arteriovenous fate development during vasculogenesis

SUMMARY

In this chapter, it was addressed that the first vessels of arteries and veins acquire their fate in stepwise manner during development. To begin with, description of the first arteries (dorsal aortae) and veins (sinus venosus/pre-vitelline veins) showed rapid and dynamic changes of vascular anatomy in mouse embryo. Angioblasts emerged at E7.5 in scattered manner, aggregated to form cords, and then eventually opened patent lumen in dorsal aortae. The first veins, vitelline veins, and cardinal veins progressed to complete tubes later than arteries. They extended from the sinus venosus towards the tail during and after embryo turning. To investigate AV fate, expression profile analysis of the most widely used AV markers was performed in early embryos at E8.25-8.75. It was shown that AV marker expression occurs in a stepwise manner, and does not coincide with the emergence of artery and vein, indicating acquisition of AV fate occurs progressively. In addition, it was examined whether AV fate is affected by hemodynamic flow. By using *in vitro* and *in vivo* 'flowless' models, embryo explants and lumenless *Rasip1* $^{-/-}$ embryos respectively, it was demonstrated that hemodynamic flow is

required for some, but not all, arterial gene expression, indicating that arterial specification does not depend on flow but is required for full differentiation.

FUTURE DIRECTIONS

Stepwise formation of arteries and veins

The first mouse vessels form via aggregation of angioblasts around E8.0, via de novo vessel formation, or vasculogenesis as previously described (Drake and Fleming, 2000). In this report, we made the striking findings that vessels emerge in a progressive manner. The dorsal aortae and vitelline veins first appear as cords, but then quickly open lumens proximal to their connections to the heart. While dorsal aortae form continuous tubes, vitelline veins remained as blind ended vessels until E8.5. During embryo turning, vitelline veins appeared to extend towards to the distal tail, and angioblasts were seen as scattered and gathering to the vitelline vein primordium. With our static observations of fixed tissues, it was indistinguishable whether these vessels form via *bona fide* vasculogenesis (angioblast aggregation), or by angiogenic sprouting. Therefore, it will be useful to investigate mouse embryos carrying *Flk1-EGFP* reporters with live imaging.

Circulatory loops

Another interesting question brought up by the anatomy investigations was when the circulatory loops are completed. It was identified that plasma circulation in murine embryos begins as early as the 3 somite stage (Lucitti et al., 2007). At this stage the heart beat is seen, and erythrocyte movement was detected. Another study demonstrated that although blood cells flow in the embryo after heart formation, a full functional loop is not formed until E10.0 (McGrath et al., 2003). It is still unclear when the intraembryonic circulatory loop closes completely. The

data presented here show that until the first main arteries have formed, veins are not formed to complete the circuit. Further studies in mice are needed to determine when a true physical vascular circulatory loop is completed.

Role of Hemodynamic flow

The data presented here addressed that blood flow influences AV fate determination during vasculogenesis. It was postulated that the embryo at 5s has hemodynamic flow as the embryo initiates heart beating at 3s (Lucitti et al., 2007). When the hemodynamic flow was abrogated in the embryo *in vitro* by bisecting the embryo or *in vivo* by using the lumenless *Rasip1* $^{-/-}$ embryo, expression of the of arterial marker Cx40 was decreased, however another arterial marker, Dll4, was not affected. With this data, it was concluded that partial arterial specification is not affected by flow, but blood flow is required for its continuous expression. Further studies will be needed to resolve the dependence of initial versus full arterial identity on hemodynamic flow with the set of the known arterial markers.

Plasticity of ECs

Here, it was shown that in the early pre-mature vessels, the arterial and venous markers are not solidified, suggesting that the vessel fate is ambiguous at early point. The fate of artery or vein is resolved as vessels become established during development. This indicates that the AV identity of early vessels is plastic. The plasticity of ECs has been considered by a number of studies. In chick-quail chimera experiments, early arterial or venous EC grafts showed that ECs can adapt to the local environment such as its flow parameters (le Noble et al., 2004). This suggests that EC fate can be manipulated due to EC plasticity. Further study is required to understand the mechanisms of AV fate determination influenced by hemodynamic forces. This will provide fundamental knowledge for clinical implications, such as arteriogenesis and coronary bypass surgery

5.2 Chapter 3:Rasip1 is required for vasculogenesis and angiogenesis

SUMMARY:

The data shown in this chapter demonstrate that Rasip1 is essential for lumen maintenance during development, embryonic vessel growth, and angiogenesis. To ablate Rasip1 at different developmental timepoints, I generated a conditional *Rasip1* mouse and bred it with different Cre drive lines. Using *Sox2-Cre* to delete Rasip1 globally from the onset of embryogenesis, I found that *Rasip1$^{fl/fl}$;Sox2-Cre* recapitulated global *Rasip1$^{-/-}$* mice, which were previously shown to completely fail to form lumens (Xu et al., 2011). To determine whether Rasip1 is required in blood vessels after their initial formation, *Tie2-Cre* driven mice was used to ablate Rasip1 expression in ECs. Vascular lumens were often observed in *Rasip1$^{fl/fl}$;Tie2-Cre* embryos at 5-10s, due to incomplete Rasip1 deletion in ECs. However, in later stages, Rasip1 deficient embryos displayed lack of blood flow due to narrow and discontinuous vascular tubes, indicating that the vessels failed to maintain lumen.

In addition, I showed that Rasip1 is also required for angiogenesis by using two models of angiogenic blood vessel growth: neonatal retinal blood vessel growth and DIVAA. In the absence of Rasip1, retinal vessels displayed decreased outgrowth, accompanied with defects in vessel remodeling and lumen formation. Decreased angiogensis was also observed in adult subcutaneous vessels. These data show that Rasip1 is necessary in growing vessels, but I found that it is dispensable for maintenance of established blood vessel lumens in adults. Together, these results suggest that Rasip1 may be a useful target for anti-angiogenic therapies.

FUTURE DIRECTIONS:

Rasip1 domains

Rasip1 has four characteristic domains: Proline rich (PR) domain, Ras associating (RA) domain, forkhead associated domain (FHA), and dilute domain. The study of the functions of the domains will provide an insight into the role of Rasip1 in ECs, however the domain study has not well dissected yet. Rasip1's only known function is GTPase interaction by the RA domain, however nothing is known about the other domains in Rasip1. In other literature, the PR domains and FHA domains are known for interaction between various types of proteins (Mahajan et al., 2008). The dilute domain is identified for its homology to myosin, which transports cargo along the actin filaments.

Rasip1 is known for its scattered puntae localization at juxta golgi region in cytoplasm (Mitin et al., 2004), so we postulated that Rasip1 may be involved in vesicles and function in vesicular transport. Co-localization with Rab GTPases, which are known for various vesicular trafficking (Somsel Rodman and Wandinger-Ness, 2000), also supports this idea. Rab5 and Rab7 positive vesicles were found localize together with Rasip1 in high percentile (data not shown).

In order to examine the functions of each domain, we investigated if each domain was required for Rasip1 localization. To investigate the loss/gain of functions of the featured domains, various versions of GFP tagged Rasip1 mutants were generated by Ke Xu or provided by Natalia Mitin. As expected, GFP control protein was seen smoothly distributed and GFP-Rasip1 full length proteins localized as punctae in the cultured ECs. Interestingly, PR domain deletion caused smoothened localization and vesicle punctae were not observed, indicating that PR domain is responsible for vesicle localization of Rasip1. Another interesting feature was dilute domain. In the absence of dilute, mutant positive vesicles were aggregated and not fused properly. When only dilute domain was overexpressed in EC, dilute domain generated bigger vesicles in the cytoplasm. These suggest that dilute domain may function in vesicle fusion. Further investigations are required to understand how Rasip1 domains regulate vesicle behavior.

In vitro- endo/exo-cytosis

One of the hypotheses was that Rasip1 regulates endocytosis. In the absence of Rasip1, junctional protein was not removed from EC-EC contacts in mouse dorsal aortae during lumen formation, indicating Rasip1 is required to remove junctional protein from luminal membranes. Therefore, Rasip1 was thought to be involved in uptake of junctional protein at the EC-EC contacts by endocytosis. To test this hypothesis, in vitro transferrin uptake was utilized with ECs in the absence of Rasip1. In this assay, fluorescence tagged transferrins were transferred into cells via endocytosis, and eventually recycled back to the cell surface. With transferrin uptake assay, it was found that Rasip1 presence or absence did not affect transferrin endocytosis. Then, I speculated that Rasip1 is involved in protein-specific endocytosis. One of available assay was VE-cadherin internalization assay, and it is known that VE-cadherin is required for lumen formation by recruiting sialomucins at aortae EC-EC contacts during vasculogenesis (Strilic et al., 2009). VE-cadherin assay didn't display any distinguishable changes in the absence of Rasip1. Then, it was tested if Rasip1 is involved in vesicle recycling. By using the same assay, we have measured the transferrin remained in cells after transferrin was translocated into the cells, and no difference was detected between control and Rasip1 deficient cells. To date, in vitro internalization and recycling assays didn't support the hypothesis that Rasip1 is involved in vesicular trafficking. For further studies of endocytosis/recycling, two aspects of Rasip1 must be considered. Rasip1 may be involved in specific protein transport. In addition, Rasip1 plays role in three dimensional EC environments *in vivo*, not in two dimensional cultures. Therefore, investigating Rasip1 function in three dimensions may yield further insight into its role in endocytosis and/or vesicular trafficking

Rasip1 functions in angiogenesis

Here, I showed that Rasip1 is required for angiogenesis using neonatal retinal angiogenesis model. This model system was used to determine if Rasip1 is required in lumen formation. As shown in Rasip1 null mouse embryo, Rasip1 plays a critical role in lumen formation (Xu et al., 2011). In the absence of Rasip1, mouse aortae were found to lack patent lumens. Therefore, I investigated lumen formation in the neonatal retinal vessels of conditional Rasip1 mice to examine whether Rasip1 depletion blocks lumen formation during angiogenesis. It was seen that lumen formation at the growing front vessels were inhibited in the absence of Rasip1. The mechanisms of Rasip1 in lumen formation remained unknown during angiogenesis. One of the hypotheses is that Rasip1 regulates junctional protein removal at EC tip cells. Failure of junctional protein redistribution may cause closed lumens, and aggregated cells. Interestingly, vessel density was increased in the absence of Rasip1. Further study will be required for determining the precise function of Rasip1 in regulating EC junctions.

Another interesting point was that Rasip1 regulates cell cytoskeleton via RhoA regulation. Indeed, it was observed that Rasip1 absence caused round shape of ECs at most stalk cells. In contrast, elongated tip cells were found in Rasip1 deficient retinal vessels. It is possible that Rasip1 induces potential of protrusion. One of the well known signaling involving angiogenesis is Notch signaling. Blockade of Notch signaling induced increased number of filopodia formation and density. It will be interesting to study whether Rasip1 is involved in Notch signaling to control angiogenesis. It was also possible that the elongated sprouts failed to anastomose with nascent vessels. Anastomosis happens via interaction between two sprouts. VE-cadherin is known to be a critical factor during the interaction (Blum et al., 2008). The mechanism of anastomosis remains to be elucidated.

Vessel growth in tumor

Excessive growth of blood vessels has been one of the prevalent symptoms in cancer, in that blood vessels facilitate cancer growth and metastasis. Consequently, blocking the vascular growth has been at the center of attention to treat cancer. As it was shown that Rasip1 is required for angiogenesis by using two different model systems, neonatal retinal vessel angiogenesis and subcutaneous vessel angiogenesis, but is dispensable for vessel maintenance in adults, Rasip1 was speculated to be a great target for inhibition of vascular growth. To test this, Rasip1 was removed in *MMTV-PyMT (*mouse mammary tumor virus-polyomavirus middle T antigen) transgenic mice, which spontaneously develop mammary tumors (Guy et al., 1992). Rasip1 was removed by tamoxifen regimen in adults containing *Cad5-Cre*^{ER} and *MMTV-PyMT* alleles, and mammary tumor growth was assessed by size during growth and by weight at 19 weeks **(Fig. 5.1 A)**. Although there was high variability, Rasip1 deletion did not affect average tumor size and weight **(Fig. 5.1 B,C)**. To evaluate whether Rasip1 deletion blocked vascularization in tumor tissue, immunohistochemistry was performed to visualize vessels **(Fig. 5.1 D)**. The number of invaded vessels into tumor tissues in Rasip1 deficient mice was comparable to that in control mice, indicating Rasip1 removal did not block the vessel growth into the tumor **(Fig. 5.1 E)**. Although the overall data suggested that depletion of Rasip1 may not inhibit tumor angiogenesis, there was high variability in the tumor growth. This is possibly resulted by using mixed background mice, different from previously reported. For further study to obtain more precise results, it will be required to unify the background of mice.

5.3 Chapter4:Arhgap29 is required for placenta and cardiovascular development

SUMMARY:

In this chapter, I demonstrated that Arhgap29 is essential for placenta and cardiovascular development. The expression profiling indicated where Arhgap29 could potentially function during murine development. Expression of Arhgap29 was detected in a widespread manner in mouse embryos, with strong expression in the allantois at E8.5 when chorion-allantois fusion occurs. Arhgap29 was also expressed around the developing heart at E8.5 through E9.5, and vascular expression of Arhgap29 was more clearly detected in head vessels and ISVs at E9.5. To study the function of Arhgap29 *in vivo*, I generated conditional *Arhgap29* knockout mouse and used *Sox2-Cre* driver line to ablate Arhgap29 expression globally. Strikingly, in the absence of Arhgap29, embryos displayed failure in allantois-chorion attachment, suggesting that Arhgap29 may play a critical role in regulation of cell adhesion in allantois at E8.5. In addition, *Arhgap29* null embryos displayed narrow and constricted dorsal aortae by E9.75, and SMA level was improperly elevated in myocardium, likely via increased RhoA activity in the absence of Arhgap29. These results suggest that Arhgap29 is essential for placenta and cardiovascular development, and provide insights for future study to better understand the function of Arhgap29.

FUTURE DIRECTIONS:

The work presented here shows that Arhgap29 plays critical roles in placenta and cardiovascular development using *Arhgap29* knockout mice. Although allantois-chorion fusion is a significant event at the onset of placenta development, it has not been well-characterized, and there have been only a few reports describing molecules involved in allantois-chorion fusion. VCAM-1 and its counter receptor, α4 integrin, have been identified as essential molecules regulating allantois attachment (Kwee et al., 1995; Yang et al., 1995). VCAM-1 and α4 integrin

are also expressed in myocardium and epicardium respectively and control cell adhesion between myocardial and epicardial cells. It will be interesting to investigate whether Arhgap29 regulates these molecules both in the allantois and heart. It will be easy to assess whether they are expressed in those tissues by *in situ* hybridization and immunohistochemistry.

The cellular and molecular functions of Arhgap29 remain to be characterized. It has been demonstrated that Arhgap29 is required for adhesion between EC and ECM (Xu et al., 2011). Arhgap29 depleted cultured ECs showed reduced adhesion to ECM proteins. siArhgap29 treated ECs displayed immature focal adhesions, and decreased levels of activated β1 and β3 integrins, resulting in reduced adhesion. In addition, it was reported that Arhgap29 is a downstream effector of Rap1 GTPase, which has been shown to regulate integrin-mediated adhesion (Post et al., 2013). Here, I showed that genetic ablation of Arhgap29 inhibited allantois attachment in mouse embryos. These data suggest that Arhgap29 regulates cell adhesion. α4 integrin is thought to be one of the candidates involved in Arhagp29 induced adhesion, as impaired VCAM-1 and α4 integrin interaction led the allantois-chorion fusion defect in embryos. Further studies will help resolve this possibility.

The study of Arhap29 was initiated by a study which showed Arhgap29 is involved in EC tubulogenesis by coordinating with Rasip1 (Xu et al., 2011). This study was followed up by other groups, supporting the idea that Rasip1 and Arhgap29 function downstream of Rap1 signaling to modulate EC permeability via RhoA inactivation using cultured ECs (Post et al., 2013; Wilson et al., 2013). Therefore, I was directed to investigate whether Arhgap29 depletion causes vascular defects in mouse embryos and adults. Global *Arhgap29* knockout embryos displayed narrow and constricted dorsal aortae. However, it was not clear whether failure in placenta development led to the vascular defect or alternatively, if Arhgap29 deficiency in ECs caused constricted vessels. To distinguish two possibilities, an EC-specific Tie2-Cre driver mouse was used to delete Arhagp29 in ECs from early developmental stage. Unexpectedly,

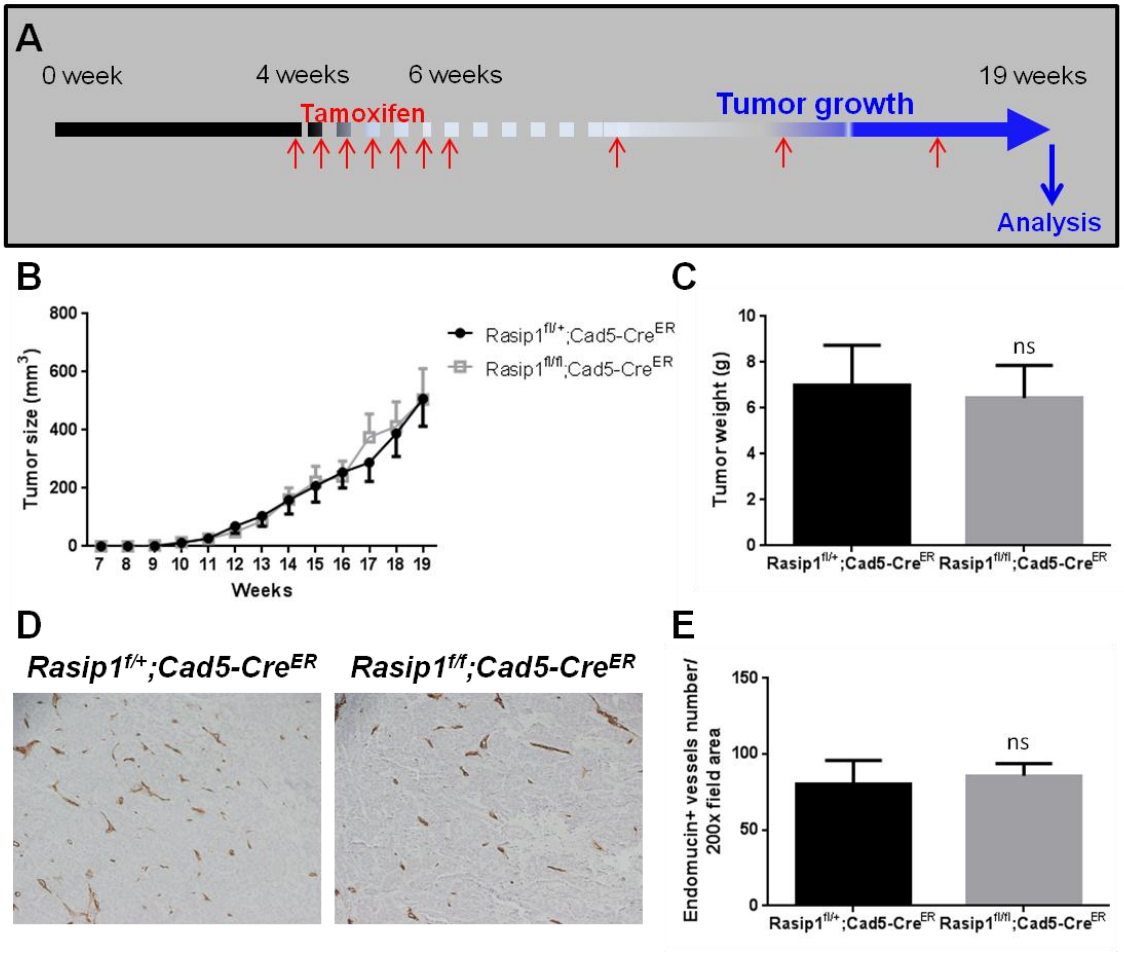

Figure 5.1. Rasip1 deficiency did not influence mammary gland tumor growth in MMTV-PyMT mice. (A) Schematic diagram for Rasip1 deletion and mammary gland tumor analysis. **(B)** Tumor size growth in Rasip1 deficient and control mice. n=9 in each group, values represents mean ± s.e.m. **(C)** Tumor weight at 19 weeks old mice. **(D)** Endomucin immunohistochemistry in tumor tissues to visualize blood vessels. **(E)** Quantification of endomucin positive blood vessel number in the field.

Arhgap29$^{fl/fl}$;Tie2-Cre was viable through adulthood without any vascular defects. Although any vascular defects have not been detected, it is possible that Arhgap29 plays a critical role in controlling vascular homeostasis as it has been reported that Arhgap29 regulates EC permeability. In addition, its function in angiogenesis has not yet been examined.

In addition, it will be interesting to study the exact function of Arhgap29 in heart development, which remains unknown due to early lethality of Arhgap29 deficient mice. It has been demonstrated that proepicardial cells initiate migration on the surface of myocardium around E9.5 to cover the naked myocardium, and the whole heart is completely covered by an epicardial sheet by E11.5 (Brade et al., 2013). As *Arhgap29$^{-/-}$* displayed delayed growth from E9.0 and lethality by E11, it was difficult to assess the exact function of Arhgap29 in epicardial cell migration and epicardium formation. To examine the function of Arhgap29 in heart development, it will be useful to use epicardial- or myocardial- specific Cre driver mice.

To dissect the function of Arhgap29, it will be a good start to investigate domains of Arhgap29. Arhgap29 has characteristic domains: a GTPase activating protein (GAP) domain, a cysteine-rich domain, ZPH region, and BIN/Amphiphysin/Rvs (BAR) domain. GAP domain of Arhgap29 has been characterized as a RhoA GTPase interacting site to inactivate RhoA. cysteine-rich domain is homologous to diacylglycerol binding domain of protein kinase C (PKC) family, and is known for its function in ligand recognition or membrane association (Saras et al., 1997). ZPH region was shown as Rap2 interacting site (Myagmar et al., 2005). It has been reported that Bar domain functions in dimerization, sensing and inducing membrane curvature, or binding to small GTPases (Habermann, 2004). It has also been shown that many of BAR domain containing proteins are involved in vesicular transport. Characterization of Arhgap29 domains will give insights to better understand the function of Arhgap29.

APPENDIX A

MATERIALS AND METHODS

COMMON METHODS

Mouse embryos

Embryos were collected from pregnant female mice. Plugging date was designated as embryonic day 0. Embryos were fixed in 4% parafoamaldehyde (PFA) in phosphate buffer saline (PBS) solution overnight at 4°C with gentle rocking. Embryos then were washed with PBS, dehydrated using an ethanol series, and stored in 75% ethanol at -20 °C. All animal handling was performed in accordance with IACUC regulations.

Sections and histology

For paraplast sectioning, embryos were dehydrated to 100% ethanol, transferred to xylene and then carried through series of rinses in 100% Paraplast Plus tissue embedding medium (McCormick) at 60 °C. The embryos were then embedded in paraplast and sectioned with a 2030 Reichert-Jung microtome and mounted on SuperfrostPlus glass slides (Fisher).

β-galactosidase reaction

Embryos were obtained from pregnant females by dissection and fixed in a 0.2% gluteraldehyde/2mM $MgCl_2$/5mM EGTA in PBS solution for 20 min on ice. After fixation, the embryos were rinsed in PBS, and incubated with lacZ staining solution (20mM $K_4Fe(CN)_6 \cdot 3H_2O$; 20mM $K_3Fe(CN)_6$; 2mM $MgCl_2$; 0.02% NP-40; 400µg X-Gal) overnight, shielded from light, to allow the color reaction to develop. Then the embryos were washed in PBS, and

transferred to 80% glycerol to be photographed by NeoLumar stereomicroscope (Zeiss) and a DP70 camera (Olympus).

Whole mount in situ hybridization

Whole mount in situ hybridization was carried out using a protocol adapted from D. Wilkinson's method (Wilkinson, 1995). Briefly, embryos stored in 75% ethanol at -20°C were rehydrated in stepwise fashion to PBST. Then, the embryos were treated with proteinase K, fixed in a 0.25% gluteraldehyde/4% PFA in PBS solution, and pre-hybridized at 60 °C for 1 hour. The samples were transferred into a hybridization mix, containing a Digoxigenin-labeled probe overnight at 60°C. Then the embryos were washed with a series of solutions. Development of color reaction was done using BM Purple (Roche). Images were taken using a Lumar dissecting microscope (Zeiss) and DP-70 camera (Olympus).

CHAPTER 2

Whole mount in situ hybridization

Whole mount in situ hybridization was performed as described above. Dig-RNA probes were generated from clones (Open Biosystems): *Cx40* (BC053054), *Cx37* (BC056613), *Nrp1* BC060129), *Nrp2*(BC098200), *Notch1* (BC010325), *Notch4* (BU703407), *Dll4* (BC042497), *Jagged1* (BC058675), *CoupTFII* (BC094360), *APJ* (BC039224), and *Flt4* (BI557457). *Hey1* and *Hey2*clones were generously provided by Dr. Eric Olson (UTSW).

Immunofluorescence

After the embryos were sectioned, they were deparaffinized in xylene, rehydrated through an ethanol series, and then equilibrated in PBS. Antigen retrieval was performed in

Buffer A solution (Electon Microscopy Sciences) by 2100 Retriever (Pickcell Laboratories). Cooled down slides after antigen retrieval were rinsed in PBS and blocked with Cas-Block (Invitrogen) before primary antibody was added for overnight incubation at 4 °C. The following primary antibodies were used at indicated concentrations: Cx40 1:200 (Santacruz) Nrp1 1:200 (R&D), Nrp2 1:200 (Cell Signaling), GFP 1:500 (Aves Labs). Signal was detected the following day using AlexaFluor 488 and AlexaFluor 555(Invitrogen). The sections were mounted with ProLong Gold Antifade (Invitrogen) and images were acquired on a LSM 510 META (Zeiss) confocal microscope.

Explants

CD1 embryos at the 5s stage were isolated in ice cold PBS at E8.0. Embryos were then bisected using Dumont #55 fine forceps (Fine Science Tools). The anterior and posterior halves were placed on separate 13 mm Watman filters (Fisher) over 500 µl of media in 4-well plates (Thermo Fisher Schientific). This created an air-surface interface and allowed the explants to grow flat to facilitate analysis of vessel morphology, Media used was DMEM (ATCC), 10% FBS (ATCC), 1% penicillin/streptomycin (Invitrogen), and 2mM glutamine (Invitrogen). After 10 or 18 hours, explants were rinsed in PBS and fixed in 4% PFA in PBS overnight at 4 °C. The tissues were rinsed and dehydrated to 75% ethanol. Whole mount in situ hybridization was then performed as previously described.

CHAPTER 3

Generation of Rasip1 conditional knockout mouse

Conditional Rasip1 founders were generated by blastocyst injection of ES cells with targeted Rasip1 allele (ID:119405), obtained from KOMP EUCOMM. *LacZ* and *Neomycin resistance cassette* were flanked by *Flp Recombinase Target (FRT) sites* and removed by breeding with Flpe mice to generate Rasip1 floxed allele (Rasip1 $^{fl/fl}$). The following primers used for genotyping; forward primer (ATGGTATGCCTGCCATTTGT), reverse primer (CGACGTCACTGTGTTCCACT). The wild-type alleles give bands of 127 base pairs, and the floxed allele gives 357 base pair bands.

In Situ Hybridization

Whole mount in situ hybridization was performed as previously described. Fixed Embryos and Retinas were incubated with DIG-labeled RNA probes overnight at 65°C. Tissues were washed with post-hybridization solutions, and then incubated in antibody overnight at 4°C. Color development was carried out using BM purple(Roche). Dig-RNA probes were generated from clones ;*CX40* (Open Biosystems, BC053054), and *Rasip1* (Made by Ke Xu in lab).

Analysis of angiogenesis in the postnatal mouse retina

To delete Rasip1 in the postnatal mice, Tamoxifen (Invitrogen) (3mg of Tamoxifen/40g mouse body weight) in Corn oil (Sigma) was applied to mother mice for six times from postnatal day0 (P0) to P5. Eyes were collected at P6 and fixed in 4% PFA for 3 hours at room temperature. Retinas were dissected and immunostained as whole mount as previously described (Pitulescu et al., 2010). For Bromodeoxyuridine (BrdU) labeling, 300µg of BrdU (Invitrogen) was injected

into P6 pups by intraperitoneal (IP) injection 2.5h before sacrifice. To visualize vascular lumen, 500ul of 15mg/ml FITC-Dextran(Invitrogen) was injected into left ventricle.

Immunofluorescence staining on sections

Fixed tissues were washed with PBS. For paraffin section, fixed tissues were dehydrated in series of ethanol, incubated in xylene, and then embedded in paraffin. For cryosection, fixed tissues were incubated in 30% sucrose at 4°C overnight, and then embedded in Tissue-Tek O.C.T. Embedded tissues were sectioned at 10 μm by Microtome or Cryostat. Sections were blocked for 30min. at room temperature in Cas-Block(Invitrogen). Primary antibodies in Cas-Block were incubated at 4°C overnight. Following day, slides were washed in PBS, and then incubated in secondary antibody for an hour at room temperature followed by incubation in DAPI. Immunoflorescence stained slides were mounted with ProLong Gold Antifade Reagent (Life Technologies). The concentrations of primary antibodies used were as follows; PECAM 1:100 , Endomucin 1:100 (Santacruz), Rasip11:100 (Abcam), VEcadherin, ZO-1, Collagen IV, pH3

Whole mount immunofluorescence staining

Fixed embryos were incubated in 5% H2O2/Ethanol at room temperature for 1 hour, then rehydrated in Series of Ethanol/PBS, and 0.1% PBST. Embryos were blocked in Cas-Block for 2 hours at room temperature, then incubated in primary antibody diluted in Cas-Block at 4°C overnight. Embryos were washed in PBS, and incubated in Biotin conjugated Secondary antibody diluted in Cas-Block at 4°C overnight. Washed embryos in PBS were then incubated in ABC Elite reagent (Vector Lab), followed by Tyramide solution (Invitrogen TSA kit).

Fixed neonatal retinas were permeabilzed in 1%Triton X-100 in PBS, and incubated in Primary antibody in 1% Triton X-100 in PBS at 4°C overnight. Tissues were washed with PBS, and incubated in secondary antibody in 1% Triton X-100 in PBS at 4°C overnight. Immunostained retinas were cut and mounted in ProLong Gold Antifade reagent (Invitrogen) as previously described [Pitulescu et al.]. Images were taken with LSM 710 Meta Zeiss Confocal microscope, Zeiss Axiovert microscope using DP70 camera (Olympus), or Zeiss Discovery Stereomicroscope.

Directed In Vivo Angiogenesis Assay (DIVAA)

Rasip1 $^{fl/fl}$*; Cad5-Cre*^{ER} mice were treated with tamoxifen (3mg of Tamoxifen/ 40g mouse body weight) at 4-5weeks old mice every other day for two weeks. At 8 weeks old, angioreactors containing basement membrane extracts with FGF and VEGF were implanted into the mice subcutaneously. After two weeks, angioreactors were removed from the mice and ECs were extracted from angioreactor and detected by FITC-lectin.

Cell culture

Human umbilical vein ECs (HUVEC, PCS100-010) and mouse pancreatic islet EC line MILE SVEN 1 (MS1, CRL-2279) were obtained from ATCC and cultured per ATCC's standard protocols. DNA constructs were transfected into the cultured ECs using Transfectin Reagent (Invitrogen). Tube formation assaywere carried out on 50 μl Matrigel (BD Matrigel) coated glass slides. Cultured ECs were fixed in 4% PFA in PBS solution, and then rinsed with PBS. ECs were permeabilized with 0.1% Ttiton X-100 in PBS, and then blocked with Cas-Block (Invitrogen) before incubation with primary antibody for 1 hour. Immunostained ECs were visualized by AlexaFluoro (Invitrogen) secondary antibodies.

CHAPTER 4

Generation of conditional Arhgap29 knockout mouse

Conditional Arhgap29 founders were generated by blastocyst injection of ES cells with targeted Arhgap29 allele (ID:36116), obtained from KOMP. *Exon4* and *exon5* are flanked by *loxp sites*. *LacZ* and *Neomycin resistance cassette* are designed being flanked by *Flp Recombinase Target (FRT) sites* forremovind if necessary. Targeting vector was electroporated into mouse embryonic stem (ES) cells by UTSW transgenic core. Genomic DNA from each ES cell clones were obtained and digested with Kpn1 and Pst1 sites. 5' and 3' external probes for Southern blot screening were performed to select ES cells with targeted allele. The correct clone was injected into blastocysts for generating Arhgap29 targeted mouse line. After germ line transmission confirmation, the animals were bred with Sox2-Cre mice to generate a Arhgap29 null allele. Litters were genotyped by PCR using primers.

In Situ Hybridization

Whole mount in situ hybridization was performed as previously described. Fixed Embryos and Retinas were incubated with DIG-labeled RNA probes overnight at 65°C. Tissues were washed with post-hybridization solutions, and then incubated in antibody overnight at 4°C. Color development was carried out using BM purple(Roche). Dig-RNA probes were generated from clones ;*Arhgap29* (Made by Ke Xu in lab).

Explants

Flk1-EGFP embryos at E8.0 were isolated in ice cold, and then allantois tissues were dissected using Dumont #55 fine forceps (Fine Science Tools). Allantoises were placed on separate 13 mm Watman filters (Fisher) over 500 μl of media in 4-well plates (Thermo Fisher

Schientific). The explants tissues were incubated in DMEM (ATCC), 10% FBS (ATCC), 1% penicillin/streptomycin (Invitrogen), and 2mM glutamine (Invitrogen). At indicated time points, images of explants were taken Images were taken by Zeiss Axiovert microscope using DP70 camera (Olympus).

Whole mount immunofluorescence staining

Fixed embryos were incubated in 5% H2O2/Ethanol at room temperature for 1 hour, then rehydrated in Series of Ethanol/PBS, and 0.1% PBST. Embryos were blocked in Cas-Block for 2 hours at room temperature, then incubated in primary antibody diluted in Cas-Block at 4°C overnight. Embryos were washed in PBS, and incubated in Biotin conjugated Secondary antibody diluted in Cas-Block at 4°C overnight. Washed embryos in PBS were then incubated in ABC Elite reagent (Vector Lab), followed by Tyramide solution (Invitrogen TSA kit).

Immunofluorescence staining on sections

Fixed tissues were washed with PBS. For paraffin section, fixed tissues were dehydrated in series of ethanol, incubated in xylene, and then embedded in paraffin. For cryosection, fixed tissues were incubated in 30% sucrose at 4°C overnight, and then embedded in Tissue-Tek O.C.T. Embedded tissues were sectioned at 10 μm by Microtome or Cryostat. Sections were blocked for 30min. at room temperature in Cas-Block(Invitrogen). Primary antibodies in Cas-Block were incubated at 4°C overnight. Following day, slides were washed in PBS, and then incubated in secondary antibody for an hour at room temperature followed by incubation in DAPI. Immunoflorescence stained slides were mounted with ProLong Gold Antifade Reagent (Life Technologies). The concentrations of primary antibodies used were as follows; PECAM 1:100 , Endomucin 1:100 (Santacruz), SMA 1:100

Bibliography

Almagro, S., Durmort, C., Chervin-Petinot, A., Heyraud, S., Dubois, M., Lambert, O., Maillefaud, C., Hewat, E., Schaal, J.P., Huber, P., Gulino-Debrac, D., 2010. The motor protein myosin-X transports VE-cadherin along filopodia to allow the formation of early endothelial cell-cell contacts. Molecular and cellular biology 30, 1703-1717.

Arora, R., Papaioannou, V.E., 2012. The murine allantois: a model system for the study of blood vessel formation. Blood 120, 2562-2572.

Bayless, K.J., Davis, G.E., 2002. The Cdc42 and Rac1 GTPases are required for capillary lumen formation in three-dimensional extracellular matrices. Journal of cell science 115, 1123-1136.

Bayless, K.J., Davis, G.E., 2004. Microtubule depolymerization rapidly collapses capillary tube networks in vitro and angiogenic vessels in vivo through the small GTPase Rho. The Journal of biological chemistry 279, 11686-11695.

Benedito, R., Roca, C., Sorensen, I., Adams, S., Gossler, A., Fruttiger, M., Adams, R.H., 2009. The notch ligands Dll4 and Jagged1 have opposing effects on angiogenesis. Cell 137, 1124-1135.

Blum, Y., Belting, H.G., Ellertsdottir, E., Herwig, L., Luders, F., Affolter, M., 2008. Complex cell rearrangements during intersegmental vessel sprouting and vessel fusion in the zebrafish embryo. Developmental biology 316, 312-322.

Bogers, A.J., Gittenberger-de Groot, A.C., Poelmann, R.E., Peault, B.M., Huysmans, H.A., 1989. Development of the origin of the coronary arteries, a matter of ingrowth or outgrowth? Anatomy and embryology 180, 437-441.

Brade, T., Pane, L.S., Moretti, A., Chien, K.R., Laugwitz, K.L., 2013. Embryonic heart progenitors and cardiogenesis. Cold Spring Harbor perspectives in medicine 3, a013847.

Bryant, D.M., Datta, A., Rodriguez-Fraticelli, A.E., Peranen, J., Martin-Belmonte, F., Mostov, K.E., 2010. A molecular network for de novo generation of the apical surface and lumen. Nature cell biology 12, 1035-1045.

Burri, P.H., Tarek, M.R., 1990. A novel mechanism of capillary growth in the rat pulmonary microcirculation. The Anatomical record 228, 35-45.

Carmeliet, P., Lampugnani, M.G., Moons, L., Breviario, F., Compernolle, V., Bono, F., Balconi, G., Spagnuolo, R., Oosthuyse, B., Dewerchin, M., Zanetti, A., Angellilo, A., Mattot, V., Nuyens, D., Lutgens, E., Clotman, F., de Ruiter, M.C., Gittenberger-de Groot, A., Poelmann, R., Lupu, F., Herbert, J.M., Collen, D., Dejana, E., 1999. Targeted deficiency or cytosolic truncation of the VE-cadherin gene in mice impairs VEGF-mediated endothelial survival and angiogenesis. Cell 98, 147-157.

Checchin, D., Sennlaub, F., Levavasseur, E., Leduc, M., Chemtob, S., 2006. Potential role of microglia in retinal blood vessel formation. Investigative ophthalmology & visual science 47, 3595-3602.

Chong, D.C., Koo, Y., Xu, K., Fu, S., Cleaver, O., 2011. Stepwise arteriovenous fate acquisition during mammalian vasculogenesis. Developmental dynamics : an official publication of the American Association of Anatomists 240, 2153-2165.

Coffin, J.D., Harrison, J., Schwartz, S., Heimark, R., 1991. Angioblast differentiation and morphogenesis of the vascular endothelium in the mouse embryo. Developmental biology 148, 51-62.

Coffin, J.D., Poole, T.J., 1988. Embryonic vascular development: immunohistochemical identification of the origin and subsequent morphogenesis of the major vessel primordia in quail embryos. Development 102, 735-748.

Datta, A., Bryant, D.M., Mostov, K.E., 2011. Molecular regulation of lumen morphogenesis. Current biology : CB 21, R126-136.

Davis, G.E., Camarillo, C.W., 1996. An alpha 2 beta 1 integrin-dependent pinocytic mechanism involving intracellular vacuole formation and coalescence regulates capillary lumen and tube formation in three-dimensional collagen matrix. Experimental cell research 224, 39-51.

Drake, C.J., Davis, L.A., Hungerford, J.E., Little, C.D., 1992a. Perturbation of beta 1 integrin-mediated adhesions results in altered somite cell shape and behavior. Developmental biology 149, 327-338.

Drake, C.J., Davis, L.A., Little, C.D., 1992b. Antibodies to beta 1-integrins cause alterations of aortic vasculogenesis, in vivo. Developmental dynamics : an official publication of the American Association of Anatomists 193, 83-91.

Drake, C.J., Fleming, P.A., 2000. Vasculogenesis in the day 6.5 to 9.5 mouse embryo. Blood 95, 1671-1679.

Eichmann, A., Yuan, L., Moyon, D., Lenoble, F., Pardanaud, L., Breant, C., 2005. Vascular development: from precursor cells to branched arterial and venous networks. The International journal of developmental biology 49, 259-267.

Ema, M., Takahashi, S., Rossant, J., 2006. Deletion of the selection cassette, but not cis-acting elements, in targeted Flk1-lacZ allele reveals Flk1 expression in multipotent mesodermal progenitors. Blood 107, 111-117.

Feinberg, R.N., Latker, C.H., Beebe, D.C., 1986. Localized vascular regression during limb morphogenesis in the chicken embryo. I. Spatial and temporal changes in the vascular pattern. The Anatomical record 214, 405-409.

Ferdous, A., Morris, J., Abedin, M.J., Collins, S., Richardson, J.A., Hill, J.A., 2011. Forkhead factor FoxO1 is essential for placental morphogenesis in the developing embryo. Proceedings of the National Academy of Sciences of the United States of America 108, 16307-16312.

Ferrari, A., Veligodskiy, A., Berge, U., Lucas, M.S., Kroschewski, R., 2008. ROCK-mediated contractility, tight junctions and channels contribute to the conversion of a preapical patch into apical surface during isochoric lumen initiation. Journal of cell science 121, 3649-3663.

Flamme, I., 1987. Edge cell migration in the extraembryonic mesoderm of the chick embryo. An experimental and morphological study. Anatomy and embryology 176, 477-491.

Folkman, J., Klagsbrun, M., 1987. Angiogenic factors. Science 235, 442-447.

Folkman, J., Shing, Y., 1992. Angiogenesis. The Journal of biological chemistry 267, 10931-10934.

Gaengel, K., Genove, G., Armulik, A., Betsholtz, C., 2009. Endothelial-mural cell signaling in vascular development and angiogenesis. Arteriosclerosis, thrombosis, and vascular biology 29, 630-638.

George, E.L., Baldwin, H.S., Hynes, R.O., 1997. Fibronectins are essential for heart and blood vessel morphogenesis but are dispensable for initial specification of precursor cells. Blood 90, 3073-3081.

George, E.L., Georges-Labouesse, E.N., Patel-King, R.S., Rayburn, H., Hynes, R.O., 1993. Defects in mesoderm, neural tube and vascular development in mouse embryos lacking fibronectin. Development 119, 1079-1091.

Gerhardt, H., Golding, M., Fruttiger, M., Ruhrberg, C., Lundkvist, A., Abramsson, A., Jeltsch, M., Mitchell, C., Alitalo, K., Shima, D., Betsholtz, C., 2003. VEGF guides angiogenic sprouting utilizing endothelial tip cell filopodia. The Journal of cell biology 161, 1163-1177.

Guy, C.T., Cardiff, R.D., Muller, W.J., 1992. Induction of mammary tumors by expression of polyomavirus middle T oncogene: a transgenic mouse model for metastatic disease. Molecular and cellular biology 12, 954-961.

Habermann, B., 2004. The BAR-domain family of proteins: a case of bending and binding? EMBO reports 5, 250-255.

Hayashi, S., Lewis, P., Pevny, L., McMahon, A.P., 2002. Efficient gene modulation in mouse epiblast using a Sox2Cre transgenic mouse strain. Mechanisms of development 119 Suppl 1, S97-S101.

Hayashi, S., McMahon, A.P., 2002. Efficient recombination in diverse tissues by a tamoxifen-inducible form of Cre: a tool for temporally regulated gene activation/inactivation in the mouse. Developmental biology 244, 305-318.

Hellstrom, M., Phng, L.K., Hofmann, J.J., Wallgard, E., Coultas, L., Lindblom, P., Alva, J., Nilsson, A.K., Karlsson, L., Gaiano, N., Yoon, K., Rossant, J., Iruela-Arispe, M.L., Kalen, M., Gerhardt, H., Betsholtz, C., 2007. Dll4 signalling through Notch1 regulates formation of tip cells during angiogenesis. Nature 445, 776-780.

Herbert, S.P., Huisken, J., Kim, T.N., Feldman, M.E., Houseman, B.T., Wang, R.A., Shokat, K.M., Stainier, D.Y., 2009. Arterial-venous segregation by selective cell sprouting: an alternative mode of blood vessel formation. Science 326, 294-298.

Herzog, Y., Guttmann-Raviv, N., Neufeld, G., 2005. Segregation of arterial and venous markers in subpopulations of blood islands before vessel formation. Developmental dynamics : an official publication of the American Association of Anatomists 232, 1047-1055.

Isogai, S., Horiguchi, M., Weinstein, B.M., 2001. The vascular anatomy of the developing zebrafish: an atlas of embryonic and early larval development. Developmental biology 230, 278-301.

Jones, E.A., Yuan, L., Breant, C., Watts, R.J., Eichmann, A., 2008. Separating genetic and hemodynamic defects in neuropilin 1 knockout embryos. Development 135, 2479-2488.

Kamei, M., Saunders, W.B., Bayless, K.J., Dye, L., Davis, G.E., Weinstein, B.M., 2006. Endothelial tubes assemble from intracellular vacuoles in vivo. Nature 442, 453-456.

Kesavan, G., Sand, F.W., Greiner, T.U., Johansson, J.K., Kobberup, S., Wu, X., Brakebusch, C., Semb, H., 2009. Cdc42-mediated tubulogenesis controls cell specification. Cell 139, 791-801.

Kisanuki, Y.Y., Hammer, R.E., Miyazaki, J., Williams, S.C., Richardson, J.A., Yanagisawa, M., 2001. Tie2-Cre transgenic mice: a new model for endothelial cell-lineage analysis in vivo. Developmental biology 230, 230-242.

Koh, W., Mahan, R.D., Davis, G.E., 2008. Cdc42- and Rac1-mediated endothelial lumen formation requires Pak2, Pak4 and Par3, and PKC-dependent signaling. Journal of cell science 121, 989-1001.

Kwee, L., Baldwin, H.S., Shen, H.M., Stewart, C.L., Buck, C., Buck, C.A., Labow, M.A., 1995. Defective development of the embryonic and extraembryonic circulatory systems in vascular cell adhesion molecule (VCAM-1) deficient mice. Development 121, 489-503.

Latker, C.H., Feinberg, R.N., Beebe, D.C., 1986. Localized vascular regression during limb morphogenesis in the chicken embryo: II. Morphological changes in the vasculature. The Anatomical record 214, 410-417, 392-413.

Lawson, N.D., Vogel, A.M., Weinstein, B.M., 2002. sonic hedgehog and vascular endothelial growth factor act upstream of the Notch pathway during arterial endothelial differentiation. Developmental cell 3, 127-136.

Lawson, N.D., Weinstein, B.M., 2002. In vivo imaging of embryonic vascular development using transgenic zebrafish. Developmental biology 248, 307-318.

le Noble, F., Moyon, D., Pardanaud, L., Yuan, L., Djonov, V., Matthijsen, R., Breant, C., Fleury, V., Eichmann, A., 2004. Flow regulates arterial-venous differentiation in the chick embryo yolk sac. Development 131, 361-375.

Leslie, E.J., Mansilla, M.A., Biggs, L.C., Schuette, K., Bullard, S., Cooper, M., Dunnwald, M., Lidral, A.C., Marazita, M.L., Beaty, T.H., Murray, J.C., 2012. Expression and mutation analyses implicate ARHGAP29 as the etiologic gene for the cleft lip with or without cleft palate locus identified by genome-wide association on chromosome 1p22. Birth defects research. Part A, Clinical and molecular teratology 94, 934-942.

Lobov, I.B., Rao, S., Carroll, T.J., Vallance, J.E., Ito, M., Ondr, J.K., Kurup, S., Glass, D.A., Patel, M.S., Shu, W., Morrisey, E.E., McMahon, A.P., Karsenty, G., Lang, R.A., 2005. WNT7b mediates macrophage-induced programmed cell death in patterning of the vasculature. Nature 437, 417-421.

Lucitti, J.L., Jones, E.A., Huang, C., Chen, J., Fraser, S.E., Dickinson, M.E., 2007. Vascular remodeling of the mouse yolk sac requires hemodynamic force. Development 134, 3317-3326.

Mahajan, A., Yuan, C., Lee, H., Chen, E.S., Wu, P.Y., Tsai, M.D., 2008. Structure and function of the phosphothreonine-specific FHA domain. Science signaling 1, re12.

Manner, J., Seidl, W., Steding, G., 1995. Embryological observations on the morphogenesis of double-outlet right ventricle with subaortic ventricular septal defect and normal arrangement of the great arteries. The Thoracic and cardiovascular surgeon 43, 307-312.

Martin-Belmonte, F., Gassama, A., Datta, A., Yu, W., Rescher, U., Gerke, V., Mostov, K., 2007. PTEN-mediated apical segregation of phosphoinositides controls epithelial morphogenesis through Cdc42. Cell 128, 383-397.

McGrath, K.E., Koniski, A.D., Malik, J., Palis, J., 2003. Circulation is established in a stepwise pattern in the mammalian embryo. Blood 101, 1669-1676.

Miller, R.A., Christoforou, N., Pevsner, J., McCallion, A.S., Gearhart, J.D., 2008. Efficient array-based identification of novel cardiac genes through differentiation of mouse ESCs. PLoS One 3, e2176.

Mitin, N., Konieczny, S.F., Taparowsky, E.J., 2006. RAS and the RAIN/RasIP1 effector. Methods in enzymology 407, 322-335.

Mitin, N.Y., Ramocki, M.B., Zullo, A.J., Der, C.J., Konieczny, S.F., Taparowsky, E.J., 2004. Identification and characterization of rain, a novel Ras-interacting protein with a unique subcellular localization. The Journal of biological chemistry 279, 22353-22361.

Monvoisin, A., Alva, J.A., Hofmann, J.J., Zovein, A.C., Lane, T.F., Iruela-Arispe, M.L., 2006. VE-cadherin-CreERT2 transgenic mouse: a model for inducible recombination in the endothelium. Developmental dynamics : an official publication of the American Association of Anatomists 235, 3413-3422.

Murakami, M., 2012. Signaling required for blood vessel maintenance: molecular basis and pathological manifestations. International journal of vascular medicine 2012, 293641.

Myagmar, B.E., Umikawa, M., Asato, T., Taira, K., Oshiro, M., Hino, A., Takei, K., Uezato, H., Kariya, K., 2005. PARG1, a protein-tyrosine phosphatase-associated RhoGAP, as a putative Rap2 effector. Biochemical and biophysical research communications 329, 1046-1052.

Outtz, H.H., Tattersall, I.W., Kofler, N.M., Steinbach, N., Kitajewski, J., 2011. Notch1 controls macrophage recruitment and Notch signaling is activated at sites of endothelial cell anastomosis during retinal angiogenesis in mice. Blood 118, 3436-3439.

Pardali, E., Goumans, M.J., ten Dijke, P., 2010. Signaling by members of the TGF-beta family in vascular morphogenesis and disease. Trends in cell biology 20, 556-567.

Phng, L.K., Gerhardt, H., 2009. Angiogenesis: a team effort coordinated by notch. Developmental cell 16, 196-208.

Pitulescu, M.E., Schmidt, I., Benedito, R., Adams, R.H., 2010. Inducible gene targeting in the neonatal vasculature and analysis of retinal angiogenesis in mice. Nature protocols 5, 1518-1534.

Post, A., Pannekoek, W.J., Ross, S.H., Verlaan, I., Brouwer, P.M., Bos, J.L., 2013. Rasip1 mediates Rap1 regulation of Rho in endothelial barrier function through ArhGAP29. Proceedings of the National Academy of Sciences of the United States of America 110, 11427-11432.

Reese, D.E., Hall, C.E., Mikawa, T., 2004. Negative regulation of midline vascular development by the notochord. Developmental cell 6, 699-708.

Retta, S.F., Balzac, F., Avolio, M., 2006. Rap1: a turnabout for the crosstalk between cadherins and integrins. European journal of cell biology 85, 283-293.

Risau, W., Flamme, I., 1995. Vasculogenesis. Annual review of cell and developmental biology 11, 73-91.

Rocha, S.F., Adams, R.H., 2009. Molecular differentiation and specialization of vascular beds. Angiogenesis 12, 139-147.

Sacharidou, A., Koh, W., Stratman, A.N., Mayo, A.M., Fisher, K.E., Davis, G.E., 2010. Endothelial lumen signaling complexes control 3D matrix-specific tubulogenesis through interdependent Cdc42- and MT1-MMP-mediated events. Blood 115, 5259-5269.

Saras, J., Franzen, P., Aspenstrom, P., Hellman, U., Gonez, L.J., Heldin, C.H., 1997. A novel GTPase-activating protein for Rho interacts with a PDZ domain of the protein-tyrosine phosphatase PTPL1. The Journal of biological chemistry 272, 24333-24338.

Shalaby, F., Rossant, J., Yamaguchi, T.P., Gertsenstein, M., Wu, X.F., Breitman, M.L., Schuh, A.C., 1995. Failure of blood-island formation and vasculogenesis in Flk-1-deficient mice. Nature 376, 62-66.

Somsel Rodman, J., Wandinger-Ness, A., 2000. Rab GTPases coordinate endocytosis. Journal of cell science 113 Pt 2, 183-192.

Strilic, B., Eglinger, J., Krieg, M., Zeeb, M., Axnick, J., Babal, P., Muller, D.J., Lammert, E., 2010. Electrostatic cell-surface repulsion initiates lumen formation in developing blood vessels. Current biology : CB 20, 2003-2009.

Strilic, B., Kucera, T., Eglinger, J., Hughes, M.R., McNagny, K.M., Tsukita, S., Dejana, E., Ferrara, N., Lammert, E., 2009. The molecular basis of vascular lumen formation in the developing mouse aorta. Developmental cell 17, 505-515.

Suchting, S., Freitas, C., le Noble, F., Benedito, R., Breant, C., Duarte, A., Eichmann, A., 2007. The Notch ligand Delta-like 4 negatively regulates endothelial tip cell formation and vessel branching. Proceedings of the National Academy of Sciences of the United States of America 104, 3225-3230.

Takai, Y., Sasaki, T., Matozaki, T., 2001. Small GTP-binding proteins. Physiological reviews 81, 153-208.

Walls, J.R., Coultas, L., Rossant, J., Henkelman, R.M., 2008. Three-dimensional analysis of vascular development in the mouse embryo. PLoS ONE 3, e2853.

Wilkinson, D.G., 1995. RNA detection using non-radioactive in situ hybridization. Current opinion in biotechnology 6, 20-23.

Wilson, C.W., Parker, L.H., Hall, C.J., Smyczek, T., Mak, J., Crow, A., Posthuma, G., De Maziere, A., Sagolla, M., Chalouni, C., Vitorino, P., Roose-Girma, M., Warming, S., Klumperman, J., Crosier, P.S., Ye, W., 2013. Rasip1 regulates vertebrate vascular endothelial junction stability through Epac1-Rap1 signaling. Blood 122, 3678-3690.

Wilt, F.H., 1965. Erythropoiesis in the Chick Embryo: The Role of Endoderm. Science 147, 1588-1590.

Xu, K., Chong, D.C., Rankin, S.A., Zorn, A.M., Cleaver, O., 2009. Rasip1 is required for endothelial cell motility, angiogenesis and vessel formation. Developmental biology 329, 269-279.

Xu, K., Sacharidou, A., Fu, S., Chong, D.C., Skaug, B., Chen, Z.F., Davis, G.E., Cleaver, O., 2011. Blood vessel tubulogenesis requires Rasip1 regulation of GTPase signaling. Developmental cell 20.

Yamaguchi, T.P., Dumont, D.J., Conlon, R.A., Breitman, M.L., Rossant, J., 1993. flk-1, an flt-related receptor tyrosine kinase is an early marker for endothelial cell precursors. Development 118, 489-498.

Yang, J.T., Rayburn, H., Hynes, R.O., 1995. Cell adhesion events mediated by alpha 4 integrins are essential in placental and cardiac development. Development 121, 549-560.

Zhao, X.H., Laschinger, C., Arora, P., Szaszi, K., Kapus, A., McCulloch, C.A., 2007. Force activates smooth muscle alpha-actin promoter activity through the Rho signaling pathway. Journal of cell science 120, 1801-1809.

Zhong, T.P., Childs, S., Leu, J.P., Fishman, M.C., 2001. Gridlock signalling pathway fashions the first embryonic artery. Nature 414, 216-220.

Zovein, A.C., Iruela-Arispe, M.L., 2009. Time to cut the cord: placental HSCs grow up. Cell stem cell 5, 351-352.

Zovein, A.C., Luque, A., Turlo, K.A., Hofmann, J.J., Yee, K.M., Becker, M.S., Fassler, R., Mellman, I., Lane, T.F., Iruela-Arispe, M.L., 2010. Beta1 integrin establishes endothelial cell polarity and arteriolar lumen formation via a Par3-dependent mechanism. Developmental cell 18, 39-51.